Design and Evaluation of Grasp Assistive Devices in an Industrial Environment

by

Daniel Philip Loewen

A thesis

presented to the University of Waterloo

in fulfillment of the

thesis requirement for the degree of

Master of Applied Science

in

Mechanical and Mechatronics Engineering

Waterloo, Ontario, Canada, 2019

© Daniel Philip Loewen 2019

Authors Declaration

I hereby declare that I am the sole author of this thesis. This is a true copy of the thesis, including any final revisions, as accepted by my examiners.

I understand that my thesis may be made electronically available to the public.

Abstract

Carpal tunnel syndrome and tendonitis are two common upper extremity cumulative trauma disorders related to repetitive and forceful activities in the workplace. The objective of this research was to reduce the hand force during an activity, as reducing task repetition would negatively affect productivity. Two devices were developed to achieve this objective: a soft pneumatic grasp assist device to augment grasp strength, and a novel grip training device to visually alert the user when more force than necessary is used. Device effectiveness was quantified by measuring muscle activity and grip force during an *in vivo* study of a common industrial activity. Nine associates experienced with power tools employed by an automobile manufacturer installed 18 fasteners using a pistol grip DC tool under three conditions: a typical manner (no device or prompting), with the grasp assist, and with the grip training device. Surface electromyography (sEMG) was used to measure the activity of four muscles commonly associated with grasping – flexor digitorum superficialis (FDS), flexor carpi ulnaris (FCU), extensor digitorum communis (EDC), and flexor carpi radialis (FCR). Results showed that both the grasp assist and grip trainer significantly reduced the mean, combined, normalized muscle activity compared to the typical condition by 18% and 23% respectively ($p < 0.05$). Muscle activation results were contextualized using the revised strain index (RSI), a clinical tool to evaluate the safety of an activity by considering activity specific ergonomic factors. The grasp assist and grip trainer both yielded a significantly lower mean RSI value than the typical condition by 13% and 17% respectively ($p < 0.05$). Grip force was measured using a flexible pressure transducer affixed to the pistol-grip handle of the DC tool. Again, the grasp assist and grip trainer yielded significantly lower values than the typical trial by 47% and 36% respectively ($p < 0.001$). Between devices, the grasp assist yielded a significantly lower grip force the grip trainer ($p < 0.001$); however, the mean muscle activation was not significantly different, which suggests that the four muscles measured in this study do not completely capture grip force. A large variation in grip force was measured for all three conditions with a weak, positive correlation between power tool experience and force applied. Knowledge of the voluntary variation in grip force can be used to educate workers on minimizing the force exerted during an activity.

Acknowledgements

I would like to thank my supervisor Dr. Naveen Chandrashekar first and foremost, for providing me with this opportunity, the support, and freedom to investigate it in the manner I deemed appropriate. The skills I have developed over the past two years have broad potential applications and I am eager to apply them towards future endeavours. I thoroughly appreciate the seemingly endless positivity that Harish Rao exudes, coupled with (somehow) limitless time to discuss my ideas and provide constructive criticism. This appreciation extends to the most experienced member of our biomechanical team, Mayank Kalra.

I would like to extend a big thank you to Honda of Canada Manufacturing for their support and feedback in my research, and the associates who participated in the study. The dedication of such a large, global company towards the health and wellbeing of its massive workforce is endearing. Thank you to Robert Bahensky and Jin Zhu for assisting me before, during, and after the study, for being pilot test subjects, and all-around great people.

Finally, and most importantly, I would like to thank my wife for ~~allowing~~ *encouraging* me to uproot our family and move to a new province so that I may sate my desire for knowledge. You constantly remind me that the best things in life are often the most challenging, and I am blessed to have you in my life.

Table of Contents

Authors Declaration ii

Abstract iii

Acknowledgements iv

List of Figures viii

List of Tables xii

List of Equations xiii

1.0 Introduction 1

1.1 Motivation 1

1.2 Anatomy of the Forearm and Wrist 2

1.3 Cumulative Trauma Disorders 4

1.4 Hand Wrist Orthoses 10

1.4.1 Passive Devices 10

1.4.2 Dynamic Devices 11

1.5 Hypotheses 18

2 Methodology 19

2.1 Grasp Assist Design 19

2.1.1 Finite Element Method 19

2.1.2 Final Design 29

2.2 Rapid Prototyping 34

2.2.1 3D Printer and Specifications 34

2.2.2 Slicer Software Settings 35
2.3 In Vivo Study 37
2.3.1 Participants 37
2.3.2 Equipment 38
2.3.3 Procedure 44
2.4 Data Processing 47
2.4.1 Grip Force 47
2.4.2 EMG 49
2.5 Statistical Analysis 50
3 Results 53
3.1 Two-way ANOVA 53
3.2 Muscle Activation 55
3.3 Grip Force 60
3.4 Revised Strain Index Results 62
3.5 Subjective Results 67
4 Discussion 68
4.1 Grasp Assist Device 71
4.2 Primary Hypothesis 72
4.3 Grip Training Device 74
4.4 Secondary Hypothesis 75
4.5 Applicability and Usefulness 76

4.6 Limitations and Recommendations 77

5 Conclusion 80

References 81

List of Figures

Figure 1 Anterior superficial layer of the forearm [7] 2

Figure 2 Anterior view of right palm with wrist cross section [8] 3

Figure 3 Posterior superficial layer of the forearm [9] 3

Figure 4 Hand wrist flexion, extension, and deviation 7

Figure 5 Hand grasp patterns a) spherical, b) cylindrical (power), c) parallel extension (palmer) [30] 7

Figure 6 Wrist extension and flexion pulley comparison [28] 7

Figure 7 Example of a split tool handle a) open, b) assembled [33] 9

Figure 8 Example of a pressure map instrumented handle [32] 9

Figure 9 Example of passive orthoses a) custom-made, b) commercially available [40] 11

Figure 10 Soft pneumatic gripper for material handling circa 1967 [50] 12

Figure 11 Example of a fiber reinforced soft actuator a) unpressurized, b) pressurized [53] 13

Figure 12 Bellows-style soft actuator inflated to six pressures, 0 kPa to 250 kPa 14

Figure 13 Fiber reinforced soft actuator manufacturing process [53] 14

Figure 14 Finite element model of a pneumatic network (pneu-net) soft actuator [57] 20

Figure 15 Finite element model of a fiber reinforced soft actuator [53] 20

Figure 16 Finite element model of a bellows-style soft actuator [52] 20

Figure 17 Isometric view of initial bellows-style actuator design (left) & section view (right) 21

Figure 18 Typical stress-strain curve for hyperelastic material (left) and elastic-plastic material (right) .. 22

Figure 19 Bottom isometric view of boundary conditions for free rotation simulation 24

Figure 20 Bottom isometric view of boundary conditions for constrained tip force simulation 25

Figure 21 Ten-node, second order, tetrahedral element C3D10H [62] (Section 28.1.4) 26

Figure 22 Isometric cross section view of bellows-style actuator with dimensional variables shown 26

Figure 23 Profile and top view of initial bellows-style actuator with 0° angle from plane of symmetry ... 28

Figure 24 Profile and top view of bellows-style actuator with 45° angle from plane of symmetry 28

Figure 25 Profile view, free rotation simulation (100kPa) for 0° (left) and 45° design (right) 29

Figure 26 Profile view, constrained tip force simulation (100kPa) for 0° (top) and 45° design (bottom).. 29

Figure 27 Final design optimized for 3D printing with flattened, adjustable digit retention loops in top view (upper left), front view (lower left) and isometric view (right)..... 30

Figure 28 Mesh convergence results for final actuator design based on free rotation simulation 31

Figure 29 Free rotation at 241kPa (~35psi) experiment (left) and corresponding simulation (right)..... 32

Figure 30 Bending ratio versus pressure results based on free rotation experiment and simulation 32

Figure 31 Constrained tip force at 138kPa (~20psi) experiment (top) and simulation (bottom)..... 33

Figure 32 Constrained tip force versus pressure, experimental and simulated results 33

Figure 33 Prusa i3 MK3 3D printer, with labeled primary components..... 34

Figure 34 Cura 3.4.1 build plate illustration with final actuator design..... 35

Figure 35 Fastener locations illustrated for the right half of the test apparatus 38

Figure 36 Pneumatic system and DC pistol grip tool 39

Figure 37 Trimmed 9830 pressure sensor (left), high density foam mounted to a measured weight to evenly distribute load across a Sensel (middle), trimmed 9830 sensor applied to the pistol grip of the DC tool with adhesive tape (right) 40

Figure 38 Example of EMG electrode and probe placement for FCU, FDS, FCR (left) and EDC (right). 41

Figure 39 Fully assembled grasp assist device 42

Figure 40 Grip trainer FlexiForce sensors (left) and visual feedback LED placement (right) on the tool . 43

Figure 41 Maximum voluntary contraction (MVC) fixture for flexion (left) and extension (right)..... 45

Figure 42 Example of identifying trigger engagement (V=0.85) and disengagement (V=~0)..... 48

Figure 43 Example of identifying fastener locations based on trigger engagement and grip force..... 48

Figure 44 Example of identifying artifacts through visual inspection 50

Figure 45 Effect of trial condition on Flexor Digitorum Superficialis (FDS) mean muscle activity (±SD) based on fastener location (low, high, overhead, all)..... 57

Figure 46 Effect of trial condition on Flexor Carpi Ulnaris (FCU) mean muscle activity (±SD) based on fastener location (low, high, overhead, all) 57
Figure 47 Effect of trial condition on Extensor Digitorum Communis (EDC) mean muscle activity (±SD) based on fastener location (low, high, overhead, all) 58
Figure 48 Effect of trial condition on Flexor Carpi Radialis (FCR) mean muscle activity (±SD) based on fastener location (low, high, overhead, all) 58
Figure 49 Effect of trial condition on FDS, FCU, EDC, and FCR combined mean muscle activity (±SD) based on fastener location (low, high, overhead, all) 59
Figure 50 Effect of trial condition on mean applied grip force (±SD) based on fastener location (low, high, overhead, all) 62
Figure 51 Minimum, mean, and maximum RSI values for FDS muscle and all trial conditions (typical, grip trainer, grasp assist) based on all fastener locations with hazardous threshold overlaid at RSI=10.0 for context (n=9) 64
Figure 52 Minimum, mean, and maximum RSI values for FCU muscle and all trial conditions (typical, grip trainer, grasp assist) based on all fastener locations with hazardous threshold overlaid at RSI=10.0 for context (n=9) 64
Figure 53 Minimum, mean, and maximum RSI values for EDC muscle and all trial conditions (typical, grip trainer, grasp assist) based on all fastener locations with hazardous threshold overlaid at RSI=10.0 for context (n=9) 65
Figure 54 Minimum, mean, and maximum RSI values for FCR muscle and all trial conditions (typical, grip trainer, grasp assist) based on all fastener locations with hazardous threshold overlaid at RSI=10.0 for context (n=9) 65
Figure 55 Minimum, mean, and maximum RSI values for FDS, FCU, EDC, and FCR combined, and all trial conditions (typical, grip trainer, grasp assist) based on all fastener locations with hazardous threshold overlaid at RSI=10.0 for context (n=9) 66
Figure 56 Subjective responses to using the grasp assist device 67

Figure 57 Normal force distribution on a split handle (left) and a pressure mapped handle (right) 69

Figure 58 Actuator design by Yap et al. (left) and improved based on presented research (right) 72

Figure 59 Averaged muscle activation profiles during active and glove-assisted trials, adapted from Yap et al 2017 [54] 74

List of Tables

Table 1 Examples of dynamic hand/wrist orthoses 15

Table 2 Summary of relevant Ninjaflex® material properties 23

Table 3 Experimentally obtained Ogden strain energy function coefficients for N=3 23

Table 4 Simulated pressure load applied per step 24

Table 5 Simulated response to dimensional variable manipulation 28

Table 6 Final actuator design parameters per hand size and digit application 30

Table 7 Mesh convergence study results for final actuator design based on free rotation simulation 31

Table 8 Optimum settings for 3D printing in Cura 3.4.1 with Ninjaflex® 36

Table 9 Summary of participant information, n=9 37

Table 10 Summary of muscle palpations and EMG electrode placement 41

Table 11 Experimental protocol summary 44

Table 12 Subjective assessment questionnaire 47

Table 13 Two-way ANOVA summary of independent and dependent variables 50

Table 14 t-Test summary of trial condition comparisons for each bolt location and independent variable 51

Table 15 Revised strain index factor description and equation 52

Table 16 Two-way ANOVA results for condition and location effects on muscle activity and grip force 54

Table 17 Post hoc significance summary of condition factor 54

Table 18 Summary of muscle activation (%MVE) mean values (±SD) based on locations: low, high, overhead, all, and conditions: typical (T), grip trainer (GT), grasp assist (GA) with significance between conditions (n=9). 56

Table 19 Summary of grip force (N) mean values (±SD) based on locations: low, high, overhead, all, and conditions: typical (T), grip trainer (GT), grasp assist (GA) with significance between conditions (n=9). 61

Table 20 Revised Strain Index (RSI) values when fastening bolts at all locations (n=9) 63

List of Equations

Equation 1 Ogden strain energy function with N=3 22

Equation 2 Radius of curvature based on three points: x, y, and z 27

Equation 3 Revised strain index (RSI) 51

1.0 Introduction

1.1 Motivation

Injuries associated with repetitive motions, such as carpal tunnel syndrome (CTS) and tendonitis of the hand and wrist, are often classified under the umbrella terms musculoskeletal disorder, repetitive strain injury, or cumulative trauma disorder (CTD). Upper extremity repetitive motions are less common in day to day life than in the workplace, and the prevalence of CTD has been shown to coincide with this. Low estimates of CTD in the general population are 3.7% (average of male and female results) [1], and rise to 10.8% in highly repetitive and forceful industrial scenarios [2]. The repetition and force of a task are both significant risk factors [3]. Task repetition in an industrial environment is typically independent of the worker and can be challenging to reduce without affecting output; however, the force applied to perform a task often varies with the individual, which may result from a number of factors including hand span, grip strength, tool experience, comfort with the task, age, etc.

Recently, the incidence rate of CTD among associates using a pistol grip DC tool has increased at Honda of Canada Manufacturing (HCM), situated in Alliston, Ontario, prompting an investigation between HCM and the University of Waterloo. In a 2017 study, Bakker, et al. measured median nerve pressure and tendon strain (two factors associated with CTS and tendonitis, respectively) on cadaveric hand/forearms during a simulated pistol grip DC tool operation [4]. Bakker determined that tendon strain is predominantly a result of the grip force required to grasp the tool (72-98%), compared to the force required to resist the applied torque (2-28%). Therefore, reducing the (grasp) force applied during a DC tool activity would lower one of the risk factors associated with injury. The objective of reducing applied grip force could have been met in multiple ways; however, it was hypothesized that using an assistive device for grasping would be most effective. This work is significant as a large portion of the workforce are employed in forceful, repetitive hand-intensive industries including food processing, and manufacturing – 1.48M in Canada [5], and 12.3M in USA [6] alone, as of 2016.

1.2 Anatomy of the Forearm and Wrist

The dexterity of the human hand can be attributed to its 27 bones, connected and articulated by a complex network of tendons, ligaments, and muscles. Its versatility means that it is used often for a wide variety of tasks, many of which can result in injury. It is important to understand the key structure of the forearm and wrist before delving into injury mechanism and prevention.

Grasp force is primarily attributed to the tertiary (deep) flexor digitorum profundus (FDP) and the superficial (surface) flexor digitorum superficialis (FDS) highlighted in Figure 1, which flex the middle phalanges of the hand. The corresponding tendons pass through the carpal tunnel, highlighted in Figure 2. Friction between these tendons and the tendon sheath can cause inflammation, resulting in tenosynovitis. Tendonitis results from repetitive use and high levels of axial loading and is commonly associated with the FDS and FDP tendons. Support for the wrist and hand is generated by the flexor carpi radialis (FCR), which flexes and abducts (radial deviation) the hand, laying superficially within the forearm. Similarly, the flexor carpi ulnaris (FCU) supports the wrist and hand, acting to flex and adduct (ulnar deviation) the hand. Both the FCR and FCU are also highlighted in Figure 1.

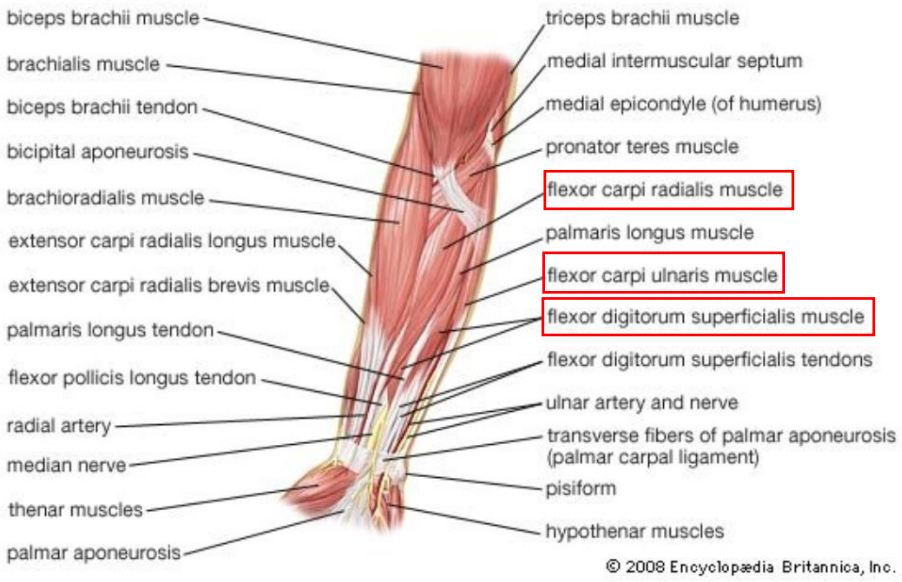

Figure 1 Anterior superficial layer of the forearm [7]

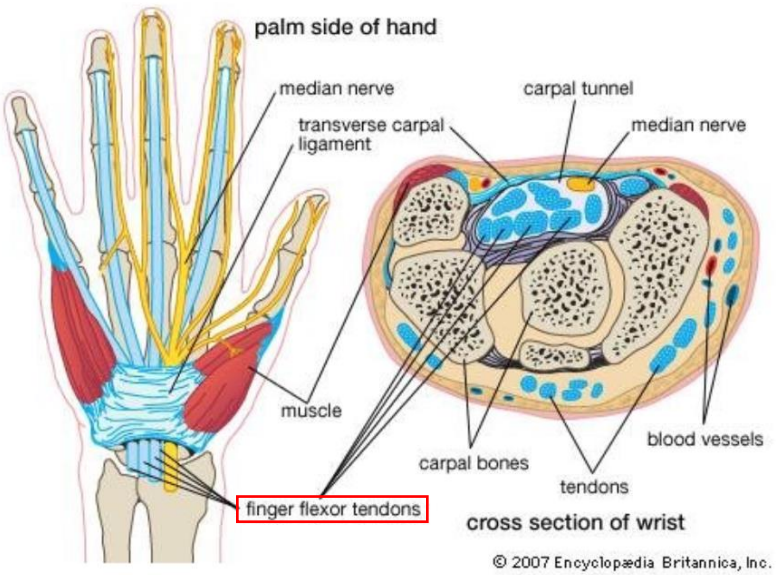

Figure 2 Anterior view of right palm with wrist cross section [8]

Extending the phalanges and wrist is attributed to the superficial extensor digitorum communis muscle (EDC), also referred to as extensor digitorum (ED), highlighted in Figure 3. The tendon forces of the EDC during a grasp activity are similar to that of the FDS [4] and are therefore relevant when determining the effects of a grasp assist device.

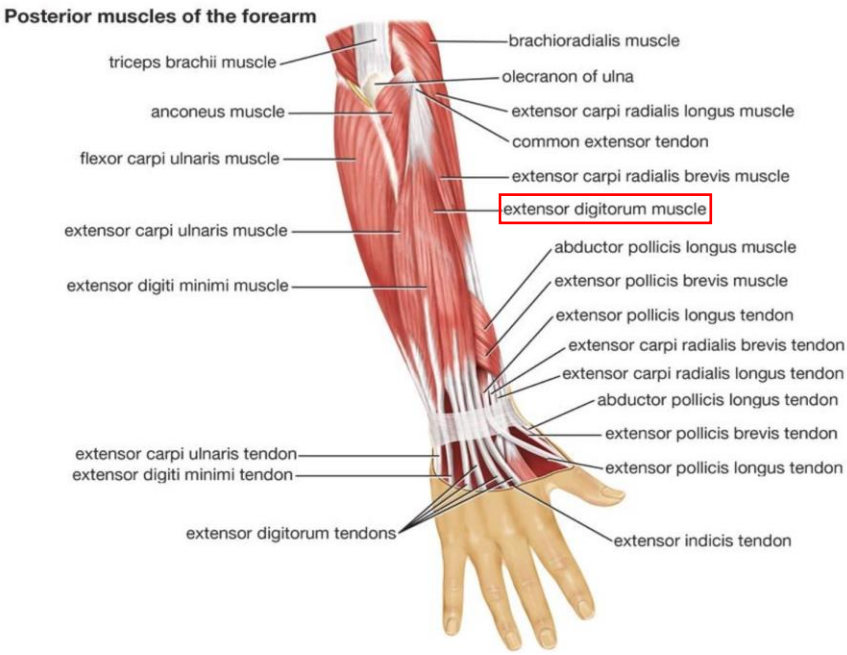

Figure 3 Posterior superficial layer of the forearm [9]

Electromyography (EMG) is a technique in which differential electrical potential within a muscle is passively measured using a pair of electrodes. The signal is on the order of microvolts and must be amplified and processed to obtain meaningful results. Electrodes can either be placed intramuscular (needle) or on the surface of the skin. The former yields a more precise, lower signal, where the latter generates an averaged, higher signal. Surface EMG (sEMG) was used in this research, as it is less invasive and many of the muscles that support and articulate the hand lay superficially. The muscles selected for evaluation in this research, noted above, were the FDS, FCR, FCU, and EDC. Previous studies measured similar muscles to quantify grip force. Bano et al. studied the effect of grip force for a torqueing task and measured muscle activity in the FCR, FCU, FDS, extensor carpi radialis (ECR) and extensor carpi ulnaris (ECU) [10]. Hoozemans and van Dieën predicted handgrip forces using sEMG of the ECR longus, ECR brevis, ED, ECU, FDS, and FCR [11], while Kadowaki et al. used sEMG to measure the FDS, FCR, FCU, and ECU to control a soft power-assist glove [12].

1.3 Cumulative Trauma Disorders

Upper extremity cumulative trauma disorders (CTD) are a major contributor to lost work, specifically in forceful, repetitive, industrial environments [13]. These injuries can take many forms, including carpal tunnel syndrome (CTS), tenosynovitis, stenosing tenosynovitis (trigger finger), lateral epicondylitis (tennis elbow), de Quervain's tenosynovitis (wrist tendonitis), among others, all of which affect an individual's ability to perform common activities without varying degrees of discomfort and physical limitations. Generally, tenosynovitis is caused by friction between the tendons of the wrist and the tendon sheaths, resulting in inflammation [14], where tendonitis is inflammation of the tendon itself as a result of accumulated strain during loading [15], and CTS occurs when the median nerve that passes through the wrist is squeezed or compressed [16]. CTS and tendonitis are the most common reported CTD [2][17][18]. They can cause limited range of motion, pain, numbness of the hand (often exacerbated nocturnally) [19], and were the two CTDs focused on in this research.

In addition to affecting an individual's health and well-being, CTDs are expensive. Yassi et al. identified 382 upper limb CTD claims in one year in Manitoba, costing a mean of $5569 (CND) per claim and requiring 71.4 days lost – both significantly more than non-CTD claims ($p < 0.0001$)[17]. Silverstein et al. evaluated claims between 1987 and 1995 in Washington State and found a mean cost of $6,977 (USD) for all hand/wrist claims, requiring 209 days lost. Claims citing CTS were significantly more expensive, with a mean of $12,794 (USD) per claim, and 228 days lost [18]. The financial cost of CTS alone based on the 2016 manufacturing industry workforce and an incidence rate of 27.3 per 10,000 [18] can be estimated at $824k (CND) in Canada, and $439M (USD) in the USA, annually. These numbers do not include lost productivity, training for replacements, administrative costs, not to mention unreported CTS cases and all other forms of CTD.

Risk factors associated with CTD are often split into two categories: occupational and non-occupational. Both are important and have been thoroughly evaluated since the 1980's, and while significant trends are consistently present, the underlying mechanisms remain largely unknown. Regardless, knowing the risk factors based on historical evidence can be used to mitigate risks for an individual or population. Non-occupational factors associated with CTDs (specifically CTS) including gender [20], age [21], body mass index (BMI) [21], and chronic diseases such as rheumatoid arthritis and gout [19]. Of these, age and BMI have the highest risk factors. Werner et al. found that in an automotive, industrial, and clerical cohort, workers over 40 years of age have a 76% increased risk of upper extremity tendonitis compared to those under 40 [21]. The same study indicated that obese workers ($BMI > 30$) are 93% more likely to be diagnosed with CTS [21]. Both of these non-occupational factors are important given trends in the workforce. The proportion of Canadian individuals aged 55 years and above reached 36% in 2016 and is projected to reach 40% by 2026 [22]. In the USA, approximately 23% of the workforce is aged 55 years or over and is increasing at a similar rate [23]. Obesity rates in the Canadian workforce were 22% in 2004, and slightly higher in the American workforce at 29% in 1999/2000 [24]. While relevant to risk of

developing a CTD and important for the general population, these factors are non-occupational and not considered from this point on.

Occupational risk factors include vibration, hand/wrist position, repetitiveness, and forcefulness [25][26]. Vibration is most often transmitted through the handle of a tool to the user's hand. Palmer et al. systematically reviewed 38 reports and found reasonable evidence that using hand-held tools that vibrate increases the risk of CTS by more than a factor of two, although these tended to be intense vibrations from tools such as rock drills and chainsaws [27]. It is therefore reasonable to assume that vibration is a less important factor compared to position, repetitiveness, and forcefulness, as tools such as wrenches, knives, and pistol grip DC drills are commonplace tools in an industrial environment with low/no vibration.

Hand/wrist position of the wrist – flexion or extension, radial or ulnar deviation, illustrated in Figure 4 – is another risk factor. The motion acts to compress the carpal tunnel (CT) by increasing the applied force, as well as increases tendon force. Different styles of grasp (illustrated in Figure 5) can also affect the CT pressure; however, the cylindrical power grasp is focused on as it is applied during a pistol grip DC tool activity. Armstrong and Chaffin found the resultant reaction force on the tendon (F_R) from the tendon tension (F_t) analogous to the force transmitted from a belt to a pulley, as $F_R = 2F_t \sin\left(\frac{\theta}{2}\right)$, where θ is the wrist angle degrees from straight Figure 6 [28]. There is zero reaction force when the wrist is neutral, 76% of the tendon force when the angle is 45°, and 100% of tendon force when the angle is 60°. Research by McGorry et al. showed that carpal tunnel pressure increased specifically during a power grasp in extension among healthy individuals, but did not increase during flexion [29]. This contradicts the work by Bakker, in which a flexed wrist significantly increased the median nerve pressure in five cadaveric samples with no history of upper extremity disorders [4]. Regardless, it is apparent that wrist position is an influential factor of CTD to some degree.

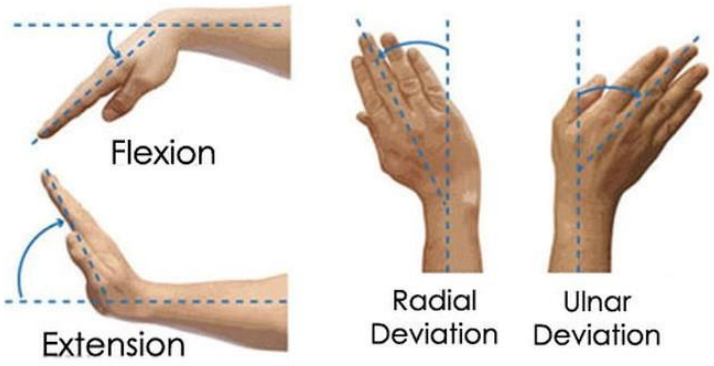

Figure 4 Hand wrist flexion, extension, and deviation

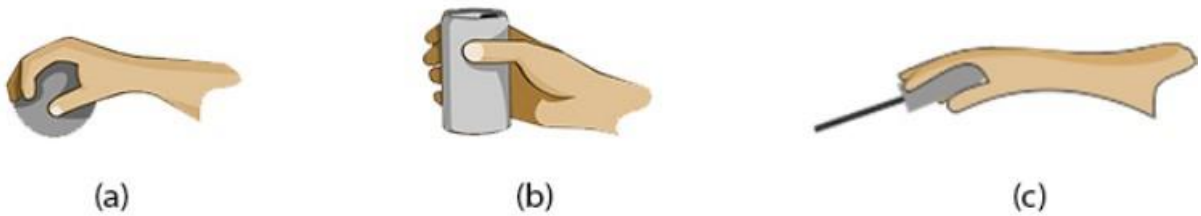

Figure 5 Hand grasp patterns a) spherical, b) cylindrical (power), c) parallel extension (palmer) [30]

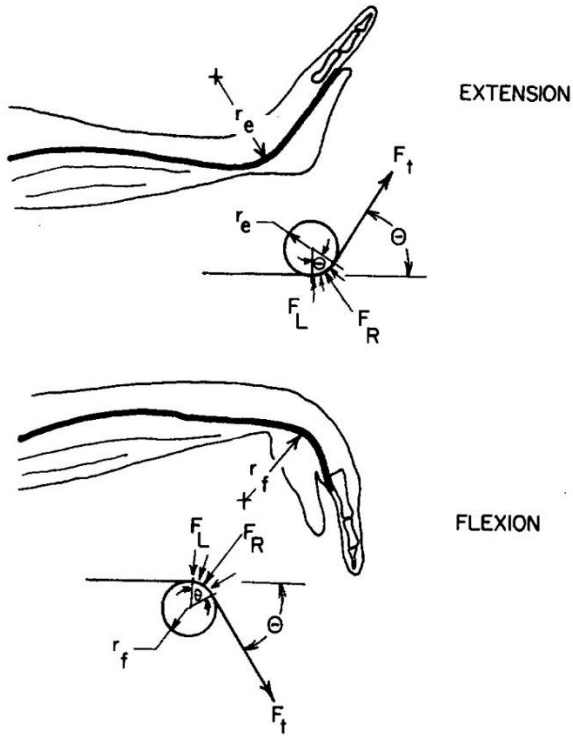

Figure 6 Wrist extension and flexion pulley comparison [28]

Repetitive and forceful tasks are commonplace in an industrial environment and are occupational risk factors. In the modern production line, workers typically perform one task dozens to hundreds of times per day. Highly repetitive tasks have been shown to increase the risk factor of CTS [27] by a factor of 5.5 times irrespective of force when compared to low repetition tasks [19]. These tasks are defined by a cycle time less than 30 seconds, or when the same kind of cycle was performed more than 50% of the cycle time. Forceful tasks were found to increase the risk factor of CTS by 2.9 times irrespective of repetition when compared to the low force tasks [19]. High force tasks were defined as requiring 142±61N, low force threshold was 31±16N (soft converted from kg_f) [19]. Regarding tendonitis, Armstrong determined the risk factor to be 3.3 times greater for jobs requiring high repetition but low force, and 6.1 times greater for jobs requiring high force but low repetition [2]. Compounded effects of high repetition and force are far more dramatic and can increase the risk of CTS by a factor of 15 times [19] and the risk of tendonitis by a factor of 29.4 times [2] when compared to low repetition and force. The force risk factor was the focus of this research, given the relative ease of measuring and mitigating it without affecting task repetition and potentially activity output.

Quantifying the effects of varying grip force on a pistol grip tool can be done in numerous ways. Typically, either a split tool handle with a strain gauge sandwiched in between (Figure 7), or pressure mapping techniques are applied (Figure 8). Seo and Armstrong compared these techniques and determined that mean normal force on a cylinder is 2.3 times greater than with a split handle [31]. This is likely because the normal force is a sum of all normal forces around the cylinder, where the load cell in the split handle only measures force normal to the sensor; however, neither method captures shear force, which may be relevant in future studies as friction between the hand and tool could act to resist torque. Nicholas et al. applied pressure mapping to compare push, pull, and grasping activities and determined that the third and fourth phalange were found to exert the highest force during grasping [32]. Where split cylinder requires a specialized tool, flexible pressure sensors can be cut to fit and applied directly to a tool. Research with the pressure mapping method has been predominantly used on cylinders to characterize the effects of diameter

on grip force with anthropometric hand variations. The need for *in situ* testing combined with the gap in literature made it an ideal choice for this research.

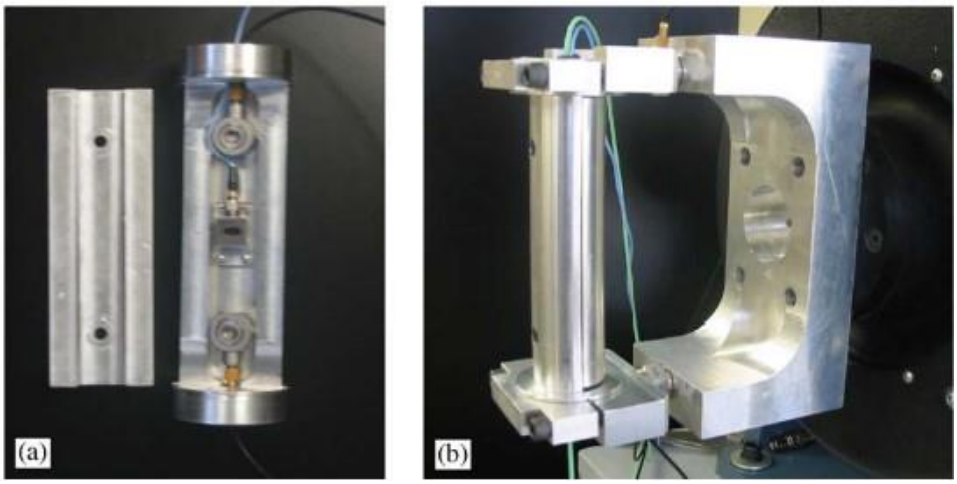

Figure 7 Example of a split tool handle a) open, b) assembled [33]

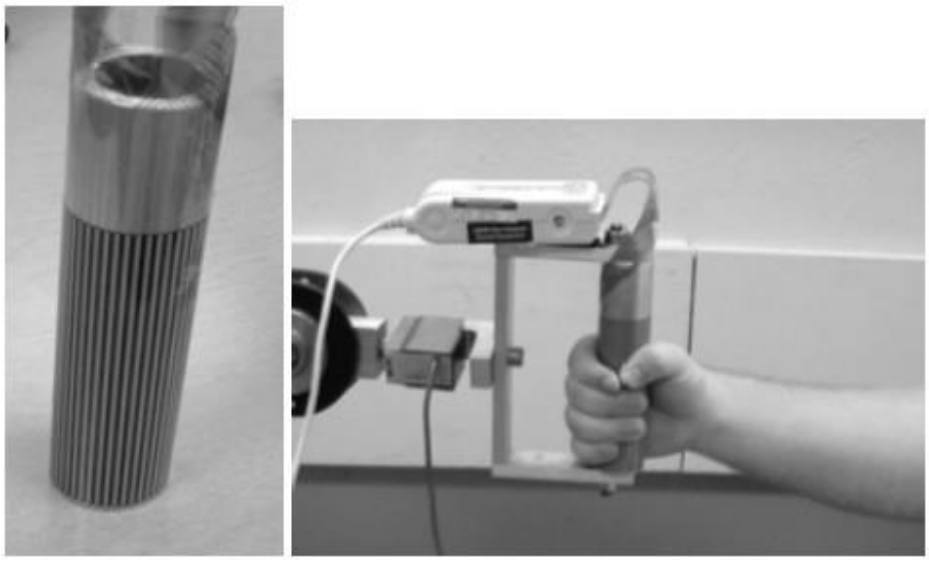

Figure 8 Example of a pressure map instrumented handle [32]

Quantifying the effects of varying muscle activity can also be done in numerous ways. The simple percent difference method is viable, as it provides a discrete mathematical comparison between trials; however, what those values translate into (i.e. muscle/tendon force) would be unknown. Alternatively, in 1995 Moore and Garg proposed a strain index (SI) by which to evaluate activities based on categorical multipliers of intensity, frequency, exertion duration, posture, speed, and the activity duration per day [34]. In 2017, Garg

et al. modified the 1995 strain index into the revised strain index (RSI), in which the formulation was continuous instead of categorical [34]. The results of some 13,944 simulated tasks aligned well with the 1995 SI, where the threshold of safe/hazardous for an activity was determined to be RSI=10.0. The risk factors described in detail above are all incorporated into the RSI. Force of exertion is defined as the percent of maximum voluntary contraction (%MVC) as measured with EMG, repetition is measured in efforts per minute, hand/wrist posture is the angle from anatomical neutral, duration of effort is measured in seconds, and duration of activity per day is measured in hours. Each multiplicative factor is based on these variables and is non-linear; therefore, the results may vary when compared with the percent difference method.

1.4 Hand Wrist Orthoses

1.4.1 Passive Devices

Passive hand wrist orthoses, such as braces and splints, are often prescribed to treat hand/wrist repetitive strain injuries such as CTS [35]. Devices such as those illustrated in Figure 9 limit extension and flexion of the wrist, both of which have been documented to increase the incidence rate of CTS by more than double [27]. Rempel et al. found that wearing a flexible wrist splint did reduce the wrist's range of motion but had no significant effect on carpal tunnel pressure [36]. This is an important finding, as individuals who suffer from CTS also have increased pressure in the carpal tunnel [37]. More recent studies comparing no orthosis, stiff orthosis, and a commercially available orthosis showed that the commercially available device had no significant effect on extensor and flexor muscle activation, but the stiff device significantly increased muscle activity [38]. Bulthaup et al. came to similar conclusions when comparing commercially available short and long orthoses to no orthosis. They found that flexion and extension muscle recruitment increased significantly for both lengths of device compared to no device, with no significance between the two [39]. Ferrigno et al. also measured a significant increase in flexion and extension muscle activation when using a custom-made splint during certain clerical tasks [40].

Figure 9 Example of passive orthoses a) custom-made, b) commercially available [40]

1.4.2 Dynamic Devices

Dynamic hand orthoses in a broad sense have a long history beginning in the late 1960's and continuing to the present, although the majority have been designed since 2010 [41]. The number of applications for dynamic orthoses are far fewer than the number of designs, focussing primarily on rehabilitation, post-stroke therapy, and general assistance. Rehabilitation and therapy devices are typically clinical tools that serve a specific purpose, such as tendon therapy [42] or kinematic analysis [43]. These devices yield accurate position measurements required for the purpose of controlling finger position but are cumbersome and typically restricted to clinical use. Alternatively, general assistance othoses can be used at home and throughout daily life, providing hand/wrist support and sufficiently augmenting the user's strength to perform daily living activities. Bos et al. compiled a thorough, if not exhaustive, review of dynamic orthoses in 2016 and classified them based on signal (controller, command, feedback), energy (storage, actuation), and mechanical (transmission, mechanism) [41]. The majority of dynamic assistive devices were portable, electromagnetically (i.e. motor) driven, transmitting force to the hand and fingers through Bowden cables or rigid linkages. This approach is apparent in designs such as the NASA/GM partnership RoboGlove [44], the SEM Glove [45], and the Exo-Glove [46]. The designs mimic human anatomy by affixing synthetic tendons to a glove actuating them elsewhere, be it the forearm, upper arm, or hip. This design has potential

to exert high forces but is also expensive and can be slower to react (actuation time > 1 sec) than other methods. The second most prominent energy source is pneumatic, and when combined with rigid linkages yields designs such as FESTO's ExoHand [47]. It is a strong design with high positional accuracy due to the rigid linkages but is encumbering, expensive, and is manufactured to fit the size of a specific hand.

The usability and acceptance of a device are related to the pressure distribution (comfort) and pressure magnitude (safety) [48]. 'Soft' robotics addresses both issues by evenly distributing pressure, and inherently generate lower magnitude forces than their rigid counterparts. Many recent designs focus on soft robotics, which typically exploit hyperelastic material properties combined with pneumatics to generate actuation. Typical soft robotic bending actuation is generated by limiting the strain along one surface and encouraging it in others. A hyperelastic chamber/body with a flexible, strain limiting lower layer such as fiberglass is an example of this style. The upper surface is free to expand and increase its length as the chamber inflates, but the lower surface is restricted by a constant length, yielding an underactuated, curling motion. Inlet pressure controls the degree of rotation and the corresponding contact force. This basic actuator design was applied to material handling grippers as early as 1967 (Figure 10), with the first application to the human hand in the early 70's, and the majority after 2010 [49].

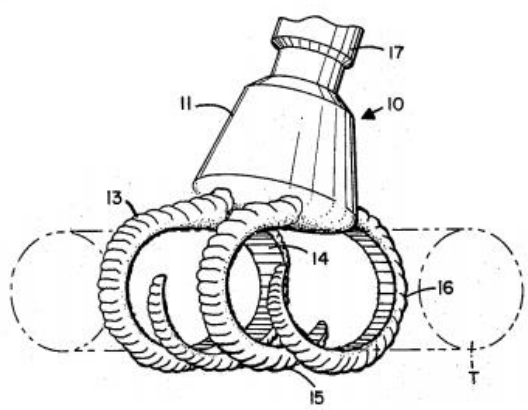

Figure 10 Soft pneumatic gripper for material handling circa 1967 [50]

Polygerinos et al. designed a dynamic orthosis in this manner, using fibers to reinforce (strain-limit) the uniform cross section at strategic locations to replicate joint/bending motion (Figure 11) [51]. Yap et al.

took a different approach in which the top surface of the actuator has more surface area (sinusoidal 'bellows') than the bottom (straight) (Figure 12) [52]. The actuator expands when inflated, lengthening the top surface while the bottom surface is limited by its original length. This change in surface length is what curls the actuator, generating motion and contact force. The benefits of both soft robotic designs include: underactuated, durable, inexpensive, relatively powerful, and quick to respond (actuation time << 1 sec). While inexpensive in terms of materials, Polygerinos' design is labor intensive, requiring multi-step molding and exact placement of the fiber reinforcement (Figure 13) [53]. Yap's design is inexpensive in terms of both materials and labour, as it can be rapid prototyped from a single material using the fused deposition modeling (FDM) method of 3D printing. However, actuators of this design can take more than 24 hours to print, making them expensive in terms of manufacturing time.

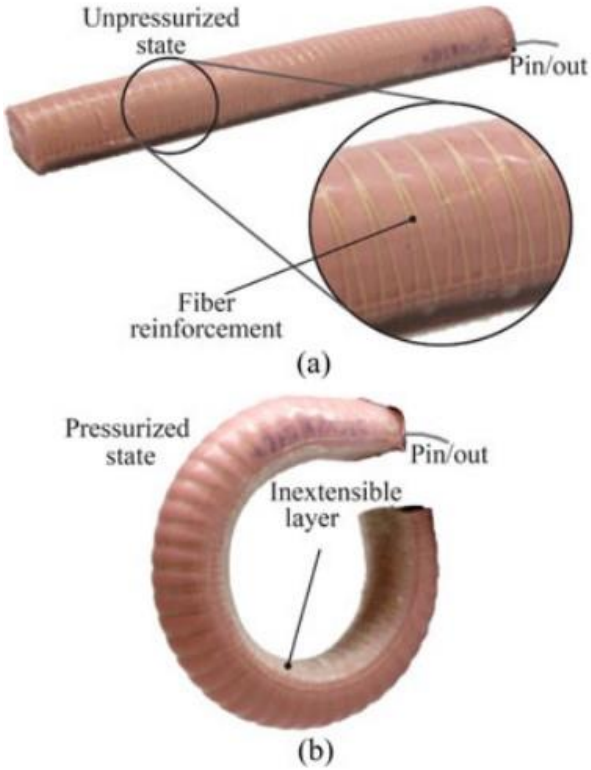

Figure 11 Example of a fiber reinforced soft actuator a) unpressurized, b) pressurized [53]

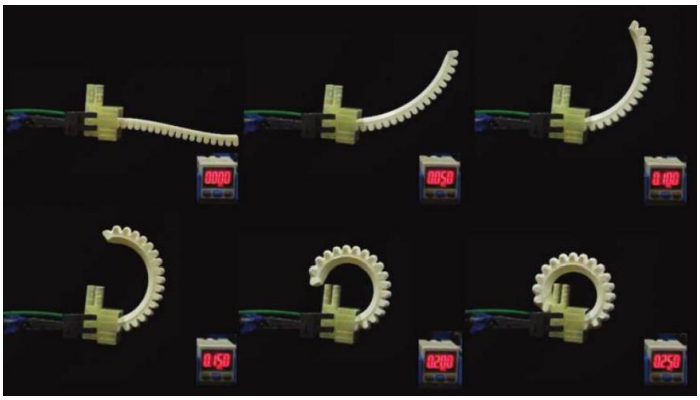

Figure 12 Bellows-style soft actuator inflated to six pressures, 0 kPa to 250 kPa

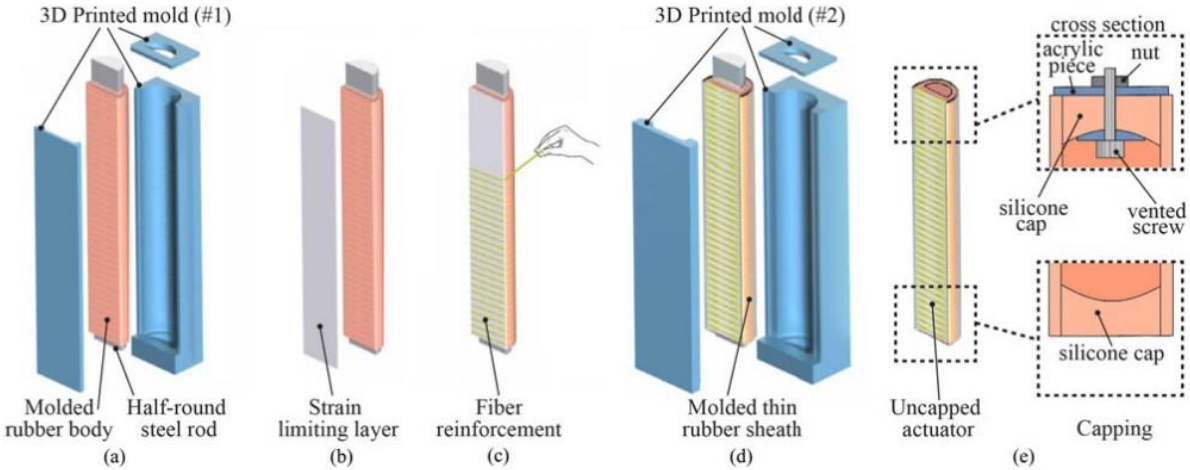

Figure 13 Fiber reinforced soft actuator manufacturing process [53]

The research presented in this thesis opted for a design similar to Yap's 3D printed bellow style of pneumatic actuator. Studies by Yap et al. have verified the performance of this actuator design; however, they do not quantify the effects of a grasp assist device utilizing these actuators on muscle activity and grip force in an able-bodied population [54]. The ability to inexpensively (~$2CDN per actuator, material cost) rapid prototype designs in under 24 hours outweighed the corresponding cumbersome design and tethered energy source. Low cost can also translate into customizable (multiple sizes based on variance in hand size), and hyperelastic materials are durable which is appropriate given the targeted industrial environment. Compressed air is also readily available in almost all industrial environments, and DC tools are commonly tethered through power and control cables. Future iterations could optimize material selection and minimize the profile to reduce the awkwardness. Select dynamic orthoses are presented in Table 1.

Table 1 Examples of dynamic hand/wrist orthoses

Device	Actuation	Application	Advantages	Disadvantages	Image	Reference
FESTO	Pneumatic & rigid linkage	Improve strength & stamina, stroke rehabilitation	Strength, position accuracy	Bulky, expensive, designed to specific hand geometry	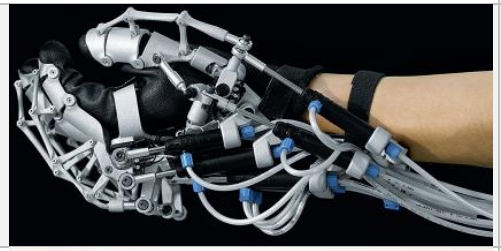	"Festo. ExoHand," [Online]. https://www.festo.com/group/en/cms/10233.htm.
Robo Glove	Linear actuators & Bowden cable	Improve strength & stamina, multipurpose	Strength, portable	Expensive, actuation time		M.A. Diftler et al., “RoboGlove – A Robonaut Derived Multipurpose Assistive Device”, 2014
SEM Glove	Linear actuators & Bowden cable	Assistive living, weak grasp force, neurological rehabilitation	Performance feedback, intuitive control, portable	Expensive, additional equip. required (power unit), no index/little finger assist		M. Nilsson, et al., "The Soft Extra Muscle System for Improving the Grasping Capability in Neurological Rehabilitation", 2012

Exo-Glove	Motor & Bowden cable	Physical disabilities, stroke & C5/C6 spinal cord injuries	Portable, inexpensive	Actuation time, trigger mechanism, pinch grip only	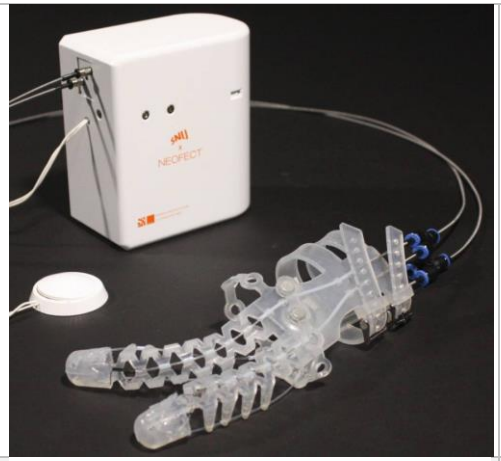	B. B. Kang, et al., “Force Transmission in Joint-less Tendon Driven Wearable Robotic Hand Brian”, 2012
Polygerinos	Pneumatic, fiber reinforced	Assisted living, stroke patients	Portable, inexpensive	Relatively weak, cumbersome	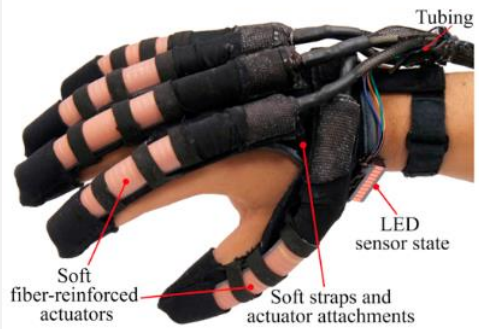	P. Polygerinos et al., “Soft robotic glove for combined assistance and at-home rehabilitation”, 2015
Yap	Pneumatic, bellows	Assisted living, stroke patients	3D Printable, inexpensive	Tethered, cumbersome		H. Yap et al., “High-Force Soft Printable Pneumatics for Soft Robotic Applications”, 2016

Data collected by Bakker from an unpublished 2017 pilot study at HCM involving a pistol grip DC tool revealed a large variation in grip force (n=8). The mean (± standard deviation), minimum, and maximum grip force was 79±15N, 45N, and 96N respectively. This was not unexpected given the anthropometric variation among people, and previous studies have shown similar variations. Nicolay and Walker measured a mean maximum grip force based on 10 repetitions of 233N (98), and a range from 91N to 491N (n=51, values soft converted from kg_f to N) [55]. While variation was expected based on physical differences, it was unexpected based on cohort. Nicolay and Walker collected data on a cohort of 51 college students with unknown power tool experience, where Bakker's cohort was experienced with the DC tool used in the experiment. The implications of this difference, while simple, are important. If one experienced individual can successfully complete a task using some minimum force, why would anyone (regardless of physical differences) require significantly more? One may argue that the term 'experienced' is subjective, and that time on a job does not definitively correlate to performance; however, Silverstein et al. measured a negative correlation between CTS incidence rate and years on the job, suggesting that experience *is* significant [19]. Gerr et al. found an increased incidence of skeletal disorder of the hand/arm among newly hired computer users, with de Quervain's tendonitis as the most common [56]. Synthesizing this information, it was hypothesized that within a capable and healthy cohort, alerting an individual to the amount of force applied during a task could significantly reduce muscle activity, thereby reducing tendon strain and CTD risk factor. Such a system could provide benefit at any level of experience, illustrating the required amount of force to a new hire or experienced individual alike.

1.5 Hypotheses

The objective of this research was to determine the effects of two devices on muscle activation and grip force – two factors associated with upper extremity cumulative trauma disorders. The first was a grasp assist device which aimed to augment the users grip strength, and the second was a grip training device which visually alerts the user as to how much force they are applying to a tool. Two hypotheses directly followed from this:

1. Primary Hypothesis: a pneumatic grasp assist device can augment the user's grip force thereby reducing the muscle activity required by the user compared to not using the device, when performing a common industrial activity using a DC tool.
2. Secondary Hypothesis: providing the worker (device user) with visual feedback of the amount of force applied to the DC tool used in the activity can reduce the grip force and muscle activation compared to typical tool usage with no visual feedback.

2 Methodology

2.1 Grasp Assist Design

For a pneumatic grasp assist device to be practical, it must be comfortable, unencumbering, and provide enough assistive force for a given activity. It should consist of enough individual actuators to provide the dexterity necessary for the activity – typically one per digit (finger). Existing pneumatic designs are too large and typically generate insufficient force to be practical for an industrial application [57][58]. The finite element method (FEM) was applied to the design process in order to optimize the actuator geometry prior to manufacturing and testing. The objective was to compare performance between designs – not to necessarily accurately simulate the response. The FEM represents a model or object as a mesh of elements with specific material characteristics. Boundary conditions such as loads, symmetry, and supports are applied to the model, and a response is simulated. Abaqus CAE 2018 [59] is a comprehensive finite element software suite, complete with modeler, mesher, solver, and post-processor and was used in this research.

2.1.1 Finite Element Method

The objective of applying the finite element method (FEM) was to optimize the profile of the bellows-style actuator so that the force output and degree of bending was maximized at a given input pressure, while the width and height were minimized.

Initial Geometry

Many soft robotics designs have been analyzed using FEM, but pneumatic networks (pneu-net, Figure 14), fiber-reinforced (Figure 15), and bellows style (Figure 16) are the three most common geometries.

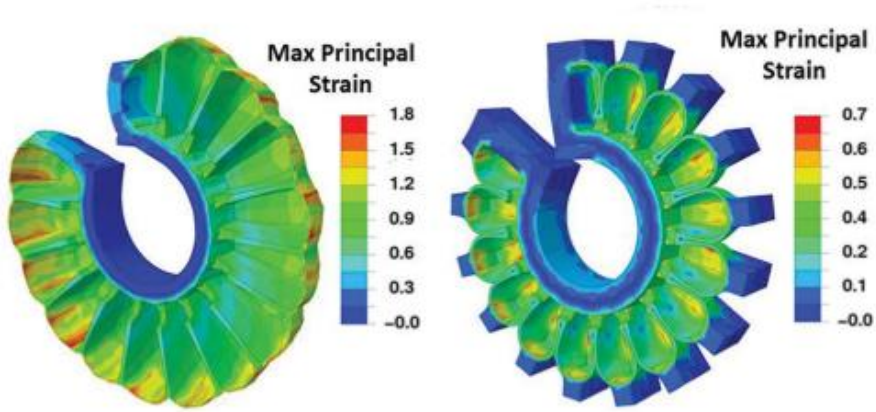

Figure 14 Finite element model of a pneumatic network (pneu-net) soft actuator [57]

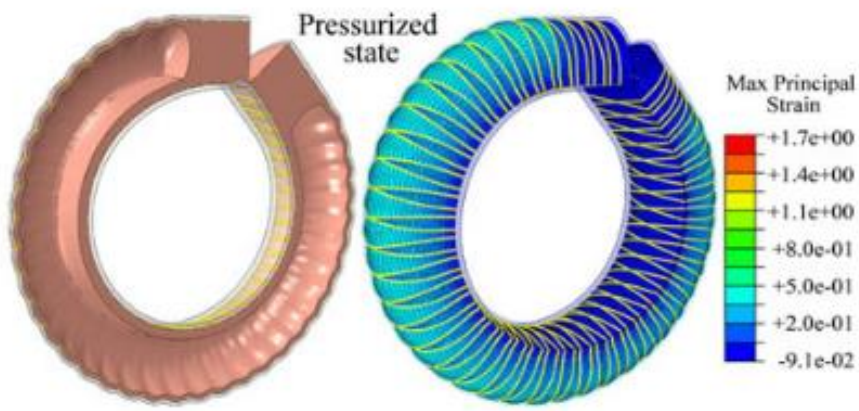

Figure 15 Finite element model of a fiber reinforced soft actuator [53]

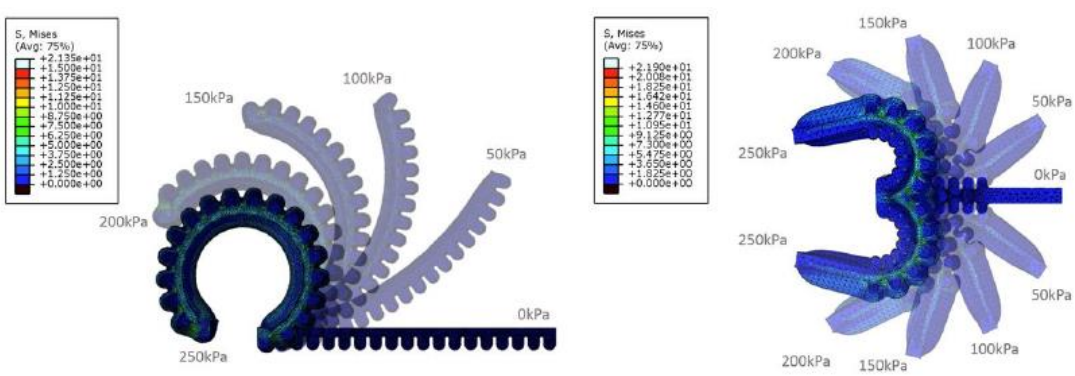

Figure 16 Finite element model of a bellows-style soft actuator [52]

The force exerted by the tip of an actuator is one performance criteria used for design evaluation and comparison. The experimental setup involves constraining the top of the actuator (to prevent bending/curling), fixing the proximal end (from which the actuator is inflated), allowing the distal surface (tip) to engage a load cell, and measuring the resulting force. Typical tip force output ranges between 5-20N at 45kPa for high-performing pneu-net actuators [60], 5-8N at 200kPa for fiber-reinforced [53], and ~40N at 200kPa for bellows actuators [52], although these values vary depending on geometry and the actuator/load cell contact area.

The manufacturing process for pneu-nets and fiber-reinforced actuators is time and labor intensive, as they are primarily molded from a degassed silicon rubber, while bellows actuators described by Yap can be 3D printed. The bellows-style actuator was selected for the initial geometry based on its superior force output, ease of manufacturing, and ability to generate complex geometries. The model illustrated in Figure 17 has dimensions 150x25x11mm (LxWxH) and wall thickness of 1.2mm [52].

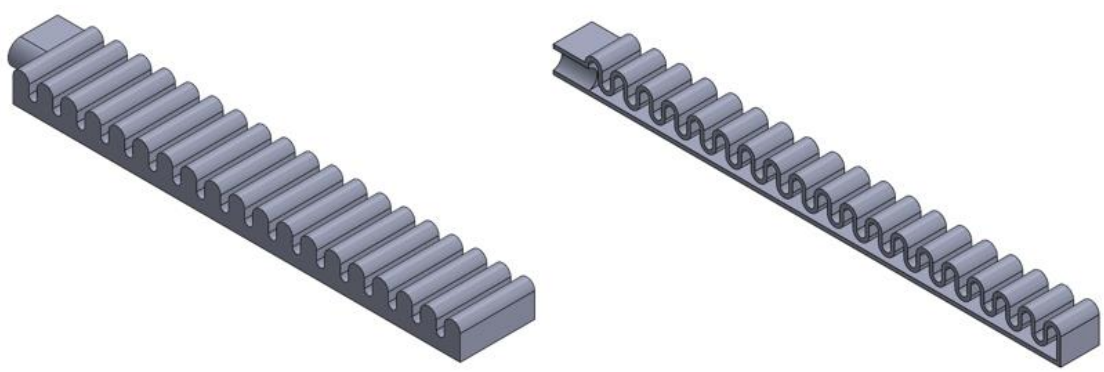

Figure 17 Isometric view of initial bellows-style actuator design (left) & section view (right)

Material

Hyperelastic materials, such as rubber, require relatively small forces to generate large deformation when compared to traditional elastic-plastic materials, such as steel, and can rapidly return to their original configuration without permanent deformation [61]. These characteristics make hyperelastic materials ideal for use in soft pneumatic actuators.

The stress-strain relationship is highly non-linear, and is therefore exceedingly important to accurately characterize the specific material prior to performing simulations. Figure 18 illustrates the typical stress-strain curve for a hyperelastic material and for a typical elastic-plastic material (section 10.6.1 and section 10.2 respectively) [62]. The entire hyperelastic stress-strain curve illustrated is within the elastic region (i.e. deformation is recovered), where that is only true for the linear region in the elastic-plastic curve.

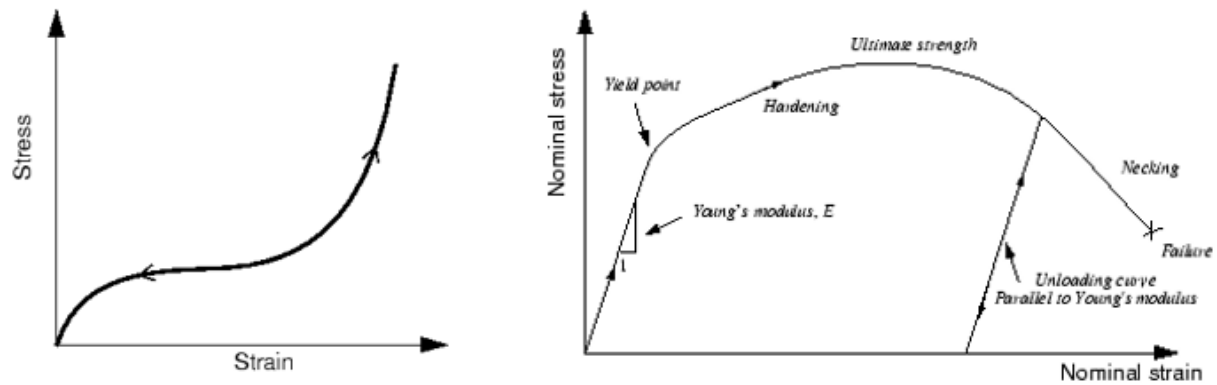

Figure 18 Typical stress-strain curve for hyperelastic material (left) and elastic-plastic material (right)

Hyperelastic response can be visualized when inflating a balloon. It initially requires high pressure to inflate (high modulus of elasticity), followed by a relatively low level of pressure, until the balloon approaches some maximum size (strain) prior to popping where the modulus of elasticity increases more dramatically.

Instead of defining a Young's modulus and Poisson's ratio, Abaqus uses a strain energy potential function, U [62] (section 10.6.3). There are multiple models readily available to characterize a hyperelastic material including Mooney-Rivlin, Neo-Hookean, Yeoh, Arruda-Boyce, and Ogden; however, the Ogden model is best able to capture the stiffening as well as the large strain deformation [61] and was applied to the model. The Ogden function can be expressed in the following form where $\lambda_1, \lambda_2, \lambda_3$ are the deviatoric principal stretches [62]:

$$U = \sum_{i=1}^{N} \frac{2\mu_i}{\alpha_i^2} \left({\lambda_1}^{-\alpha_i} + {\lambda_2}^{-\alpha_i} + {\lambda_3}^{-\alpha_i} - 3 \right) + \sum_{i=1}^{N} \frac{1}{D_i} \left(J^{el} - 1 \right)^{2i}$$

Equation 1 Ogden strain energy function with N=3

An off-the-shelf, relatively low cost (85 USD/kg [2.11 fennerdrives.com]) material with desirable strength and elasticity characteristics was used for all actuator designs. NinjaFlex® by NinjaTek [63] is a flexible, polyurethane filament 3D printing filament with excellent strength and elasticity (Table 2). Yap experimentally tested the material according to ISO37 and determined Ogden N=3 to best represent the results (Table 3) [52].

Table 2 Summary of relevant Ninjaflex® material properties

Property	**Test Method**	**Metric**
Specific Gravity	ASTM D792	1.19 g/cc
Tensile Strength, Yield	ASTM D638	4 MPa
Tensile Strength, Ultimate	ASTM D638	26 MPa
Tensile Modulus	ASTM D638	12 MPa
Elongation at Yield	ASTM D638	65%
Elongation at Break	ASTM D638	660%

Table 3 Experimentally obtained Ogden strain energy function coefficients for N=3

μ_1	α_1	μ_2	α_2	μ_3	α_3	D_1	D_2	D_3
-30.921	0.508	10.342	1.375	26.791	-0.482	0	0	0

Solving Method

Abaqus provides different solving methods depending on the simulation – static and dynamic. Given that the problem of comparing designs can be performed in an equilibrium state (i.e. fully inflated at a given pressure) a dynamic analysis was not required. A static analysis is appropriate for comparing actuator designs and can be solved by either the *static general* or *dynamic implicit* solver. The latter was used for all simulations – specifically the *quasi-static dynamic implicit* solver – as it efficiently solves problems with contact, complex geometry, and non-linearity [62] (section 6.3.2). Four identical steps were created, one for each pressure as defined in the boundary conditions section below.

Boundary Conditions

Two unique configurations were simulated with similar boundary conditions. The first simulated free rotation in order to determine the degree to which the actuator would curl. The second simulated constrained

tip force to determine the force output of the actuator. Simulation time was optimized by modeling half of an actuator with Z-symmetry boundary condition [U3, UR1, UR2] = 0.

Free Rotation

A fixed (encastre) boundary condition of [U1, U2, U3, UR1, UR2, UR3] = 0 was applied to the width of the bottom surface, 20mm proximally, illustrated in Figure 19. This minimized simulation time and closely simulated the actuator clamped during experimental verification. A pressure load was applied to the entire internal surface and modified at each step as per Table 4.

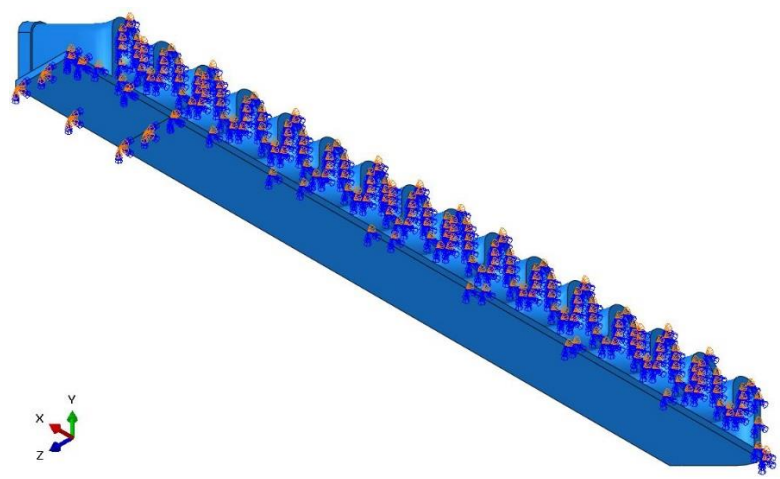

Figure 19 Bottom isometric view of boundary conditions for free rotation simulation

Table 4 Simulated pressure load applied per step

Step	P1	P2	P3	P4
Pressure (MPa)	0.138	0.172	0.207	0.241

Constrained Tip Force

The same fixed and Z-symmetry boundary conditions were applied as in the case of free rotation; however, two additional components were added – a contact surface to represent a load cell, and a constraining surface above the actuator to prevent rotation (Figure 20). The bottom surface of the load cell and the top surface of the constraint were also fixed. Self-contact was defined along the top surface of the actuator, surface-to-surface contact defined between the top surface of the actuator and the constraining component,

and surface-to-surface contact was defined between the bottom surface of the actuator and the load cell representation. A history output request was defined for the normal contact force between the load cell and bottom actuator surface contact pair. A frictionless interaction property was defined for all contact cases.

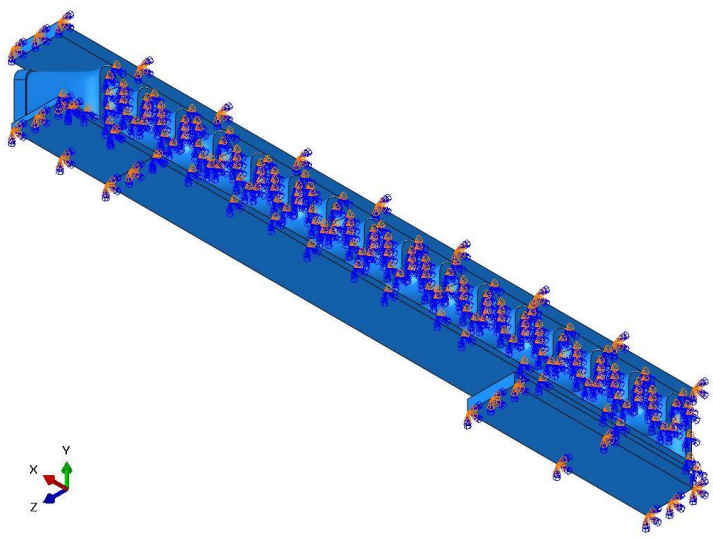

Figure 20 Bottom isometric view of boundary conditions for constrained tip force simulation

Element

Solid elements can model stress/displacement in complex, non-linear geometry where contact and large displacements are involved [62] (section 27.1.3). Although shell elements also model bending efficiently (particularly in-plane deformations), given the flexible nature of hyperelastic materials and the out-of-plane bending, shell elements were not used. Solid (continuum), hybrid, 3-dimensional, quadratic, tetrahedral elements (Figure 21) were selected for simulating the final design, as tetrahedral geometry was best able to capture the complex geometry. The hybrid formulation is required for incompressible and nearly incompressible ($0.475 < \nu \leq 0.500$) materials to prevent volumetric locking. This occurs when the volume of the element and integration points within it must remain constant, which over constrains – or locks – the element [64]. Hybrid elements treat pressure stress as "an independently interpolated basic solution variable, coupled to the displacement solution through the constitutive theory" [64]. Hybrid, first-order tetrahedra are still over constrained, hence second order tetrahedra are required. The C3D10H element was selected for simulating the final actuator design.

- C – Continuum
- 3D – 3 Dimensional
- 10 – Number of notes within the element, second order (quadratic)
- H – Hybrid type to capture the incompressible nature of the hyperelastic material

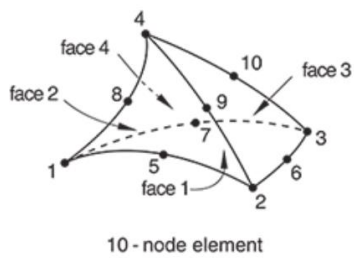

Figure 21 Ten-node, second order, tetrahedral element C3D10H [62] *(Section 28.1.4)*

Design Iterations

There are many variables in even the simplest bellows design as illustrated in Figure 22, including: length, width, height, wall thickness, diameter, ratio of diameters – all which impact performance to some degree. Given the grasp assist application, length and width were based on finger geometry, while the height was fixed at 11mm to minimize the profile and obtrusiveness.

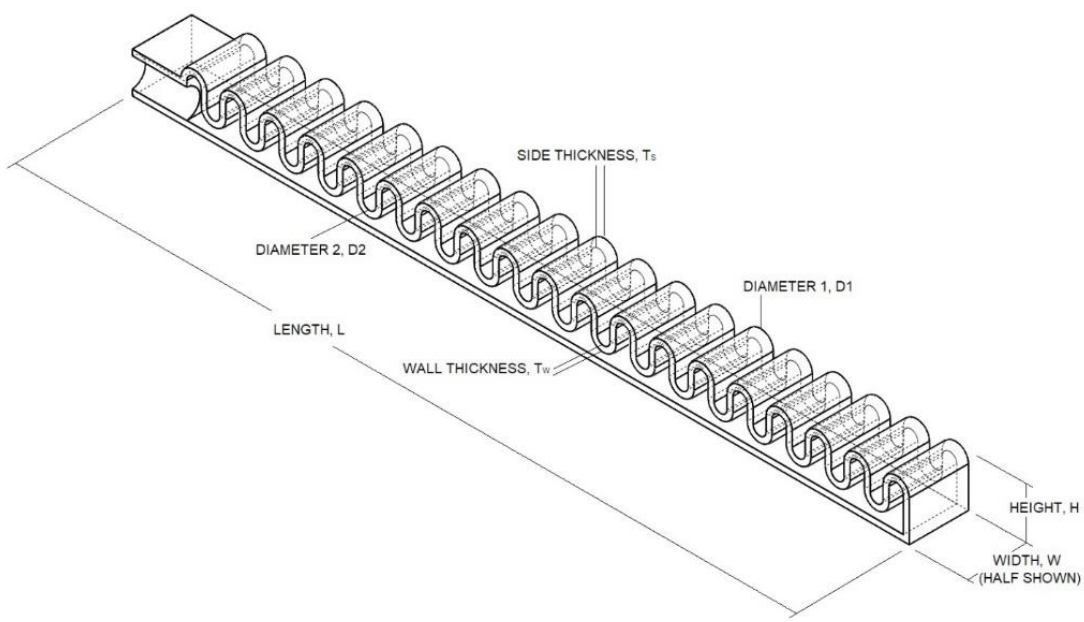

Figure 22 Isometric cross section view of bellows-style actuator with dimensional variables shown

Actuator performance was based on:

1. Bending ratio, R – defined as the radius of curvature divided by original length, as $R = \frac{r_c}{L_0}$, where performance is considered to increase as R decreases [52]. This was a performance characteristic adopted by Yap et al. which facilitated easy comparison. When applied to a grasp assist device, a lower R value will more effectively curl the fingers. The radius of curvature was calculated as the Menger curvature, Equation 2, which relates area of a triangle to the lengths of its sides as defined by three points. The boundary conditions applied are described above in 2.1.1.

$$r_c = \frac{|x-y||y-z||z-x|}{4A}$$

Equation 2 Radius of curvature based on three points: x, y, and z

2. Contact force, F – the force measured between the contact pair was defined by the load cell representation and the bottom actuator surface, described above in 2.1.1. Performance was considered to increase as F increases, as the actuator will provide more assistance to the grasping activity.

Wall Thickness

Durability and R both increase proportionally with wall thickness. Thicker walls increase stiffness and resistance to bending. Where increased durability is preferred, an increase in R is not; therefore, it was important to optimize the wall thickness. The 3D printer nozzle diameter of 0.4mm was also considered, as printing in multiples will optimize layer adhesion. A wall thickness of 1.6mm was compared to 1.2mm, and a side thickness of 1.5mm is compared to 1.2mm.

Diameter

Setting the height at 11mm and varying wall thickness between 1.2mm and 1.6mm, the bellows diameter could not vary much. Instead, the ratio of D1:D2 was compared for cases 2:1, 1:2, and 1:4 to measure the effect on performance.

Angle

During the iteration process, it was hypothesized that increasing the angle with respect to the centre symmetry plane would increase the actuators performance. Actuators with 0° and 45° bellows from plane XY (Figure 23 and Figure 24, respectively) were modeled and simulated to compare performance.

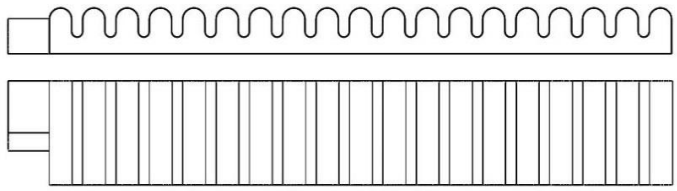

Figure 23 Profile and top view of initial bellows-style actuator with 0° angle from plane of symmetry

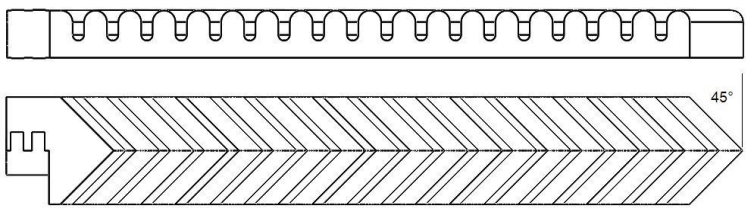

Figure 24 Profile and top view of bellows-style actuator with 45° angle from plane of symmetry

Design Summary

The performance results are summarized below in Table 5. Thinner walls and a D1:D2 ratio of 1:2 are typically preferable, as the lower resistance to bending translates to a lower bending ratio. A bellows angle of 45° further optimizes performance by minimizing R and maximizing F; however, the trade-off is increased stress as illustrated in Figure 25 and Figure 26.

Table 5 Simulated response to dimensional variable manipulation

D1:D2	Angle (°)	L (mm)	H (mm)	W (mm)	Tw (mm)	Ts (mm)	Pressure (kPa)	Force F (N)	Bending Ratio, R
1:2	0	150	11	30	1.6	1.5	100	18.0	0.597
1:4	0	150	11	30	1.6	1.5	100	25.5	0.618
2:1	0	150	11	30	1.2	1.2	100	31.3	0.291
1:2	0	150	11	25	1.2	1.2	138	17.1	0.236
1:2	45	150	11	25	1.2	1.2	138	42.7	0.174

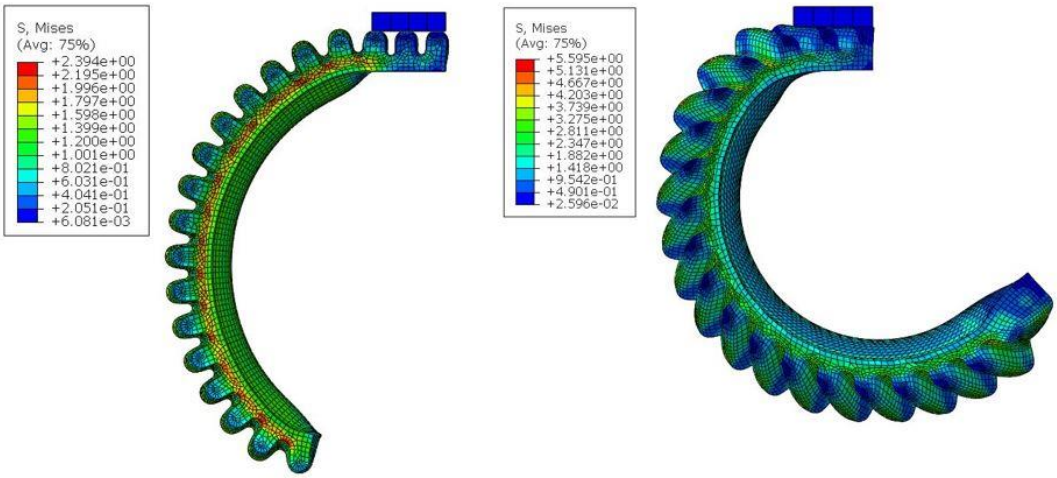

Figure 25 Profile view, free rotation simulation (100kPa) for 0° (left) and 45° design (right)

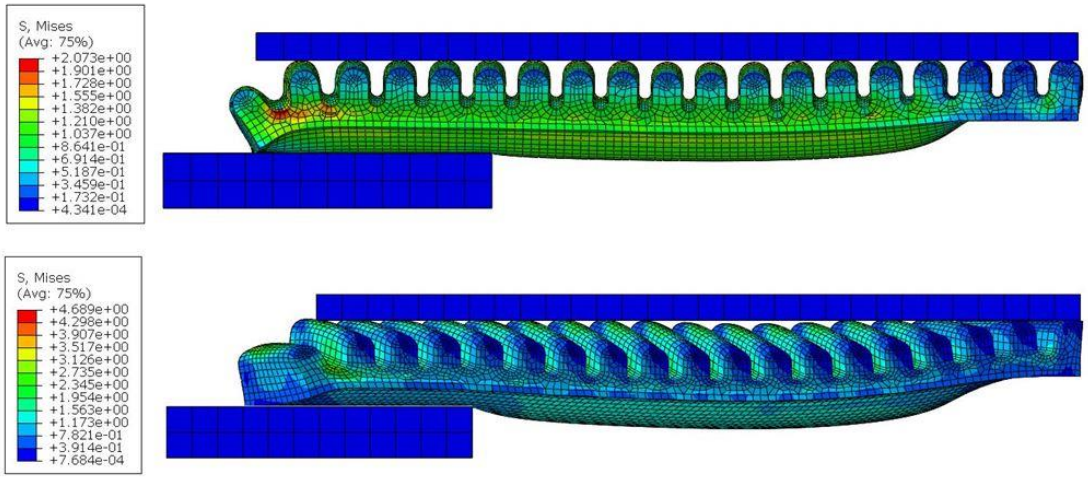

Figure 26 Profile view, constrained tip force simulation (100kPa) for 0° (top) and 45° design (bottom)

2.1.2 Final Design

The final design parameters are represented in Table 2Table 6, where the length and width vary with corresponding digit application and hand size. The stress concentrations associated with the high performing 45° bellows were mitigated by introducing a 5mm radius about the plane of symmetry, illustrated in Figure 27. Adjustable digit retention loops were incorporated into the final actuator design to facilitate quick fitment adjustments between participants.

Table 6 Final actuator design parameters per hand size and digit application

Hand Size	Digit Application	D1:D2	Bellows Angle (°)	L (mm)	H (mm)	W (mm)	Tw (mm)	Ts (mm)
Small, Medium	Middle	1:2	45, Rounded r=5mm	150	11	20	1.2	1.2
	Index, Ring	1:2	45, Rounded r=5mm	126	11	20	1.2	1.2
	Thumb, Little	1:2	45, Rounded r=5mm	102	11	20	1.2	1.2
Large, X-Large	Middle	1:2	45, Rounded r=5mm	150	11	25	1.2	1.2
	Index, Ring	1:2	45, Rounded r=5mm	126	11	25	1.2	1.2
	Thumb, Little	1:2	45, Rounded r=5mm	102	11	25	1.2	1.2

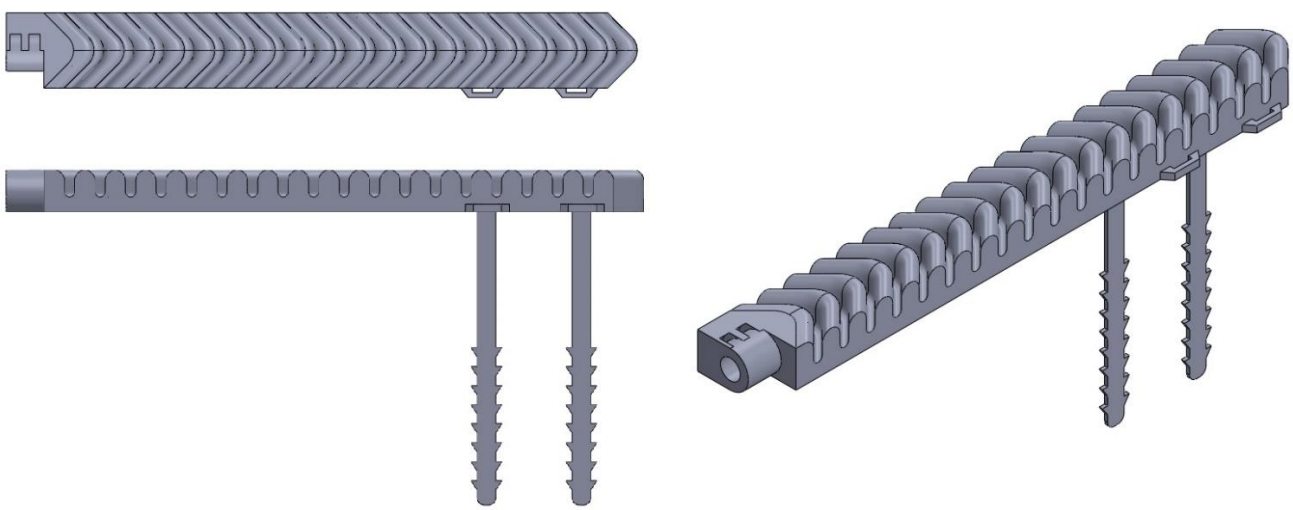

Figure 27 Final design optimized for 3D printing with flattened, adjustable digit retention loops in top view (upper left), front view (lower left) and isometric view (right)

2.1.2.1 Mesh Convergence

A mesh convergence study was performed by comparing the resultant stress and strain versus number of elements based on a global seed size. This study verified that the mesh was sufficiently refined (stress/strain plateaued as element size decreased) while considering the computational time. This study was performed for the free rotation scenario. Stress (von Mises, MPa) and strain (LE Max Principal) were used as the metrics for comparison. From the results illustrated in Table 7 and Figure 28, a global seed size of 1.2mm was selected for simulations with this model geometry.

Table 7 Mesh convergence study results for final actuator design based on free rotation simulation

Global Seed Size (mm)	Number of Elements	von Mises Stress (MPa)	LE Max Principal
4.8	46721	23.27	1.056
3.6	55905	33.61	0.8456
2.4	70286	25.94	0.8414
1.2	**77972**	**22.55**	**0.8412**
1.0	104911	21.17	0.8378

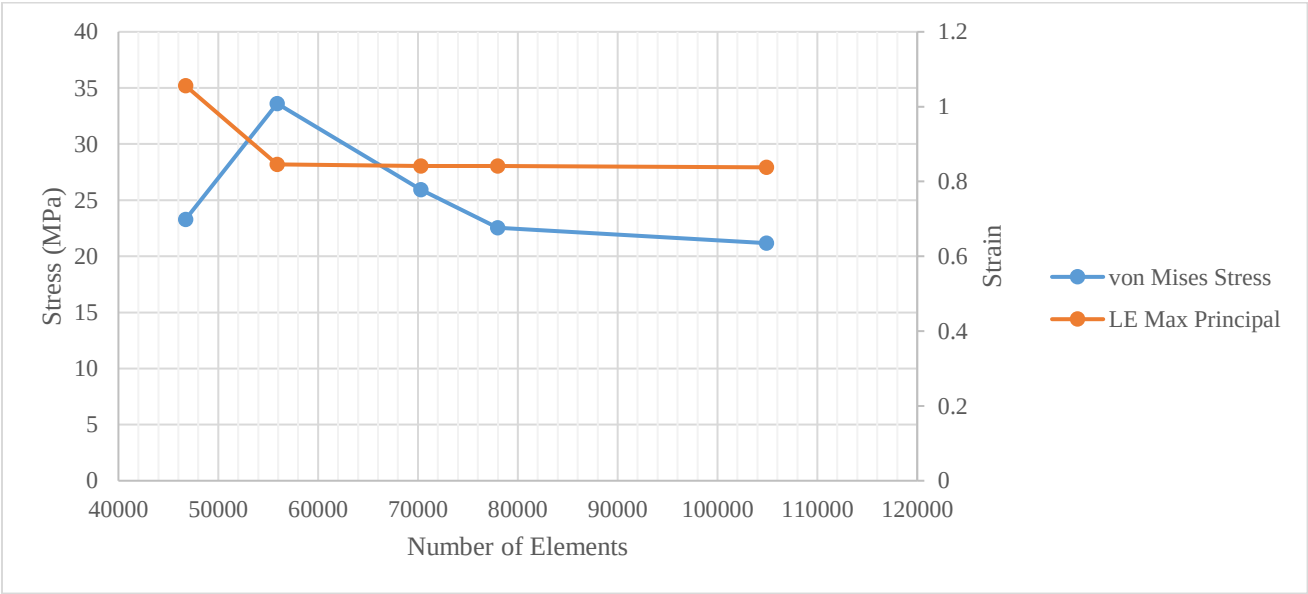

Figure 28 Mesh convergence results for final actuator design based on free rotation simulation

2.1.2.2 Experimental Verification

To verify the simulation results, an actuator of the final design (Table 6 small/medium, index/ring) was printed and tested experimentally. Experimental verification confirms the accuracy of the simulated model (element selection, material properties, boundary conditions), thereby providing confidence for simulated design iterations without needing to experimentally verify each one. The two performance measures experimentally verified were bending ratio and constrained tip force.

Bending Ratio

The actuator was constrained within a custom 3D printed apparatus 20mm proximally (Figure 29), inflated three times, to four pressures successively, and the corresponding radius of curvature values were calculated

from the digitized images from Equation 2 and averaged. The camera was mounted to a tripod to insure a constant field of view throughout the experiment. The experimental results are compared to the simulation output in Figure 30.

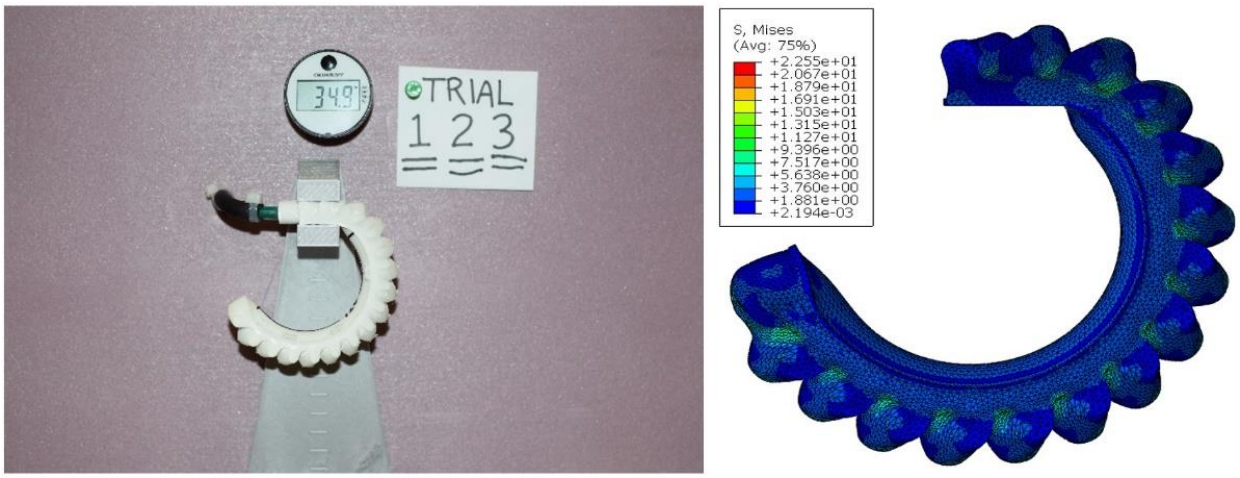

Figure 29 Free rotation at 241kPa (~35psi) experiment (left) and corresponding simulation (right)

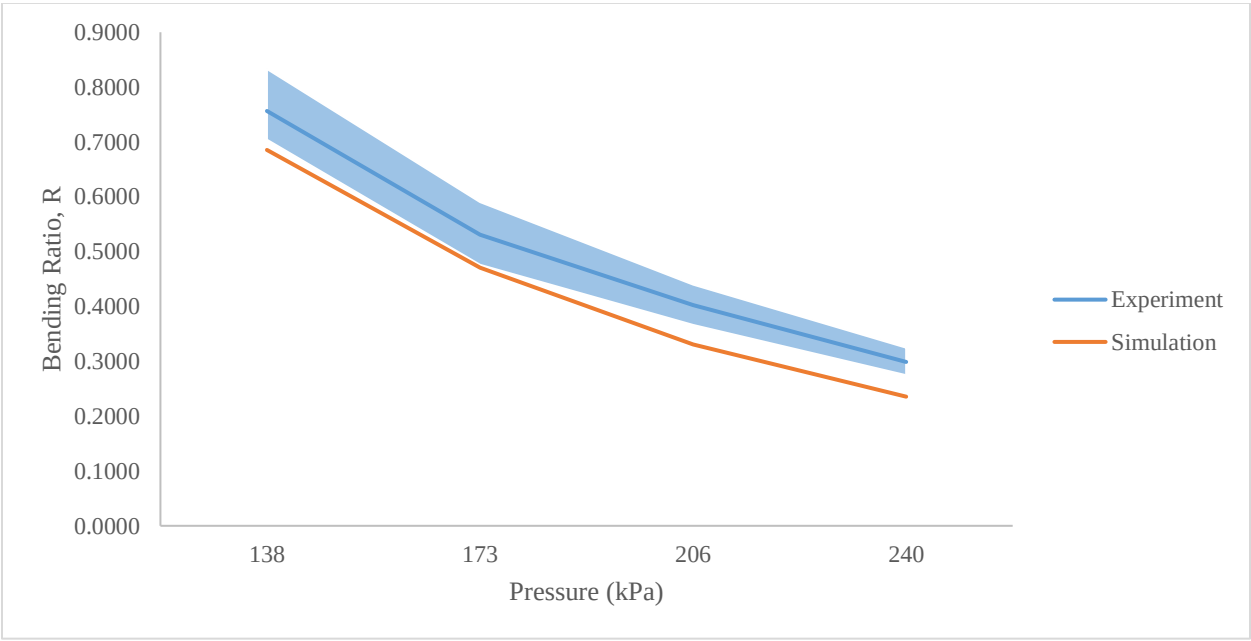

Figure 30 Bending ratio versus pressure results based on free rotation experiment and simulation

The results indicate that the experiment closely matches the simulation with a constant offset of approximately R=0.07; however, the simulation overestimates the performance (lower R is better).

Constrained Tip Force

Similarly, the actuator was constrained within a custom 3D printed apparatus 20mm proximally (Figure 31), inflated three times, to four pressures successively, and the resultant force was measured using a Mark-10 MG50 force gauge [65] and averaged. The experimental results are compared to the simulation output in Figure 32.

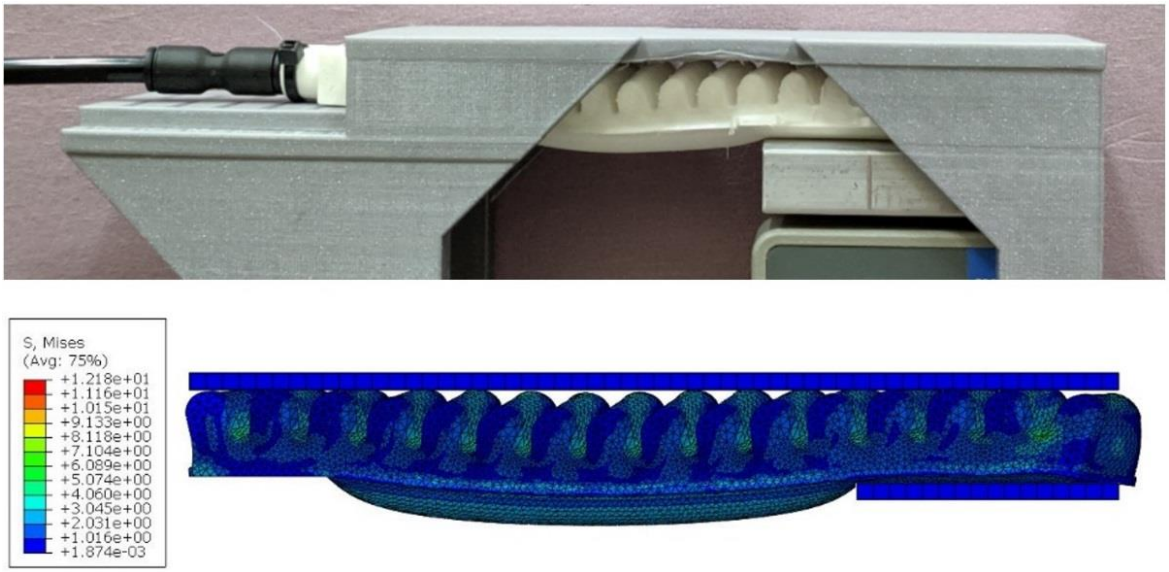

Figure 31 Constrained tip force at 138kPa (~20psi) experiment (top) and simulation (bottom)

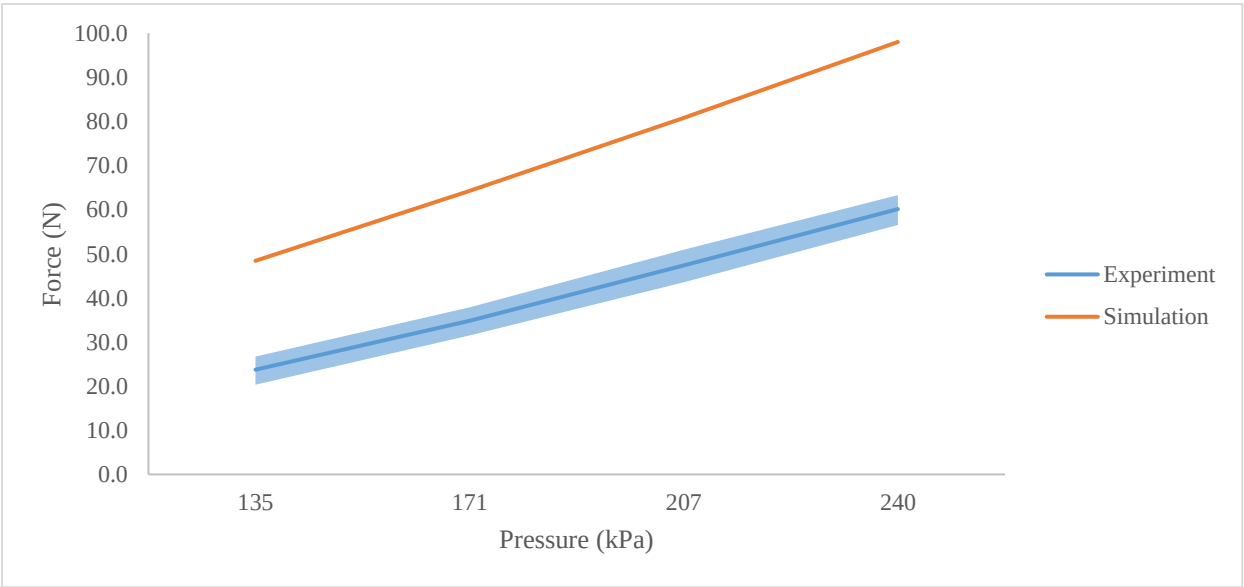

Figure 32 Constrained tip force versus pressure, experimental and simulated results

Again, although the simulation overestimates the performance of the actuator, the trend of contact force versus pressure is similar. These results indicate that simulated results can reasonably be compared between designs, but actual performance would be lower. Changes could be made to improve the model's accuracy (ex. more thorough material characterization); however, it was deemed sufficient for the comparison of designs used in this research.

2.2 Rapid Prototyping

2.2.1 3D Printer and Specifications

A Prusa i3 MK3 filament deposition modeling (FDM) 3D printer [66] was selected for all actuator rapid prototyping based on its performance, resolution, and reliability. In the FDM printing method, filament feeds from a spool into a heated extruder by a pair of gears, where it is extruded through a nozzle onto a surface and rapidly cooled by a fan to form a layer (Figure 33). The FDM method was selected because the desired hyperelastic material (NinjaFlex) was only available in spooled filament.

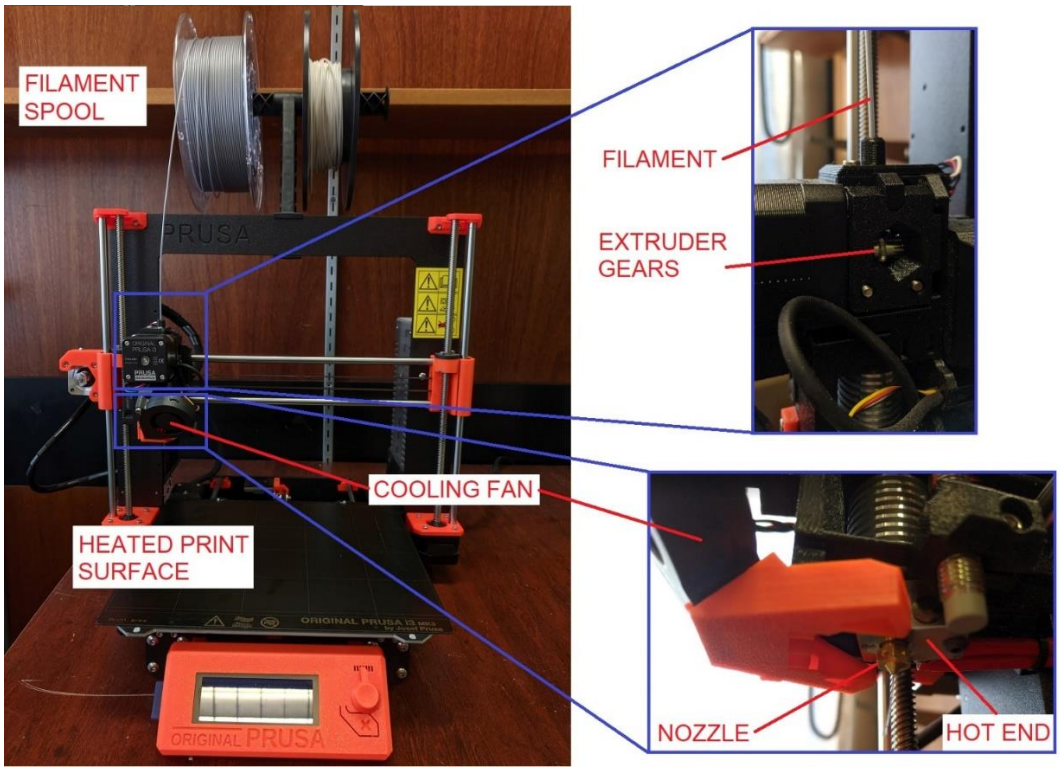

Figure 33 Prusa i3 MK3 3D printer, with labeled primary components

2.2.2 Slicer Software Settings

Printing flexible filament can be very challenging. The print temperature, extrusion rate, and speed are the most critical factors in a successful print. If the temperature is too low or the extrusion rate too high, the material will bind and become lodged in the extruder. If the print speed is too fast, the material cannot be properly extruded and cooled, resulting in a weak, porous print that is not airtight. The software suite Cura 3.4.1 [67] was used to generate the code required to print the actuators, with optimum settings as detailed in Table 8. The actuators were printed on their side to optimize bridging, illustrated in Figure 34.

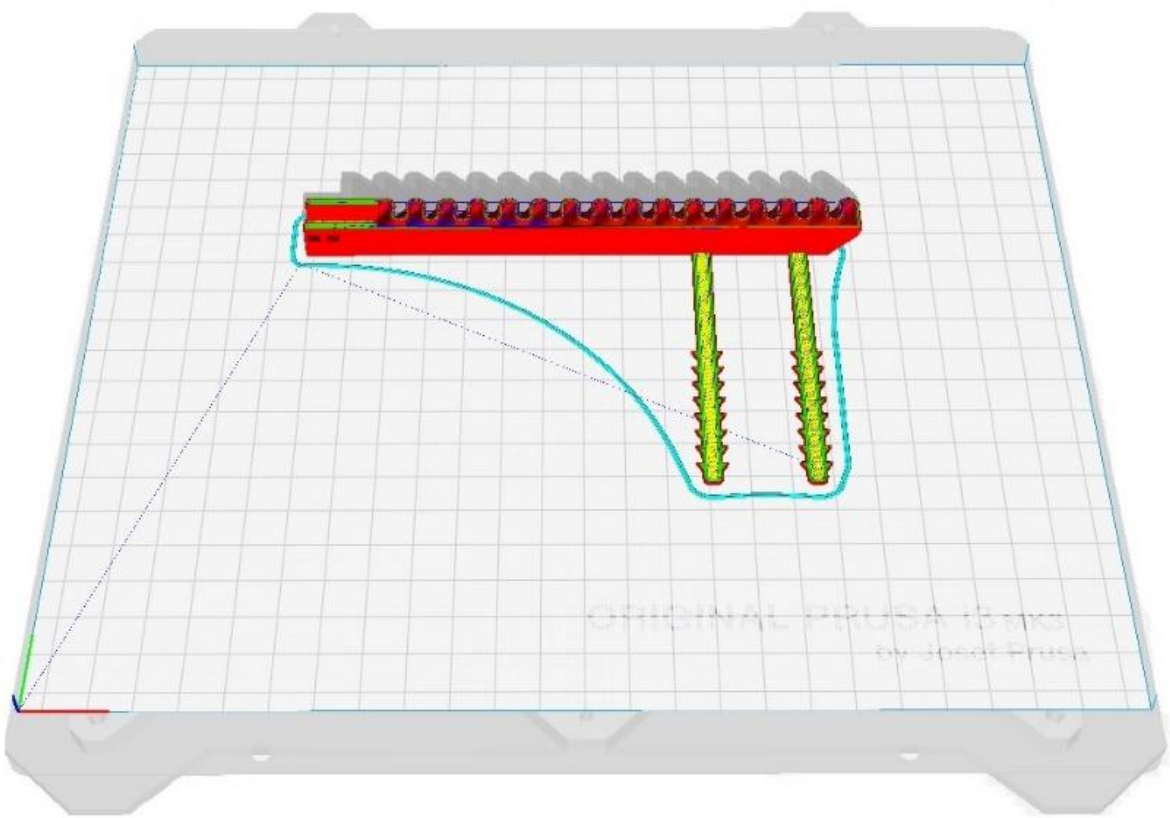

Figure 34 Cura 3.4.1 build plate illustration with final actuator design

Table 8 Optimum settings for 3D printing in Cura 3.4.1 with Ninjaflex®

	Setting	Value	Units
QUALITY	Layer Height	0.05	mm
	Initial Layer Height	0.02	mm
	Line Width	0.40	mm
	Initial Layer Line Width	150	%
SHELL	Wall Thickness	1.20	mm
	Wall Line Count	3	
	Top/Bottom Thickness	1.20	mm
	Top Layers	24	
	Bottom Layers	24	
	Top/Bottom Pattern	Lines	
	Optimize Wall Printing Order	YES	
INFILL	Infill Density	20	%
	Infill Pattern	Grid	
MATERIAL	Printing Temperature	235	°C
	Printing Temperature Initial Layer	235	°C
	Initial Printing Temperature	225	°C
	Final Printing Temperature	220	°C
	Build Plate Temperature	40	°C
	Flow	120	%
	Initial Layer Flow	120	%
	Enable Retraction	OFF	
SPEED	Print Speed	15	mm/s
	Infill Speed	15	mm/s
	Wall Speed	7.5	mm/s
	Outer Wall Speed	7.5	mm/s
	Inner Wall Speed	15	mm/s
	Top/Bottom Speed	7.5	mm/s
	Travel Speed	120	mm/s
	Initial Layer Speed	7.5	mm/s
	Initial Layer Print Speed	7.5	mm/s
	Initial Layer Travel Speed	60	mm/s
COOLING	Enable Print Cooling	ON	
	Regular Fan Speed	100	%
	Initial Fan Speed	0	%
	Regular Fan Speed at Height	0.02	mm

2.3 In Vivo Study

The objective of the *in vivo* study was to test the primary and secondary hypotheses discussed in section 1.5. Specifically, to quantify the effects of the grasp assist and grip trainer devices on muscle activity and grip force compared to a typical trial without the device(s) during a controlled activity on able-bodied participants employed at an automobile manufacturer. The effects of the two devices presented in this research on muscle activity and grip force within an industrial cohort act to bridge a gap in existing literature on passive and dynamic orthoses.

2.3.1 Participants

Ten associates at Honda of Canada Manufacturing (HCM) voluntarily participated in the study; however, due to equipment issues, only data from nine participants were usable (Table 9). Of the nine participants, five were male, four were female, seven were right-handed, and two were left-handed. The experimental procedure, equipment used, and potential risks were explained to each participant. The participants were informed that if at any point during the trial they felt uncomfortable or wished to stop for any reason they could do so with no repercussions. They were encouraged to ask questions throughout the study and were provided with contact information should they have questions at a later time. The Office of Research Ethics approved the study, and each participant voluntarily signed a consent form.

Table 9 Summary of participant information, n=9

	Female		**Male**	
	Mean	SD	Mean	SD
Height (cm)	160.3	3.4	178.3	10.9
Hand Span (cm)	18.5	0.8	20.7	1.0
Age (yr)	48.5	2.3	40.0	10.1
Power Tool Experience (yr)	10.6	6.9	17.4	7.1
Employed at HCM (yr)	23.5	4.5	14.0	8.5

2.3.2 Equipment

Test Apparatus

The test apparatus consisted of an L-shaped frame with six steel plates fastened at three heights – low, high, overhead – each with three exposed threaded receiving holes, for a total of 18 receiving holes (Figure 35). The frame was fastened to a table 76cm from the ground, yielding receiving hole location heights of 130/180/180cm for low/high/over head respectively. These locations are typical at HCM and within reasonable reach of all participants whose mean height (±SD) was 170.3cm (12.3).

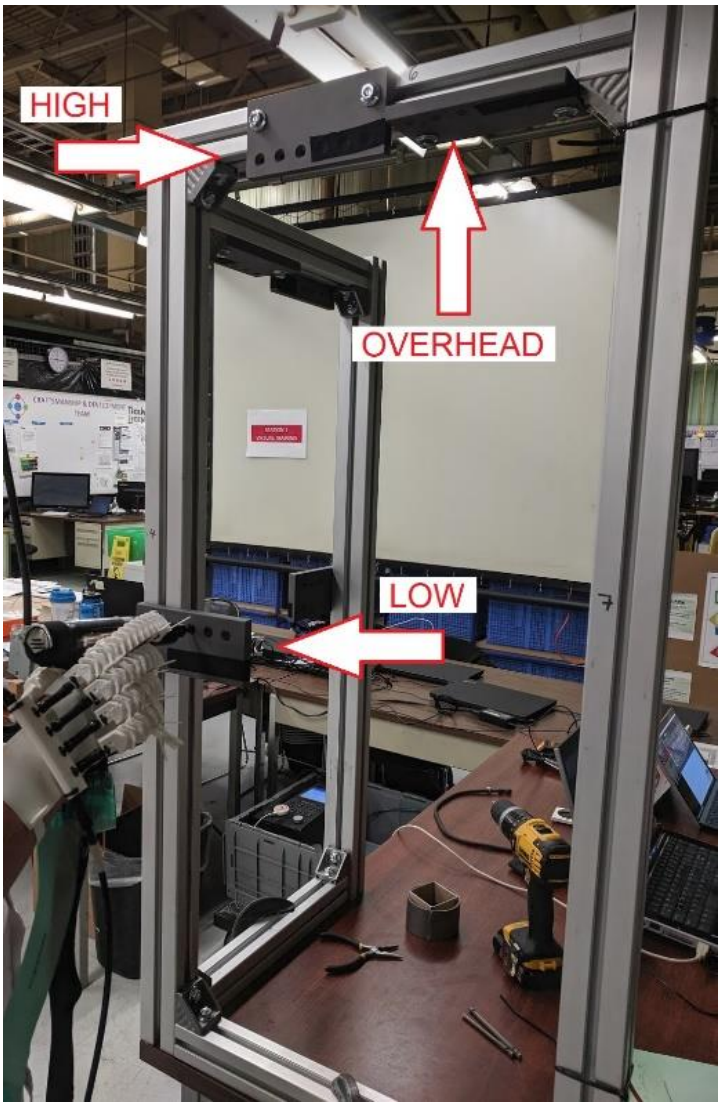

Figure 35 Fastener locations illustrated for the right half of the test apparatus

Pneumatic System and DC Tool

DC Pistol grip tools are routinely used to install fasteners at HCM. These tools have an embedded motor and encoder for operation using a controller. The controller allows for setting various operational parameters such as torque, speed, build-up time, etc. A pneumatic system was built by HCM to work with the controller (Figure 36). The pneumatic system was connected to a compressed air supply, which supplied air at the desired pressure when the DC pistol grip tool trigger was engaged and vacuums out the air when the trigger was disengaged. The grasp assist device was connected to this system, inflating and deflating with the engagement and disengagement of the trigger by the participant. All bolts were fastened using the DC tool [68] to a torque of 5Nm. Actuator response time using this inflation/deflation method was much approximately one tenth of a second.

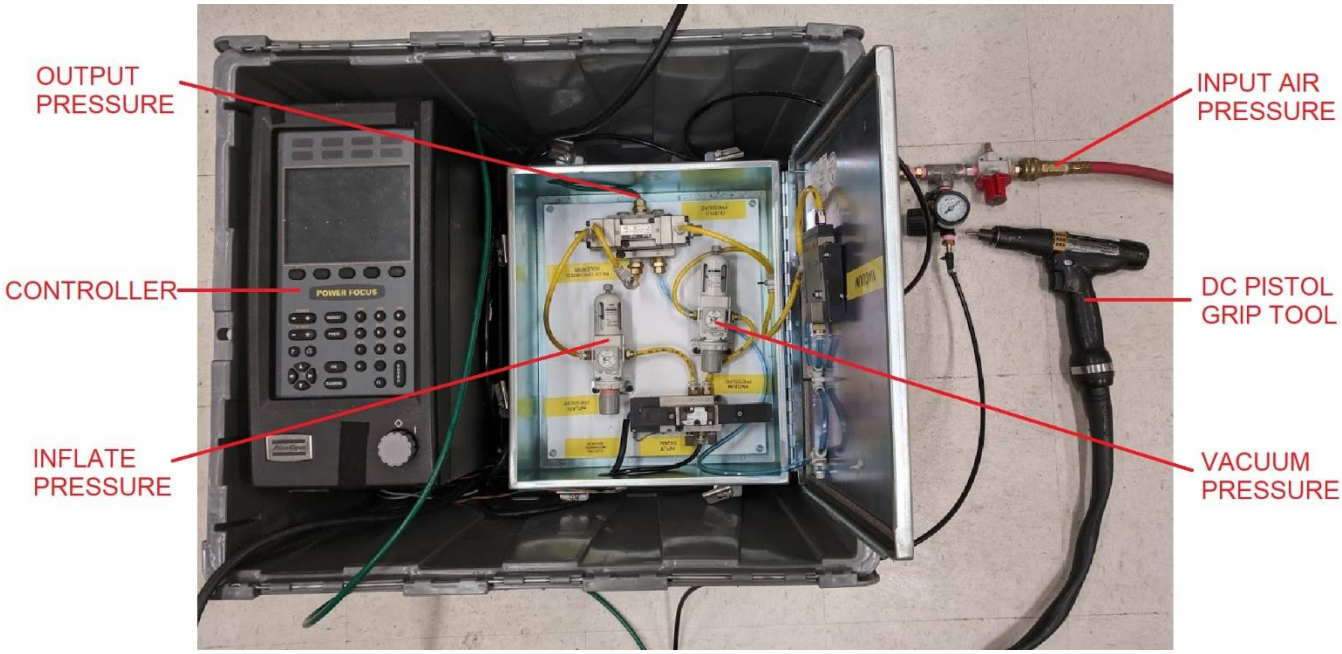

Figure 36 Pneumatic system and DC pistol grip tool

Grip Force Sensor

A Tekscan Evolution I-Scan 9830 pressure sensor with a sensing element (Sensel™) density of 0.5/cm^2 and a max pressure of 69kPa [69] was trimmed and applied to the handle of the DC tool using soft, flexible tape (Figure 37). The sensor was calibrated before and after the trial by applying an evenly distributed known load to individual Sensels and measuring the raw sum output (0-255), then averaged. The calibration factor was determined to be 0.0973N/sum. Corresponding Tekscan I-Scan software [69] was used to collect the data at a sample frequency of 25Hz.

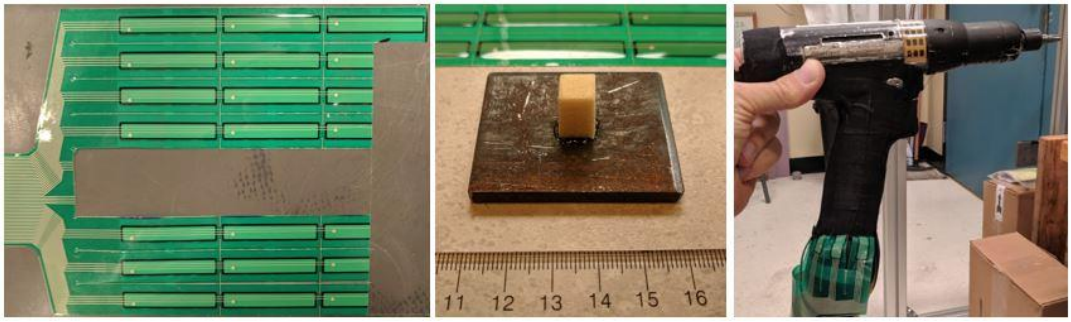

Figure 37 Trimmed 9830 pressure sensor (left), high density foam mounted to a measured weight to evenly distribute load across a Sensel (middle), trimmed 9830 sensor applied to the pistol grip of the DC tool with adhesive tape (right)

Electromyography

The right forearm of each participant was prepared by shaving excess hair, wiping with isopropyl alcohol, followed by a mild abrasive gel to remove dead skin and improve conductivity. Foam electrodes with a conductive adhesive hydrogel were applied in pairs, approximately 2cm apart. Muscle palpation and electrode placement was performed as per Delagi et al. [70], summarized in Table 10. Each pair of electrodes were connected to a 2-channel wireless Bioelettronica DUE probe [71]. The analogue signals were converted to digital signals at a resolution of 16 bits. An analog bandpass filter was applied to the raw EMG signal with corner frequencies 10Hz and 500Hz and amplified (common mode rejection ratio > 100dB) with a gain of 200V/V. Electrode wires were secured to the participants skin with masking tape. Typical electrode and wireless probe application are illustrated in Figure 38. Trigger pull signal from the DC tool was captured using an AUX input to a wireless DUE probe for simplicity and time synchronization. Signals were sampled at 2048Hz and raw data was collected wirelessly through OTBioLab+ v1.2.0 [71].

Table 10 Summary of muscle palpations and EMG electrode placement

Muscle	Palpation Maneuver	Electrode Position
Flexor Carpi Radialis (FCR)	Supine, wrist flexion with radial deviation	Three to four finger widths distal to midpoint of a line connecting the medial epicondyle and biceps tendon
Flexor Digitorum Superficialis (FDS)	Supine, flexion of interphalangeal joints	Grasp with operator's palm to volar surface of subject's wrist, point index finger to biceps tendon and place electrode ulnarly to tip of index finger
Flexor Carpi Ulnaris (FCU)	Supine, wrist flexion with ulnar deviation	Two finger widths volar to ulna at the junction of the upper and middle thirds of forearm
Extensor Digitorum Communis (EDC)	Pronated, extend metacarpophalangeal joints	Grasp the forearm at function of upper and middle third with thumb and middle finger on radius and ulna, electrode position at bisection these two points

Figure 38 Example of EMG electrode and probe placement for FCU, FDS, FCR (left) and EDC (right)

Grasp Assist

A glove-like interface was designed to affix the actuators to the dorsal aspect of the hand and 3D printed using Ninjaflex®. A manifold was also printed to enable all actuators to inflate simultaneously and was connected to the actuators with 6mm OD semi-rigid tubing, 6mm ID flexible tubing, a semi-flexible adhesive, and zip-ties (Figure 39). Two assembly sizes were generated (Table 6) and the most appropriate size was fitted to each participant. Each actuator's position with respect to the corresponding digit was adjusted as best as possible for optimal contact.

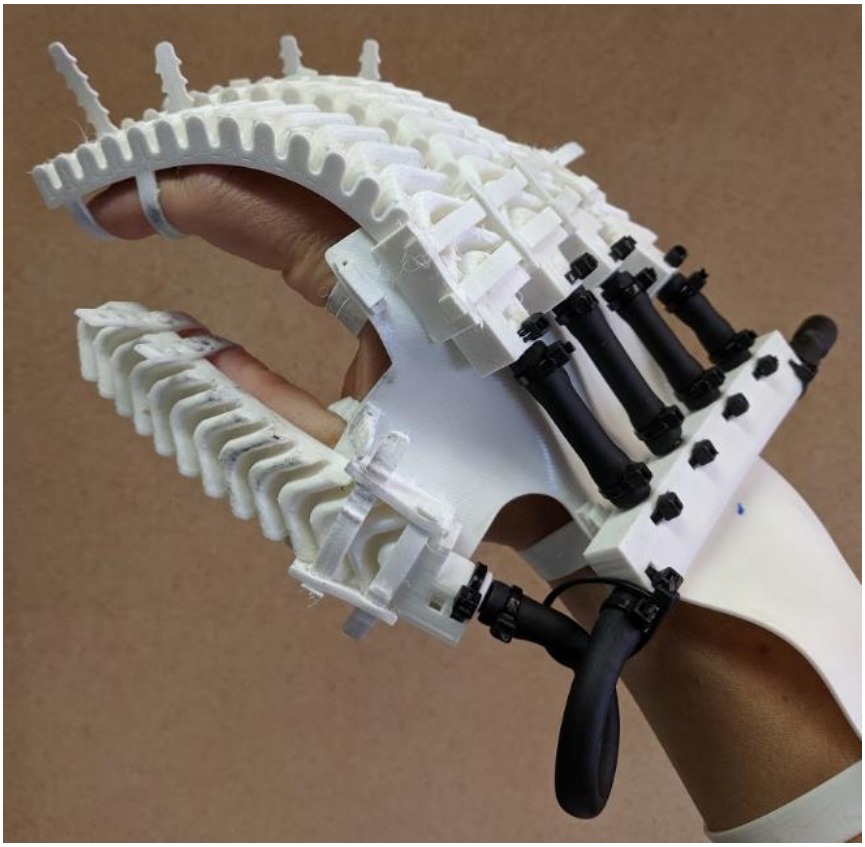

Figure 39 Fully assembled grasp assist device

Grip Trainer

As discussed in section 1.4 and 1.5, the secondary hypothesis of this research involved a grip training system. The system was designed and fabricated using two Tekscan FlexiForce A201 [69] sensors connected in parallel to a Tekscan QSB [69] and an Arduino microcontroller [72] which was programmed to vary the colour and brightness of an LED based on force threshold values determined during a pilot study. The sensors were applied to the trigger and the handle at the location most likely to experience the greatest force, approximately where the third and fourth phalanges contact the tool [32]. The LED was affixed proximally on the top of the housing so that it was clearly visible at every bolt location. Final sensor and LED placement are illustrated in Figure 40.

Figure 40 Grip trainer FlexiForce sensors (left) and visual feedback LED placement (right) on the tool

2.3.3 Procedure

Experimental Protocol

A single data collection session took between 45 and 60 minutes per participant, and all ten trials were captured over two successive days. The equipment was left untouched between sessions. The complete experimental protocol is summarized in Table 11.

Table 11 Experimental protocol summary

Background & Experiment Explanation	1. The purpose of the experiment was explained along with a general procedure 2. The equipment and potential risks were explained, participant consent was given, and basic participant information was collected
EMG Setup	3. The right forearm was prepared by removing excess hair, cleansed with alcohol, and dead skin removed with an abrasive, conductive gel 4. Target muscles were palpated and electrode pairs were placed 5. Electrode pairs were connected to probes, wires and probes secured to forearm 6. Probes were turned on and confirmed operational through OT BioLab+
Subject Profile	7. A participant profile was generated in OT BioLab+, including name, participant number, birth date, hand dominance, height, hand span, power tool experience, and years worked at HCM
Maximum Voluntary Contraction	8. The importance of accurate MVC data was reiterated 9. MVC Flexion – two trials, at least two minutes rest in between 10. MVC Extension – two trials, at least two minutes rest in between
Data Trials	11. Typical tool use, no prompting 12. Using the trainer, prompted to use as little muscle activation as necessary and that the LED would change colour/intensity with applied force 13. Using the assist, prompted to let the assistance device provide as much of the force as possible
Disconnect System	14. Grasp assist device and tape were removed from the participant 15. Probes were disconnected and electrodes were removed
Subjective Assessment	16. Participants were given a voluntary survey to complete 17. Any follow up questions were answered

Maximum Voluntary Contractions

The magnitude of an EMG signal varies between individuals and must be normalized to the maximum voluntary electrical activity (MVE) during a maximum voluntary contraction activity (MVC) before results can be compared [73]. Each participant performed two flexion MVCs to capture the MVE of the FCU, FDS, and FCR, and two extension MVCs to capture the MVE of the EDC. They were given one minute of rest between flexion and extension MVCs, resulting in a rest greater than two minutes between similar

MVCs. Both flexion and extension trials were captured on a simple fixture illustrated in Figure 41. For the flexion trial, the participants were instructed to squeeze and rotate the grip in an attempt to flip the fixture. For the extension trial, the participants were instructed to squeeze and rotate the grip similar to accelerating a motorcycle. The duration of each contraction was ten seconds and verbal encouragement was provided to better elicit the participants true maximum [74].

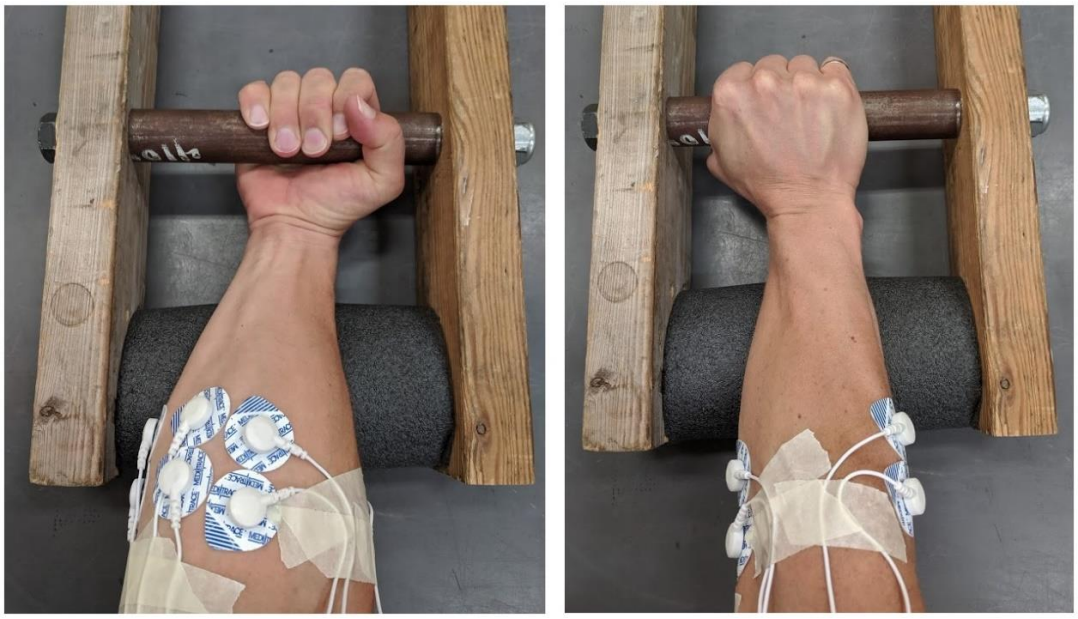

Figure 41 Maximum voluntary contraction (MVC) fixture for flexion (left) and extension (right)

Trial Data Collection

Once per participant, a ten second trial with no applied load was recorded. This bias was later removed from each participant grip force data (i.e. zeroed), as residual force generated a raw sum from the pressure map that varied between participants. Participants were encouraged to practice fastening bolts until they felt comfortable with the specific activity (all trials) and device (trial 2 and 3). For each of the three data trials, the pressure map (I-Scan) and EMG (OT BioLab+) recordings were initiated simultaneously and the participants were cued to begin with a 3-2-1 countdown. Once the trial was complete, both data recording systems were stopped simultaneously. Fasteners were handed to the participant as required so as to encourage focus on the activity. Between trials, all 18 fasteners were removed by a research assistant, not the participant.

Trial 1 – Typical

The first trial was designed as the baseline for comparison. Participants were instructed to fasten three bolts into receiving holes on each of the six plates (18 total) as they typically would. The sequence was Low → High → Overhead → Low → High → Overhead, as the participant moved left to right around the test apparatus. No other instruction or prompting was provided.

Trial 2 – Grip Trainer

The second trial tested the secondary hypothesis that visual grip force feedback could reduce muscle activation. Participants were informed that previous studies indicate associates apply more grip force than is required for an activity. They were instructed to use as little force as possible to successfully complete the same activity in the same sequence, and that the colour and intensity of the tool-mounted LED would vary with applied force.

Trial 3 – Grasp Assist

The third trial tested the primary hypothesis that the designed pneumatic grip assist device could reduce muscle activation. Participants were again instructed to use as little force as possible to successfully complete the same activity in the same sequence, and to let the grasp assist device provide as much of the force as possible. The device inflated when the DC tool trigger was engaged and deflated when the trigger was released. A pressure of 172kPa (~25psi) was applied to the small/medium size, and 138kPa (~20psi) to the large/x-large size.

Subjective Assessment

Each participant voluntarily participated in questionnaire after the trials (Table 12). The grip force and EMG data provided objective data, where the questionnaire provided subjective data. This information may be important for future development of the device.

Table 12 Subjective assessment questionnaire

Comfort	0 to 10, where 0 is uncomfortable and 10 is comfortable
Support	0 to 10, where 0 the device provided no support, and 10 the device provided ample support
Force	0 to 10, where 0 the device provided no assistance, and 10 the device provided all the assistance required
Did you like wearing it?	YES or NO, and WHY
Would you wear it for a 2-hour shift?	YES or NO

2.4 Data Processing

All data was processed using MATLAB R2019a [75]. Raw pressure map data was imported as text, EMG and trigger pull data was first exported from OT BioLab+ as a .m file, then imported to MATLAB. The data was analyzed during the fastening phase only (i.e. when the trigger was pulled) as the grip assist was only active when the trigger was engaged. Given the 5mm trigger displacement and a typical actuator response time of less than 0.1s, there was no significant difference in trigger engagement times between trials.

2.4.1 Grip Force

Bias data was removed from the raw pressure map data for each trial. Raw sum pressure data was resampled from 25Hz to 2048Hz and bandpass 4th order Butterworth dual pass filtered with corner frequencies [20Hz, 400Hz] to match EMG filtering. The raw sum data was summed and converted to Newtons by multiplying by the calibration factor (0.0973N/sum) discussed in section 2.3.2. Grip force versus time was plotted for each trial and participant individually and visually inspected to determine when the trigger was engaged (Figure 42) and the corresponding fastener location (Figure 43). The start/stop time for each trigger pull was determined using a custom MATLAB function, stored, and used for both grip force and EMG processing. Mean grip force values were recorded for Low, High, Overhead, and All bolt locations for each of the nine participants and four trials.

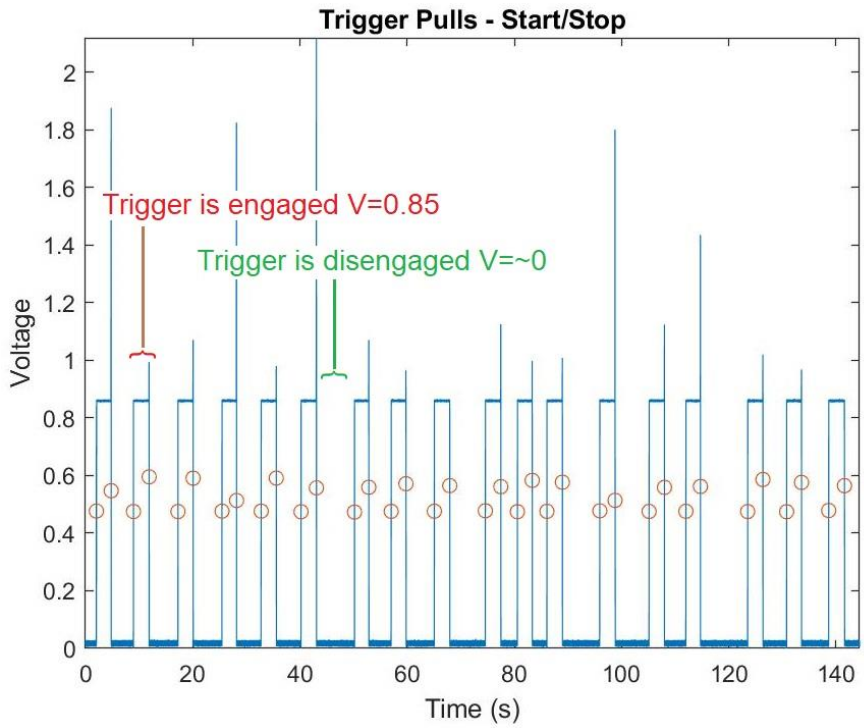

Figure 42 Example of identifying trigger engagement (V=0.85) and disengagement (V=~0)

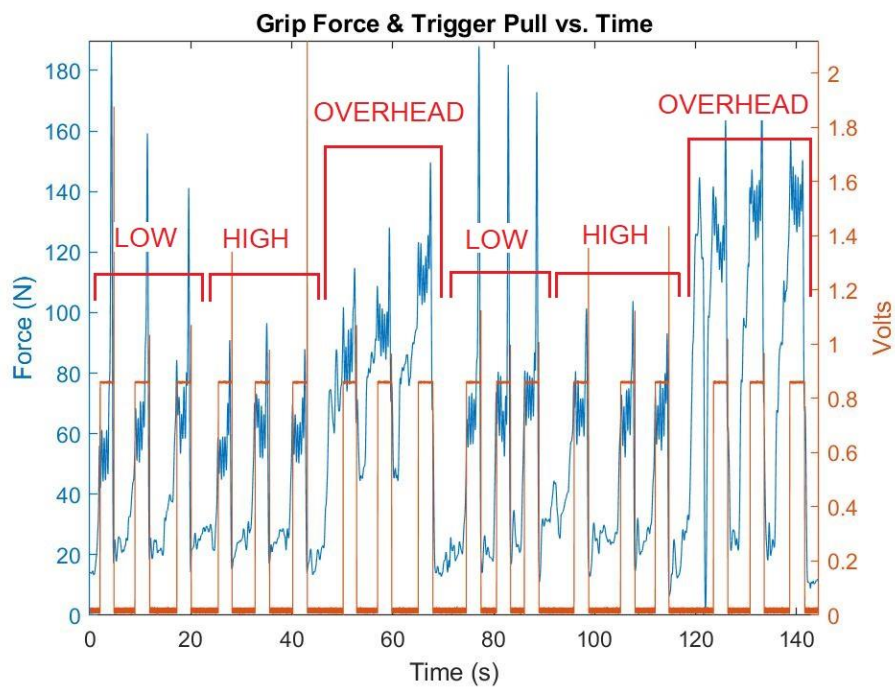

Figure 43 Example of identifying fastener locations based on trigger engagement and grip force

2.4.2 EMG

All EMG signals (MVC and trials) were individually filtered to improve the signal to noise ratio (SNR) by applying a dual pass, 4th order Butterworth bandpass filter with corner frequencies [20Hz, 400Hz] [76]. A linear envelope was applied to the filtered signals by subtracting the mean, full wave rectifying, and filtering with a low pass 2nd order Butterworth filter. The low pass cut-off frequency was calculated to be $f_c = \frac{1}{2\pi T} = 3Hz$ based on upper extremity muscle twitch time $T = 52ms$ [77]. Corser et al. reported similar delays between onset of EMG activity and onset of movement of 25-75ms [78][79]. A phase shift was intentionally introduced using a single pass filter to digitally reproduce the electromechanical delay [80]. A moving window average of 52ms was applied to the linear enveloped MVE data to determine the peak amplitude to be used for EMG normalization [81]. This was performed for each of the four MVC trials, and the maximum MVE value was selected per muscle. Trial data was normalized by dividing it by the corresponding muscle MVE and multiplied by 100 to yield results in percent MVE.

Normalized EMG data was plotted versus time and visually inspected for artifacts (Figure 44), as per trigger pull start/stop times determined from the grip force analysis. If artifacts existed during any part of a trigger pull, data from the entire trigger pull duration was removed from the analysis. The mean percent MVE values were recorded for Low, High, Overhead, and All bolt locations for each of the nine participants and four trials.

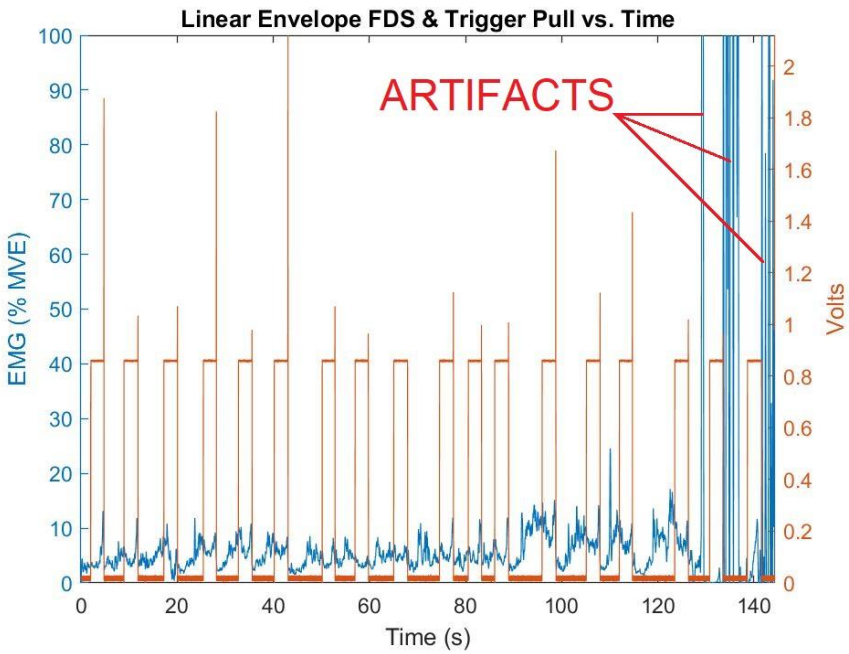

Figure 44 Example of identifying artifacts through visual inspection

2.5 Statistical Analysis

All statistical analysis was performed using IBM SPSS Statistics version 26.0 [82]. A two-way repeated measure analysis of variance (ANOVA) was performed for each of the dependent variables (muscle activation, grip force) on the two dependent variables (bolt location and trial condition). The analysis was performed using the mean and peak/maximal values at a $p < 0.05$ level of significance (Table 13).

Table 13 Two-way ANOVA summary of independent and dependent variables

Independent	**Dependent**		
FCU, FDS, FCR, EDC, Grip Force	Value	Bolt Location	Trial Condition
	Mean, Peak/Maximal	LOW, HIGH, OVERHEAD, ALL	Typical, Grip Trainer, Grasp Assist

Both a Bonferroni and Tukey HSD post-hoc analysis were performed to determine significant interaction between bolt location and trial condition. The null hypotheses were as follows:

1. H_{01}: Bolt location will have no significant effect on muscle activation or grip force.
2. H_{02}: Trial condition will have no significant effect on muscle activation or grip force.

3. H_{03}: Bolt location and trial condition interaction will have no significant effect on muscle activation or grip force.

The grip trainer and grasp assist trial conditions were compared to the typical trial condition at each bolt location for each independent variable using a compared means t-test. This analysis was performed using the mean values at a $p < 0.05$ level of significance (Table 14). The results help illustrate the effect of the grip trainer and grasp assist devices on muscle activation and grip force at different bolt locations.

Table 14 t-Test summary of trial condition comparisons for each bolt location and independent variable

Trial Condition Comparison	Bolt Location	Independent Variable
Grip Trainer vs. Typical	LOW, HIGH, OVERHEAD, ALL	FCU, FDS, FCR, EDC, Grip Force
Grasp Assist vs. Typical		

As discussed in section 1.3, the revised strain index is a tool to evaluate the safety level of a task [34]. It is the product of five non-linear factors (Equation 3), which means that the results will not necessary match the muscle activation and grip force results. A description of each factor as well as how to calculate it is described in Table 15. The effect of the grip trainer and grasp assist device compared to no device on the RSI was also analyzed using a compared means t-test.

Equation 3 Revised strain index (RSI)

$$RSI = IM * EM * DM * PM * HM$$

Table 15 Revised strain index factor description and equation

Factor	Description	Equation	Variable	Range
IM	Intensity of exertion multiplier (force)	$30I^3 - 15.60I^2 + 13I - 0.40,$ $0.0 < I < 0.4$ $36I^3 - 33.33I^2 + 24.77I - 1.86,$ $0.4 < I < 1.0$	I – Intensity of exertion (%MVE)	0 to 1
EM	Exertions per minute multiplier (frequency)	$0.10 + 0.25E, E \leq 90/m$ $0.00334E^{1.96}, E > 90/m$	E – Efforts	0 to >100 (effort/min)
DM	Duration per exertion multiplier	$0.45 + 0.31D, D \leq 60s$ $19.17 \log_e D - 59.44, D > 60s$	D – Duration per exertion	0 to >100 (seconds)
PM	Hand/wrist posture multiplier	$1.2e^{0.009P} - 0.2, P = Deg\ flexion$ $1.0, P \leq 30\ Deg\ extension$ $1.0 + 0.00028(P - 30)^2, P > 30\ Deg\ extension$	P – Hand/wrist posture (degrees from anatomical neutral) Flexion and Extension	0 to 90 (degrees)
HM	Duration of task per day multiplier	$0.2, H \leq 0.05h$ $0.042H + 0.090 \log_e H + 0.477, H > 0.05h$	H – Duration of task per day	0 to 12 (hours)

3 Results

The results are presented to help answer the primary and secondary hypotheses of this research. To reiterate, the primary hypothesis proposed using a pneumatic grasp assist device can lower superficial forearm muscle activation associated with grasping tasks compared to not using the device. The secondary hypothesis proposed using a grip force visual feedback device can lower superficial forearm muscle activity associated with grasping tasks compared to not using the device. The mean grip force and EMG values for each fastener were analyzed only while the trigger was engaged (18 total – 6 Low, 6 High, 6 Overhead), per muscle (FDS, FCU, EDC, FCR) and per participant (n=9).

A small number of actuators ruptured at lower pressures (172kPa for the small/medium, 138kPa for the large/x-large) than achieved during experimental verification (345kPa for all sizes). Although the actuators still performed to some degree when ruptured, it was not at the designed level. Ruptured actuators were either replaced in between trials if the trial had progressed past halfway or else replaced immediately and the trial was re-run.

A significance level of $p < 0.05$ was used unless otherwise stated. Mean values were analyzed to generally describe the effects of the devices and to allow comparison with similar studies where forearm muscle activation was measured using othoses [38][40][83]. The mean values were approximately normally distributed across the three trial conditions, activation of four muscles, combined muscle activation, and grip force based on a Shapiro-Wilk's test ($p > 0.05$) [84], a visual inspection of the corresponding histograms, normal Q-Q and box plots – except for the FCU muscle under the typical condition trial ($p = 0.022$).

3.1 Two-way ANOVA

A two-way analysis of variance (ANOVA) study was performed to determine the effects of the trial condition factor (typical (T), grip trainer (GT), grasp assist (GA)) and the fastener location factor (low, high, overhead).

A significant difference was found for the condition factor for the FDS, FCU, and grip force. There was no significant difference found for the condition factor in the EDC and FCR muscle groups. For the fastener location factor, a significant difference was found for the FCU and grip force. There was no significant difference found for the fastener location factor in the FDS, EDC, and FCR muscle groups. When considering the interaction between factors condition and location, there was no significant difference found. The results are summarized in Table 16.

Table 16 Two-way ANOVA results for condition and location effects on muscle activity and grip force

P-Values					
	FDS	**FCU**	**EDC**	**FCR**	**GRIP**
Condition (T, GT, GA)	0.011	0.000	0.567	0.286	0.000
H_{01}	Reject	Reject	Fail to Reject	Fail to Reject	Reject
Location (low, high, overhead)	0.315	0.004	0.059	0.980	0.000
H_{02}	Fail to Reject	Reject	Fail to Reject	Fail to Reject	Reject
Condition and Location	0.999	0.976	0.945	0.977	0.927
H_{03}	Fail to Reject	Fail to Reject	Fail to Reject	Fail to Reject	Fail to Reject

The significance of the fastener location factor on the FCU muscle activity and the grip force was left for future analysis, as the focus of this research was on the condition factor and its effect on muscle activity. For the FDS muscle activity, FCU muscle activity, and grip force, both the Bonferroni and Tukey post hoc analysis agreed that there was a significant difference between the typical trial and both the grip trainer and grasp assist trials. The Bonferroni correction was determined based on $\frac{\alpha}{N}$, where $\alpha = 0.05$ and $N = 3$ (muscle activation OR grip force, condition, and location). A summary of the significance is presented in Table 17.

Table 17 Post hoc significance summary of condition factor

P-Values					
Condition 1	**Condition 2**	**Post-hoc Test**	**FDS**	**FCU**	**Grip Force**
Typical	Grip Trainer	Tukey HSD	0.036	0.006	0.000
		Bonferroni	0.040	0.007	0.000
	Grasp Assist	Tukey HSD	0.016	0.000	0.000
		Bonferroni	0.018	0.001	0.000

3.2 Muscle Activation

Muscle activation for all fastener locations and all muscles combined in terms of %MVE was determined to be 11.9, 9.1, and 9.7 for the typical (T), grip trainer (GT), and grasp assist (GA) trials respectively. The FCR yielded the lowest amount of activity ranging from 4.2%MVE to 5.7%MVE across all trial conditions and fastener locations. The EDC yielded the highest amount of activity, ranging from 13.3%MVE to 25.2%MVE across all trial conditions and fastener locations. The magnitudes of muscle activation measured in this study align with previous studies [38][40]. Significance was determined using paired samples t-tests to compare the means of the trials.

The flexion muscles (FDS, FCU, FCR) responded favorably to the grip trainer, significantly reducing muscle activity compared to the typical trial at every fastener location. With all fastener locations considered, the grip trainer also significantly reduced the muscle activity of the extension muscle (EDC). The grasp assist device also significantly reduced the muscle activity compared to the typical trial, but results were sporadic. At no fastener location did the trainer or assist device increase muscle activity significantly compared to the typical trial. Mean muscle activation for all fastener locations, trial conditions, and muscle groups are summarized in Table 18. Results are presented in a similar fashion as by Johansson et al. [38] to succinctly summarize mean results and compare significance.

Combined muscle activation was significantly reduced considering all fastener locations when using the grip trainer (9.1%MVE) and the grasp assist (9.7%MVE) compared to the typical trial (11.9%MVE). Overall, this confirmed the primary and secondary hypothesis as they relate to muscle activation.

Table 18 Summary of muscle activation (%MVE) mean values (±SD) based on locations: low, high, overhead, all, and conditions: typical (T), grip trainer (GT), grasp assist (GA) with significance between conditions (n=9).

%MVE						
Location	**Condition**	**FDS**	**FCU**	**EDC**	**FCR**	**Combined**
Low	T	7.0 (5.1)	10.5 (5.5)	16.0 (7.1)	5.5 (2.8)	9.7 (4.1)
	GT	4.5 (3.3)	6.4 (3.2)	13.3 (6.7)	4.2 (2.2)	7.1 (3.3)
	GA	4.4 (2.2)	5.7 (2.4)	18.2 (8.1)	5.6 (3.1)	8.6 (3.6)
Significance		GT<T*	GT<T* GA<T*	ns	GT<T**	GT<T*
High	T	8.8 (4.6)	16.7 (7.8)	24.0 (13.3)	5.7 (3.1)	13.8 (6.4)
	GT	5.9 (3.2)	11.2 (4.9)	20.5 (10.5)	4.2 (2.4)	10.4 (4.8)
	GA	5.8 (2.8)	9.9 (3.9)	25.2 (15.5)	5.1 (3.6)	11.5 (6.0)
Significance		GT<T** GA<T*	GT<T* GA<T*	ns	GT<T**	GT<T*
Overhead	T	7.5 (3.9)	13.1 (6.1)	22.5 (12.9)	5.6 (2.8)	12.2 (6.0)
	GT	5.3 (2.7)	9.2 (4.5)	20.3 (10.6)	4.5 (2.3)	9.8 (4.7)
	GA	4.7 (2.3)	7.3 (3.1)	19.8 (8.7)	4.7 (2.5)	9.1 (3.9)
Significance		GT<T** GA<T*	GT<T** GA<T*	ns	GT<T**	GT<T**
All	T	7.8 (4.6)	13.4 (7.0)	20.8 (12.0)	5.6 (2.9)	11.9 (5.8)
	GT	5.2 (3.1)	9.0 (4.7)	18.0 (10.0)	4.3 (2.3)	9.1 (4.5)
	GA	4.9 (2.5)	7.7 (3.7)	21.0 (11.7)	5.1 (3.1)	9.7 (4.8)
Significance		GT<T*** GA<T***	GT<T*** GA<T***	GT<T***	GT<T***	GT<T*** GA<T*
ns = not significant, *p < 0.05, **p < 0.01, ***p < 0.001						

The significance summarized in Table 18 is illustrated and further investigated per muscle group based on the fastener location and the trial condition in the following figures.

The grip trainer mean %MVE values for the FDS muscle were significantly lower than the typical trial for low, high, overhead, and all fastener locations illustrated in Figure 45. The grasp assist mean %MVE values were significantly lower than the typical trial for the high, overhead, and all fastener locations (not low).

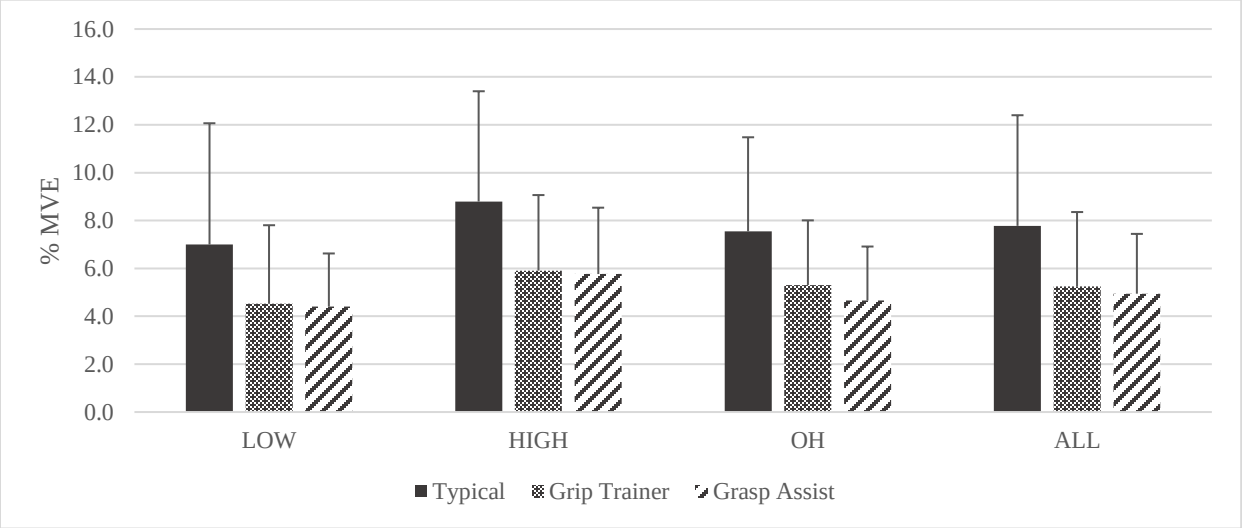

Figure 45 Effect of trial condition on Flexor Digitorum Superficialis (FDS) mean muscle activity (±SD) based on fastener location (low, high, overhead, all)

Both the grip trainer and grasp assist mean %MVE values for the FCU muscle were significantly lower than the typical trial for low, high, overhead, and all fastener locations illustrated in Figure 46.

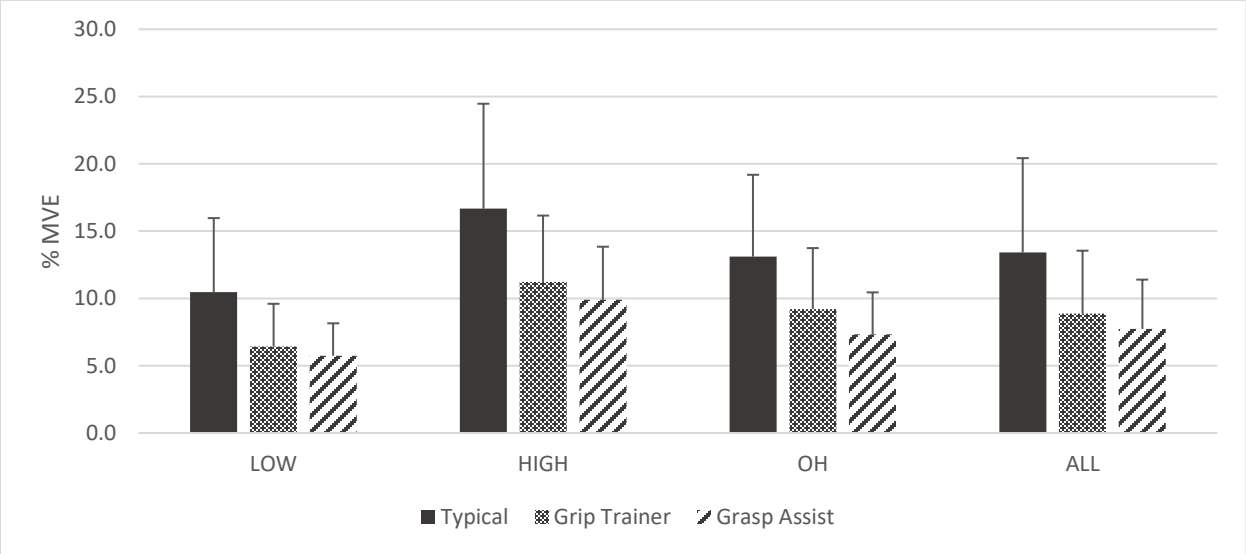

Figure 46 Effect of trial condition on Flexor Carpi Ulnaris (FCU) mean muscle activity (±SD) based on fastener location (low, high, overhead, all)

The grip trainer mean %MVE values for the EDC muscle were significantly lower than the typical values only for all bolt locations illustrated in Figure 47. While the grasp assist appeared to increase EDC muscle activity compared to the typical trial for low and high fastener locations, it was not significant.

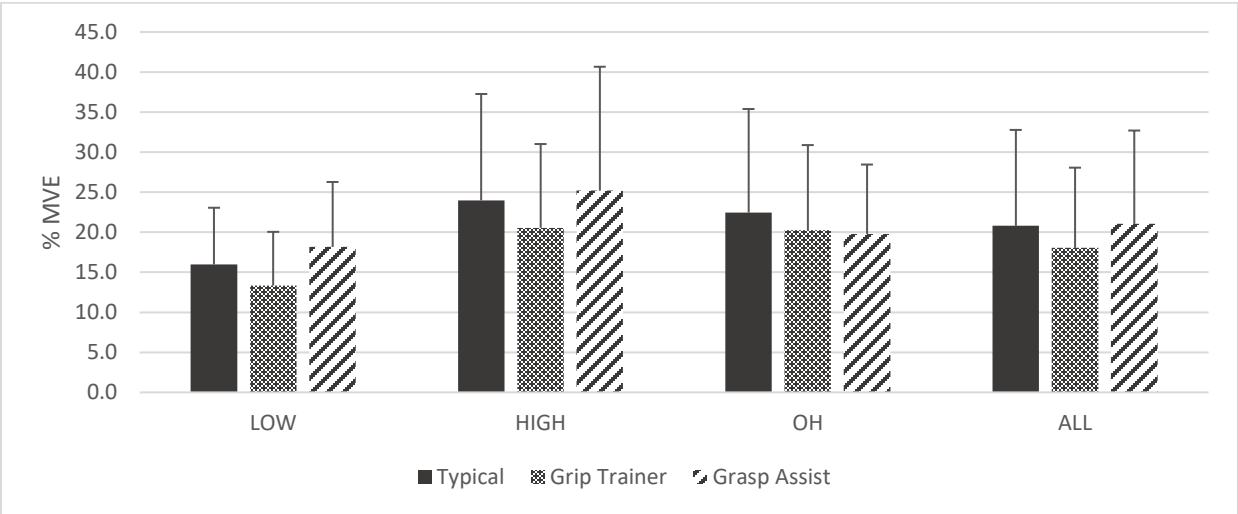

Figure 47 Effect of trial condition on Extensor Digitorum Communis (EDC) mean muscle activity (±SD) based on fastener location (low, high, overhead, all)

The grip trainer mean %MVE values for the FCR muscle were significantly lower than typical values for low, high, overhead, and all bolt locations, illustrated in Figure 48. The grasp assist mean %MVE values were not significantly different than the typical trial at any fastener location.

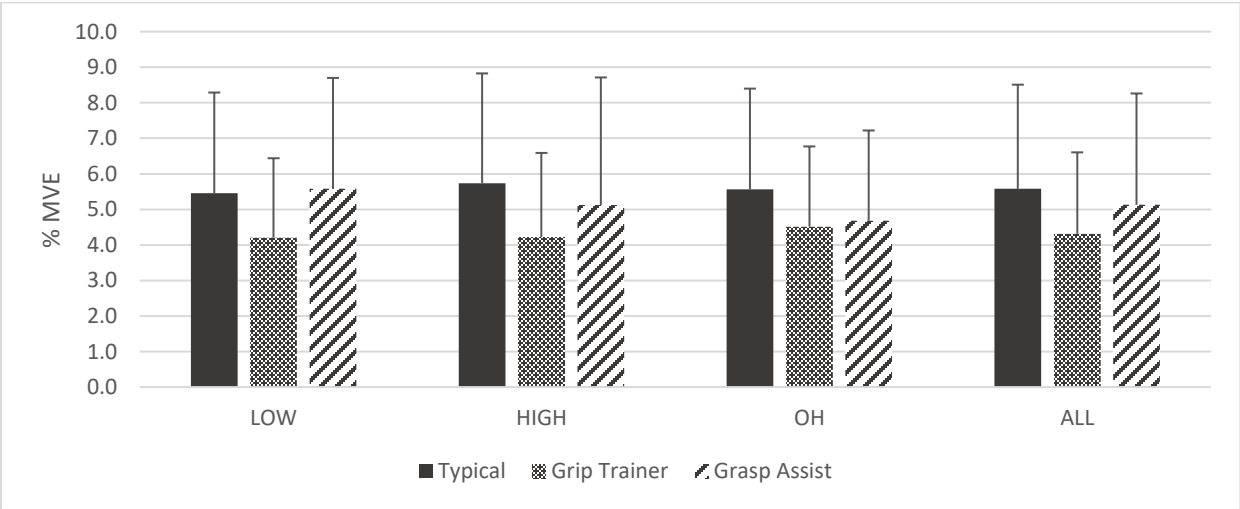

Figure 48 Effect of trial condition on Flexor Carpi Radialis (FCR) mean muscle activity (±SD) based on fastener location (low, high, overhead, all)

When the muscle activation values for all muscle groups were combined, the grip trainer mean %MVE was significantly lower than the typical trial for low, high, overhead, and all fastener locations illustrated in Figure 49. The grasp assist mean %MVE was significantly lower for all fastener locations.

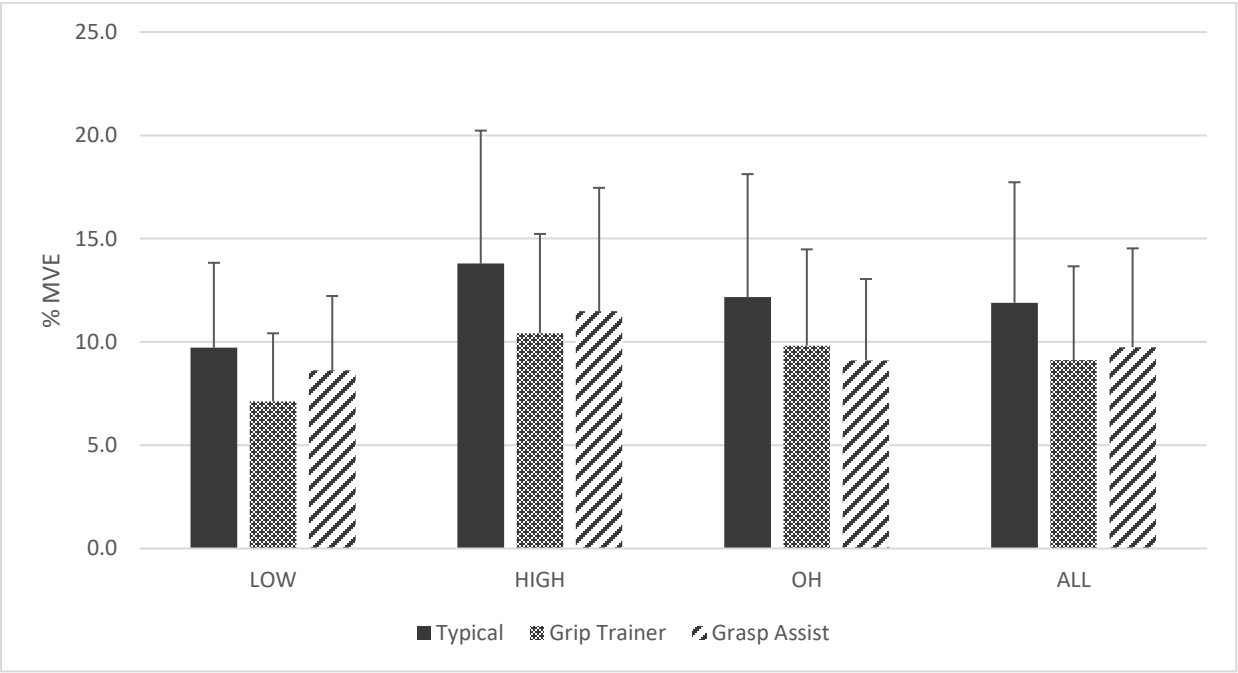

Figure 49 Effect of trial condition on FDS, FCU, EDC, and FCR combined mean muscle activity (±SD) based on fastener location (low, high, overhead, all)

The general trend of the grip trainer was to reduce mean muscle activation compared to the typical trial. Low fastener muscle activation was significantly reduced by 27%, high by 24%, overhead by 19%, and for all fastener locations by 23%. The grasp assist device also reduced mean muscle activation compared to the typical trial by 18%, but it was only significant when considering all of the fastener locations combined.

3.3 Grip Force

The grip force per complete trial (all fastener locations) was found to be 114.8N for the typical condition (T), 73.3N for the grip trainer condition (GT), and 61.2N for the grasp assist condition (GA). Low fasteners required the least amount of force at 99.9N, 55.7N, and 47.9N for T, GT, GA respectively. High fasteners grip forces were similar to the low location at 100.3N, 60.6N, and 50.6N for T, GT, GA respectively. Overhead fasteners were applied with significantly more force at 144.3N, 103.7N, and 85N for T, GT, GA respectively. Given that the tool was oriented vertically for the overhead trial the DC tool could be pushed, and combined with the weight of the tool, the "grip" force may have been artificially increased. The magnitudes of forces in this submaximal, *in situ* study align with previous studies in which maximal grip forces range from 318±66N to 535±129N and higher [38][55]. Mean grip forces with standard deviation (±SD) for all fastener locations and trial conditions are summarized in Table 19. Paired sample t-tests were performed between trial conditions and it was determined that participants used significantly less force during the grip trainer and grasp assist trials than for the typical trial at all fastener locations. This confirmed the primary and secondary hypothesis as it relates to applied grip force.

Table 19 Summary of grip force (N) mean values (±SD) based on locations: low, high, overhead, all, and conditions: typical (T), grip trainer (GT), grasp assist (GA) with significance between conditions (n=9).

Location	Condition	Grip Force (N)
Low	T	99.9 (18.7)
	GT	55.7 (17.6)
	GA	47.9 (19.7)
Significance		GT<T*** GA<T***
High	T	100.3 (17.5)
	GT	60.6 (19.1)
	GA	50.6 (14.6)
Significance		GT<T*** GA<T***
Overhead	T	144.3 (25.7)
	GT	103.7 (21.2)
	GA	85.1 (22.3)
Significance		GT<T** GA<T**
All	T	114.8 (29.6)
	GT	73.3 (29.0)
	GA	61.2 (25.5)
Significance		GT<T*** GA<T***
**p < 0.01, ***p < 0.001		

The results from Table 19 are illustrated in Figure 50, providing a clear, visual representation of the data. When considering all fastener locations, the percent reduction in grip force compared to the typical trial was 36% and 47% for the grip trainer and grasp assist trials, respectively.

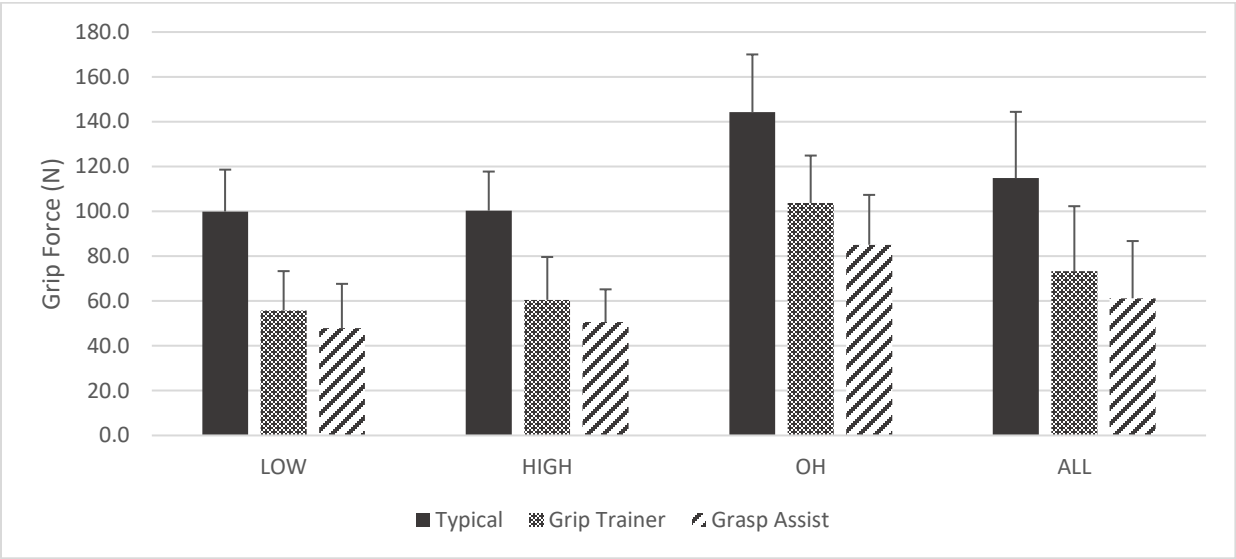

Figure 50 Effect of trial condition on mean applied grip force (±SD) based on fastener location (low, high, overhead, all)

3.4 Revised Strain Index Results

The revised strain index values (RSI) were calculated according to Equation 3 in section 2.5 as $RSI = IM * EM * DM * PM * HM$. The exertions per minute was based on average values from the trial and determined to be approximately 14 efforts per minute ($EM = 2.0$). The duration of the exertion was typically 3.5 seconds ($DM = 1.5$). The drill speed (fastening time) was controlled by the DC tool, however it sometimes took multiple attempts to engage the fastener with the receiving hole, resulting in multiple trigger engagements in a short period of time. Hand/wrist posture was not measured and assumed to be neutral ($PM = 1.0$). The duration of task per day was assumed to be 8 hours ($HM = 1.0$). Therefore, results were based on the intensity multiplier (IM) only.

The RSI was significantly lower for every muscle group when the grip trainer (GT) was used compared to the typical trial (T), and for muscle groups FDS and FCU when the grasp assist (GA) was used compared

to the typical trial (T). When muscle %MVE was combined (per participant, per fastener location) both GT and GA were determined to yield significantly lower RSI values compared to the typical trial. Statistical significance was based on the mean values; however, the minimum and maximum values are also displayed to illustrate the range of RSI (Table 20).

Table 20 Revised Strain Index (RSI) values when fastening bolts at all locations (n=9)

Condition		**FDS**	**FCU**	**EDC**	**FCR**	**Combined**
Typical (T)	Mean (±SD)	3.9 (2.9)	5.7 (3.7)	8.0 (5.3)	3.2 (2.3)	5.2 (3.3)
	Min	2.0	3.7	2.6	1.7	2.8
	Max	6.2	10.1	13.0	4.8	7.9
Grip Trainer (GT)	Mean (±SD)	3.1 (2.3)	4.3 (2.9)	7.1 (4.7)	2.8 (2.0)	4.4 (2.8)
	Min	1.6	2.3	2.3	1.6	2.1
	Max	4.7	6.0	10.2	4.0	6.1
Grasp Assist (GA)	Mean (±SD)	3.0 (2.1)	3.9 (2.5)	8.0 (5.2)	3.0 (2.3)	4.6 (2.9)
	Min	1.6	1.9	2.4	1.6	2.1
	Max	4.0	4.9	13.6	4.6	6.5
*p<0.05, **p<0.01, ***p<0.001		GT<T***	GT<T***	GT<T**	GT<T***	GT<T***
		GA<T***	GA<T***			GA<T*

The following figures (Figure 51 through Figure 55) illustrate the RSI values summarized in Table 20. Garg et al. determined the safe/hazardous threshold to be 10.0 [34]. This value is overlaid on each figure to provide context.

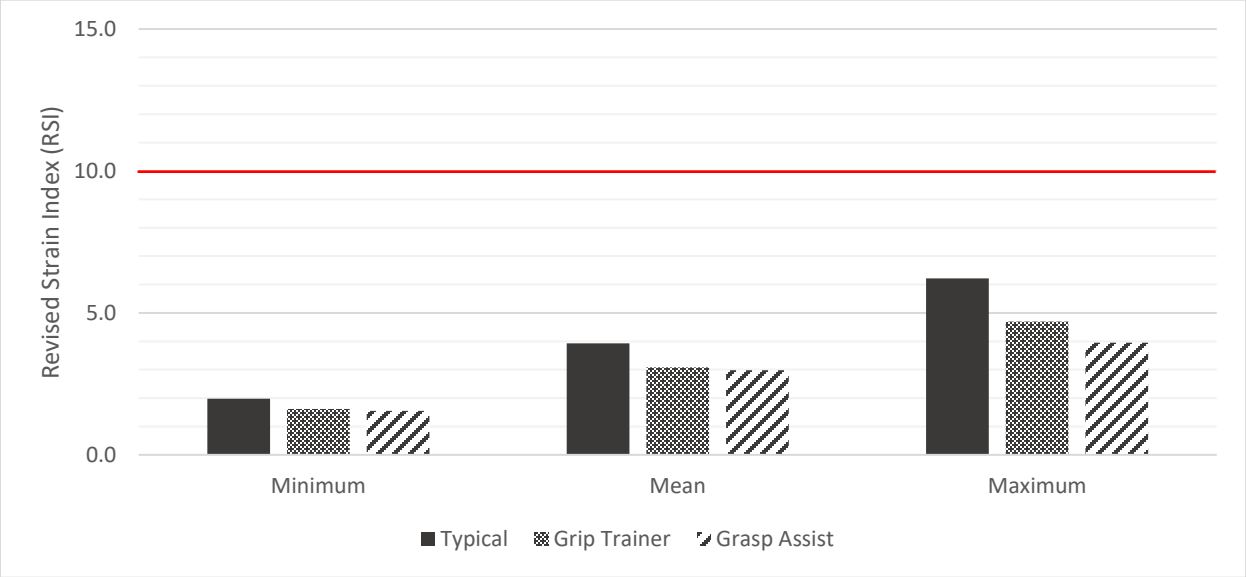

Figure 51 Minimum, mean, and maximum RSI values for FDS muscle and all trial conditions (typical, grip trainer, grasp assist) based on all fastener locations with hazardous threshold overlaid at RSI=10.0 for context (n=9)

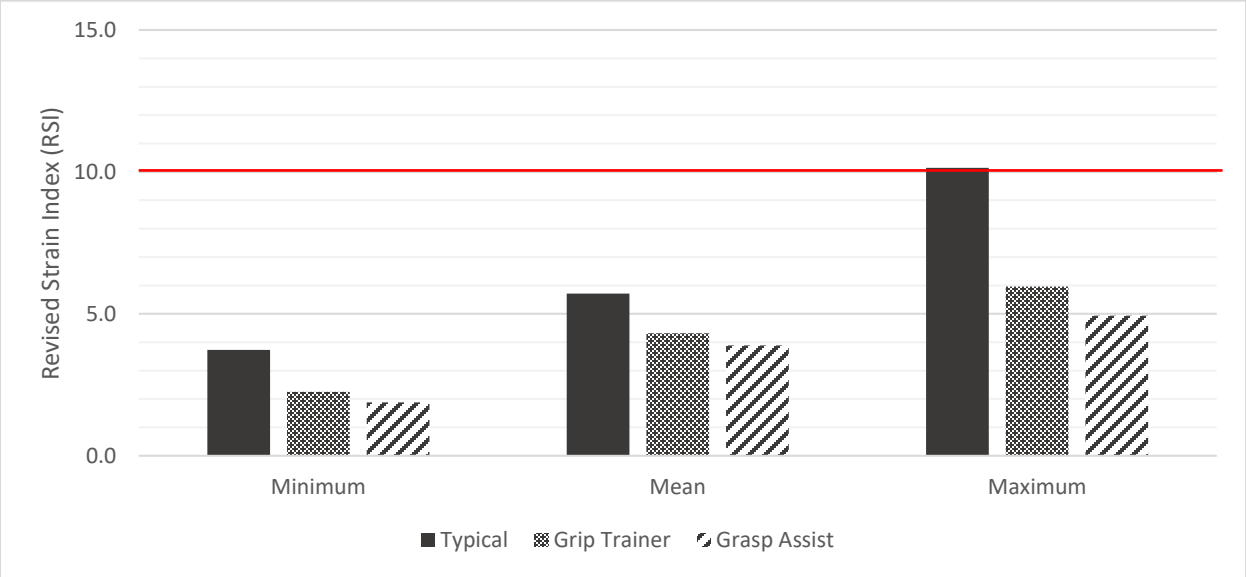

Figure 52 Minimum, mean, and maximum RSI values for FCU muscle and all trial conditions (typical, grip trainer, grasp assist) based on all fastener locations with hazardous threshold overlaid at RSI=10.0 for context (n=9)

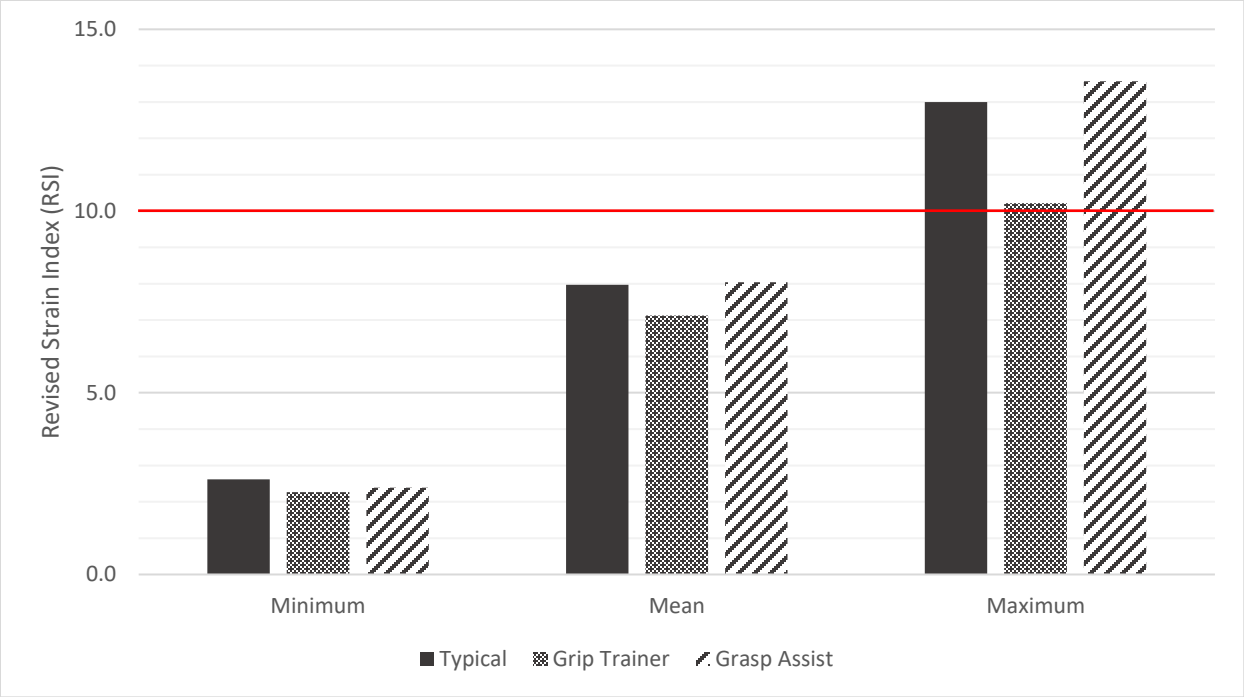

Figure 53 Minimum, mean, and maximum RSI values for EDC muscle and all trial conditions (typical, grip trainer, grasp assist) based on all fastener locations with hazardous threshold overlaid at RSI=10.0 for context (n=9)

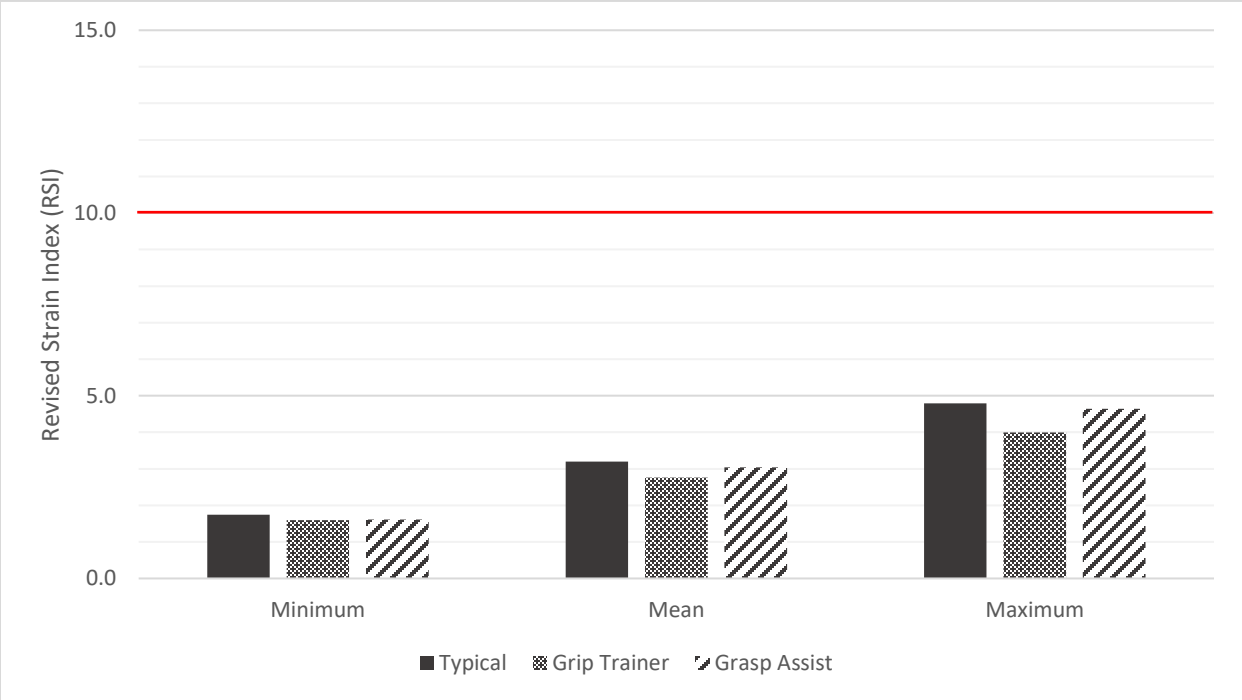

Figure 54 Minimum, mean, and maximum RSI values for FCR muscle and all trial conditions (typical, grip trainer, grasp assist) based on all fastener locations with hazardous threshold overlaid at RSI=10.0 for context (n=9)

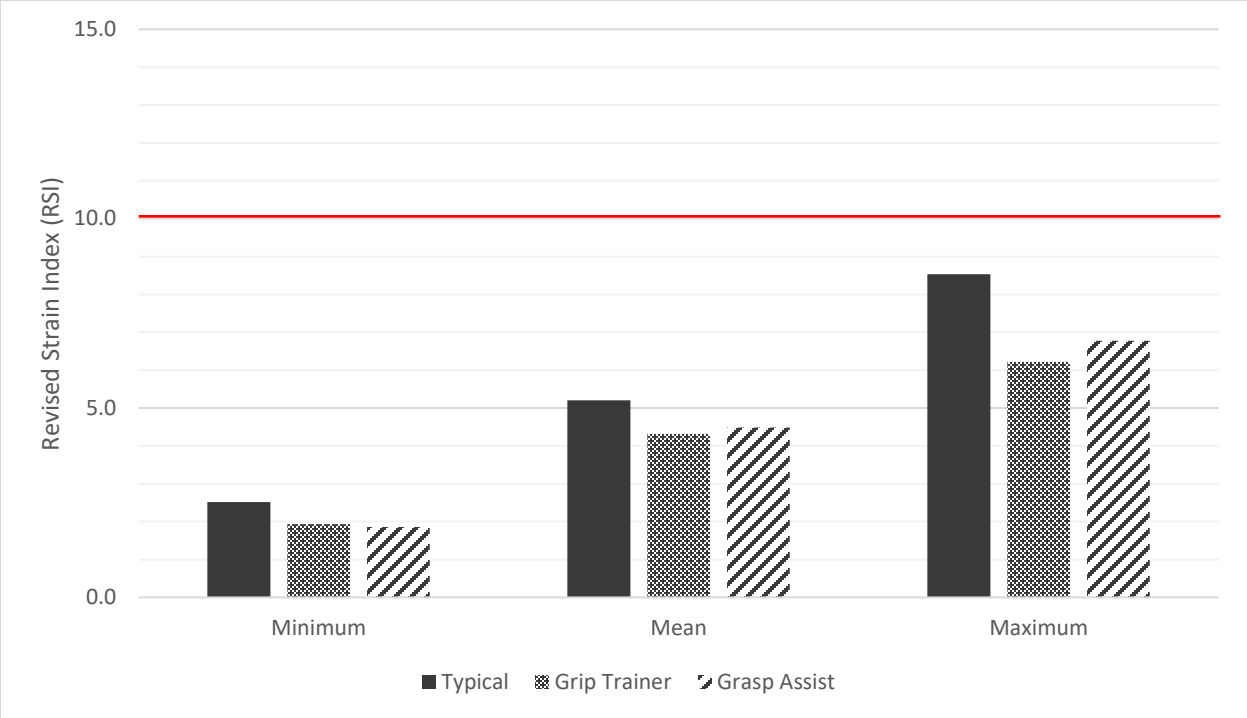

Figure 55 Minimum, mean, and maximum RSI values for FDS, FCU, EDC, and FCR combined, and all trial conditions (typical, grip trainer, grasp assist) based on all fastener locations with hazardous threshold overlaid at RSI=10.0 for context (n=9)

Figure 55 illustrates that although the grip trainer and grasp assist device significantly lower the RSI, the entire activity is still deemed safe. Percent reductions in mean, minimum, and maximum RSI compared to the typical trial were 17%, 23%, and 22% respectively for the grip trainer, and 13%, 25%, and 17% respectively for the grasp assist.

3.5 Subjective Results

Participants opinions of the grasp assist device are important, as they must be willing to use such a device regardless of the objective results previously presented. Furthermore, feedback could be used to further develop and refine the device to improve both performance and comfort. Figure 56 illustrates that the device was deemed reasonably comfortable (mean of 7.4), supportive (mean of 7.6), and provided ample force (mean of 8.2).

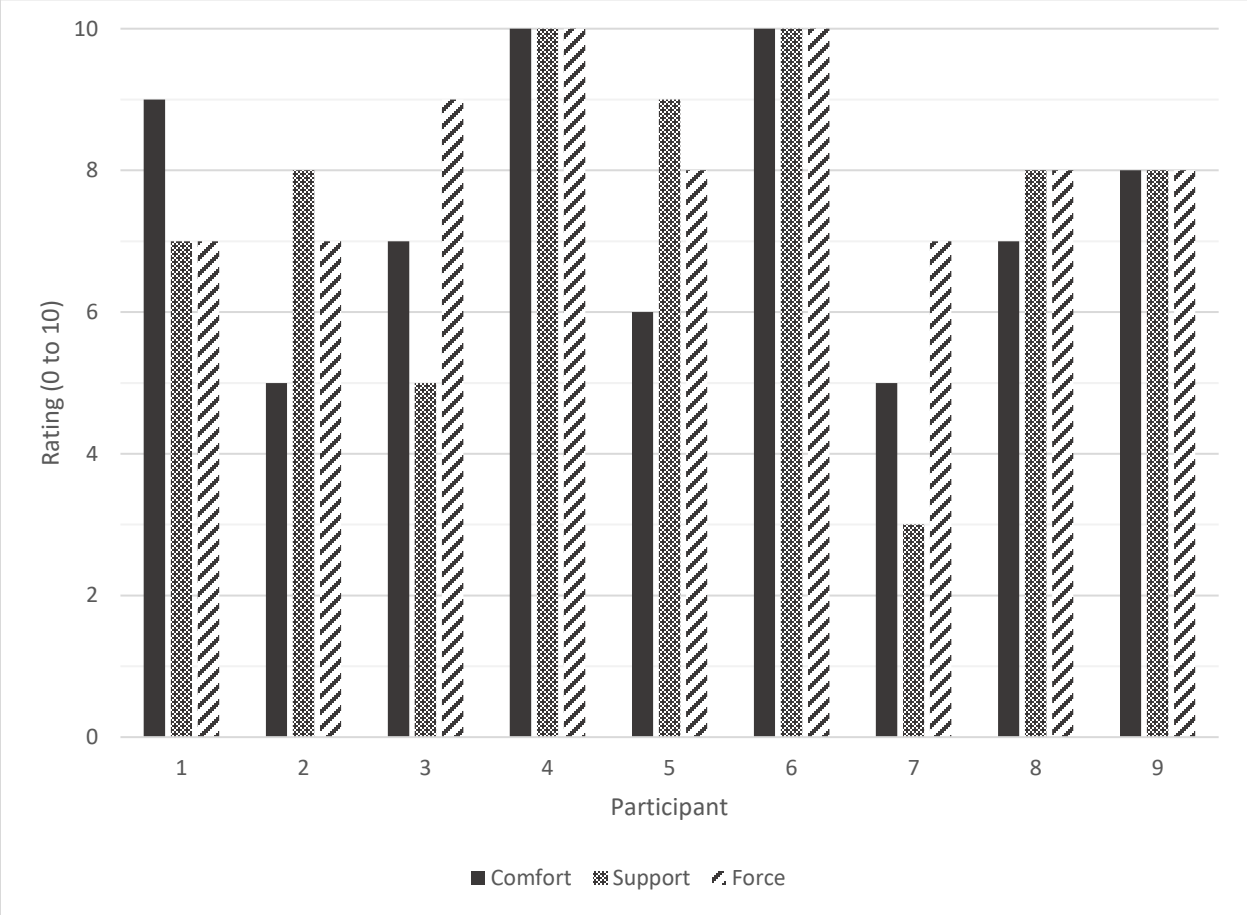

Figure 56 Subjective responses to using the grasp assist device

Written feedback about the grasp assist device was constructive, quoted as follows: “ring finger & pinky were a little uncomfortable”, “awkward”, “need thinner version”, and “would be better in a glove version”. One response indicated that in regard to fastening the bolts, “makes it effortless”.

4 Discussion

The primary purpose of this research was to evaluate the effects of a dynamic hand-wrist orthosis (grasp assist) on flexor and extensor forearm muscle activity and grip force in an industrial environment on healthy, able-bodied participants using a common pistol grip DC tool. A second, passive device was developed to provide visual grip force feedback to the participants (grip trainer) whose effects were also evaluated based on muscle activity and grip force. The study had participants install mechanical fasteners using the DC tool at three locations, all of which were reasonable based on daily workplace activities. The effectiveness of both devices was determined by comparing results with a baseline trial where no device was used.

To the best of our knowledge, this research is unique based on a number of factors. First and foremost is the *in situ* nature of the study. Previous studies have investigated the individual components of such a study, but not combined as this research presents it. In 1989 Radwin et al. measured the muscle activity of the flexor palmaris longus, FCR, and EDC during the installation of mechanical fasteners using a right-angled pneumatic drill [85]. The tool was modified with a brake to simulate fastener response; however, no fasteners were used, and the study was not performed in a workplace. Grip force was not directly measured during the study. Instead, it was inferred from EMG results that were calibrated using a strain gauge dynamometer with two bars spanning 3cm. More recently, Hoozemans and van Dieën commented that even in 2005 *in situ* testing was difficult to perform in the workplace and also attempted to estimate grip force based on EMG results [11]. They measured flexor and extensor forearm muscle activity during a calibration task with a strain gauge split handle and developed a predictive model. The model was applied to voluntarily varied levels of grasp force lasting eight seconds, with reasonable agreement between observed and predicted output. Measured output forces were less than 300N, and error between measured and predicted ranged from 27N to 41N. While the method of predicting grip force using EMG is convenient, it is not complete. Deep muscles such as the flexor digitorum profundus (FDP) and the flexor pollicis longus (FPL) also affect grip force and cannot be measured using sEMG. All forearm muscles contribute simultaneously

to grasping activities to some degree, and tasks may require more of certain muscles than others; therefore, using sEMG to predict grasping force cannot be conclusive.

A study by Seo and Armstrong in 2008 assisted in providing the groundwork necessary to overcome the need to predict grip force using EMG by instrumenting handles with pressure sensors [31]. In this study, grip forces were measured using a strain gauge split handle device and a pressure mapping system applied to a cylinder with the same diameter were compared. They determined that pressure-mapped mean normal forces were 2.3 times greater (R^2=0.65) than those measured with the split handle. Both devices measured normal force, however the split handle was limited to a single orientation where the pressure map covered 360°, illustrated in Figure 57. A pressure mapped handle is therefore more capable of accurately measuring force applied to a tool, as the user may apply more force parallel to the split tool sensor than normal to it, depending on preference. More recently in 2012 Nicholas et al. studied the force interaction between the hand and a pressure mapped cylinder during grasping, pushing, and pulling, isolating the locations of maximum contact force [32]. While useful in their own regard, neither of these studies recorded EMG and both used cylindrical handles in a laboratory environment. What they did provide, is verification towards the application of the equipment to the *in situ* testing in this research.

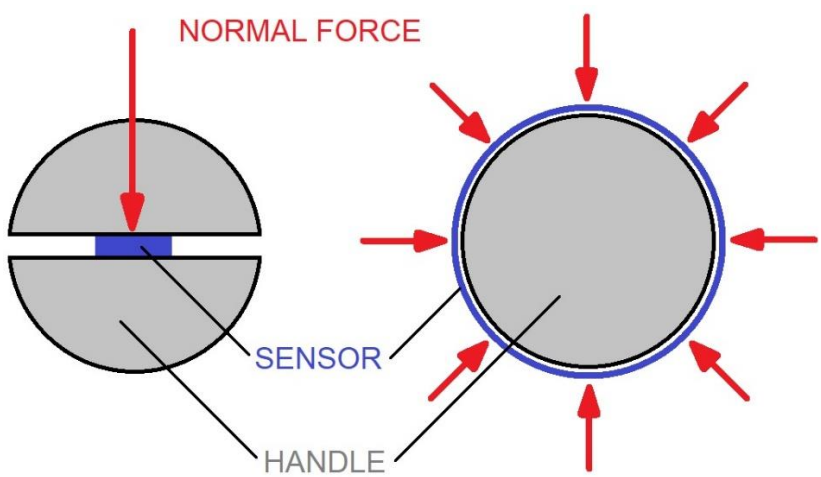

Figure 57 Normal force distribution on a split handle (left) and a pressure mapped handle (right)

In addition to the *in situ* factor, the cohort contributed to the uniqueness of this research. While Radwin's et al. 1989 study discussed earlier used real-world tools, the power tool experience of the participants ranged from zero to over 30 years, with no indication of their employment [85]. Potvin et al. evaluated and compared the risk of CTD injury using a pneumatic tool versus a DC tool using sEMG and a cohort of college students – 15 male (age = 22.9±4.3 years) and 15 female (age = 21.7±0.8 years) [86]. They found that using a DC tool can reduce muscle activity of the FCU, FCR, ECU, and ECR; however, grip force was not measured. Johnson suggested in 1988 that the occupation and the level of experience of a cohort is irrelevant, as industrial workers do not use tools differently than the general public [87]. This is counterintuitive, as an individual with sufficient training and experience with a tool will likely use it differently. It is therefore not unreasonable to imagine a negative correlation between power tool experience and grip force – as experience increases and the participant becomes more comfortable with a tool, grip force would decrease. However, a weak *positive* correlation between experience and grip force was determined from this research for typical (0.21), grip trainer (0.48), and grasp assist (0.27) scenarios, indicating that grip force increases with experience, albeit weakly.

Johansson et al. measured the effects of a stiff orthosis and a commercially available orthosis on forearm muscle activity during tasks involving holding weighted cylinders, a simulated cutting task, and striking a bar on 12 non-professional tool users – six male (age = 38±8 years) and six female (age = 36±6 years) [38]. Ferrigno et al. also measured the effects of passive orthoses on muscle activity in healthy individuals, though they used real-world, typical clerical tasks [40]. Although this work applied orthoses to a real-world application, the force applied during clerical tasks is less than industrial tasks and grip force was not measured.

Dynamic orthoses are primarily applied to individuals with reduced muscle strength, stroke patients, and/or the elderly, to assist in daily living activities (see section 1.4.2). Although many of these devices have been designed for the aforementioned applications, few have been tested. Even commercially available devices such as the SEM Glove are still undergoing clinical studies at the time of this writing. One applicable

example by Yap et al. demonstrated the effectiveness of a soft, pneumatic grasp assist device with the help of two stroke survivors. They showed a significant reduction in muscle activation when the device was used compared to when it was not, performing standardized Jebsen hand function tests – grasping and manipulating an empty water bottle (20g, diameter = 60mm) and a tin can (454g, diameter = 75mm) [54].

Finally, the devices used in the study contributed to making this research unique. The design of the dynamic grasp assist device has improved upon previous works by Yap et al., and we are not aware of another passive grip training system. Both of these devices are discussed in their own sections below, along with the primary and secondary hypotheses.

4.1 Grasp Assist Device

The actuator designed and applied to the grasp assist device in this research offers a marketed improvement over existing soft pneumatic actuators. Cast silicone pneu-net actuators generate tip forces between 9N [53] and 27N [88] at approximately 225kPa, and given their relative low force generation were not considered further. The design most similar is by Yap et al., as it was the starting point for the actuators used here, discussed in section 2.1.1. Their straight bellow design generated approximately 63N of constrained tip force and a bending ratio of 0.23 at 240kPa experimentally, with dimensions 150mm, 25mm, and 11mm (length, width, height) [52]. The modified design presented here also generated 63N of constrained tip force and a bending ratio of 0.30 at 240kPa experimentally; however, the dimensions were 126mm, 20mm, and 11mm (length, width, height). The modified design generates the same force but is 20% narrower (22% less active width, with a 1.2mm thickness) and 16% shorter. Furthermore, where Yap constrained the actuator on the most proximal surface, the actuators tested in this work were constrained 20mm proximally, essentially reducing the length to 106mm. Keeping other dimensions constant, longer actuators generate more force and a lower (better) bending ratio. The two designs are presented in Figure 58 to illustrate their similarities and differences.

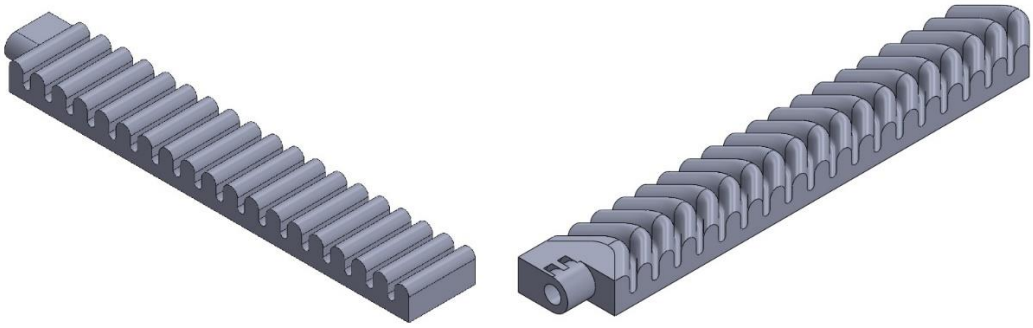

Figure 58 Actuator design by Yap et al. (left) and improved based on presented research (right)

4.2 Primary Hypothesis

The primary hypothesis was proven correct – using a grasp assist device significantly reduced combined mean muscle activation and grip force compared to a typical condition in which no device is used. Combined mean (±SD) muscle activation for all fastener locations was 9.7%MVE (4.8) with the grasp assist device, and 11.9%MVE (5.8) for the typical scenario, yielding a significant overall reduction of 18.5% ($p < 0.05$). When considering individual muscles, the device significantly reduced the muscle activity of the FDS and FCU muscles compared to the typical trial by 37.2% and 42.5% respectively; however, the EDC and FCR muscles were not found to be significantly different than the typical trial. This suggests that the device supports the hand in ulnar deviation (FCU) and grasping (FDS). It is possible that this was a result of participants using their right hand on right-handed fasteners, which pressed the tool into the hand due to the torque direction; however, a separate study would be required to verify this. Mean (±SD) grip force for all fastener locations was significantly lower at 61.2N (25.5) with the grasp assist device compared to 114.8N (29.6) for the typical scenario ($p < 0.001$). Mean (±SD) revised strain index values were also found to be significantly lower for the grasp assist trial compared to the typical trial, 4.6 (2.9) and 5.2 (3.3) respectively ($p < 0.05$). While both scenarios are deemed "safe" (RSI < 10.0) [34], the grasp assist device significantly reduced both the mean RSI value and its range by 13% compared to without the device. Furthermore, the hazardous threshold for RSI was based on biceps brachii data and may be different for forearm muscles.

Limited data was available regarding the effect of a grasp assist device on the muscle activity in an able-bodied population. Previous studies by Ferrigno et al. and Johansson et al. have shown that during daily living activities passive orthoses do not reduce muscle activity, and instead tend to *increase* muscle activity, while Jansen et al. concluded that grip strength significantly decreased but extensor muscle activity did not [83]. Ferrigno et al. measured a significant increase in muscle activity of flexor (FDS) and extensor (ECU) muscles during computer work using a mouse with a stiff, passive orthosis by 51.3% and 13.1% respectively ($p < 0.05$), when compared to no orthosis [40]. Johansson et al. performed a similar study comparing passive orthosis and measured a significant increase in FDS muscle activity of 39.3% and 47.9% (at 20%MVC ($p < 0.05$) and 40%MVC ($p < 0.001$), respectively) and no significant change in extensor muscle activity when using a stiff orthosis compared with no orthosis [38]. The grasp assist device investigated in this research could be considered "stiff" when inflated; however, a significant *decrease* in flexor (FDS) muscle activity was measured when considering all fastener locations of 37.2%, and no significant difference to extensor (EDC) muscle activity (Table 18). While not a direct comparison given the nature of the devices and the tasks performed, the results presented here support the effectiveness of the grasp assist device.

In a non-able-bodied population, Yap et al. measured a remarkable difference in both flexor and extensor muscle activation during a standardized gripping task when using a pneumatic grasp assist device compared to without, illustrated in Figure 59. Similar to the passive othoses studies described above, Yap's study does not directly compare to this research. The participants were stroke victims (n=2), and the tasks performed were simulated daily living activities [54].

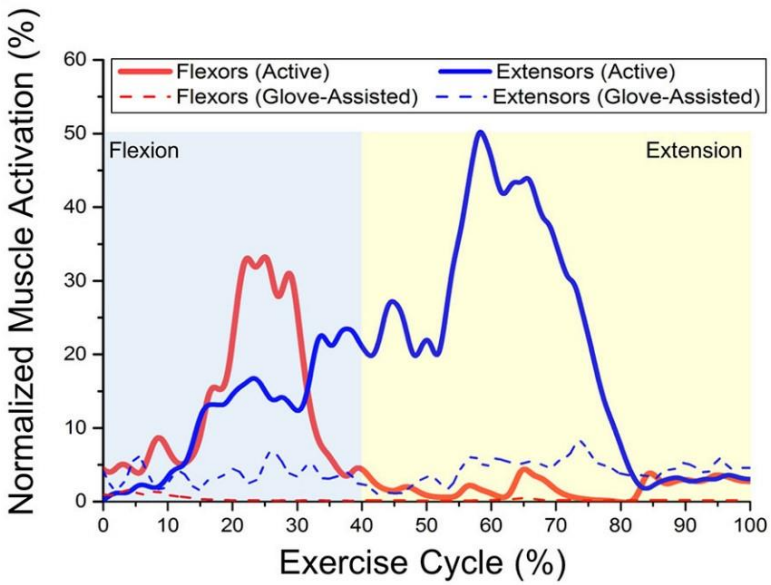

Figure 59 Averaged muscle activation profiles during active and glove-assisted trials, adapted from Yap et al 2017 [54]

4.3 Grip Training Device

To the best of our knowledge, a grip trainer device has not been previously designed or investigated. Many studies use visual feedback to target certain force values, but not in a laboratory environment and not as the primary purpose. For example, in 1999 Burden and Bartlett used a digital system to display 50N, 100N, 150N, and 200N grasp force targets for an EMG normalization study – not for a workplace activity [81]. In 2004 Johansson et al. used an analog meter in front of the participant to allow them to target 5%, 20%, and 40%MVC to evaluate muscle activation using passive orthoses during a custom grasping activity – not for a workplace activity [38]. Rossi et al. used a grip force visual feedback system in 2012, but it was displayed on a computer screen with the purpose of characterizing grip force versus handle diameter – again, not for a workplace activity [89]. More recently in 2012, Nicholas, et al. recorded trials at 100%, 50%, 25%MVC using a grip dynamometer with a digital readout from a Tekscan pressure map on a computer to determine contact force and area between the hand and the handle [32]. The concept between the grip training device and these studies is similar, however the application differentiates it.

Industrial ergonomics focuses on reducing CTD risk factors by improving posture, reducing task repetition, as well as the required force for a task. Posture is visually apparent (i.e. flexed or extended wrist), as is

repetition – one can readily see the frequency of a movement or task. It is easy to overlook force applied to a tool however, as there is no apparent difference between too much force and the correct amount of force for a task. For example, a grasping task may be designed to require only 50N of force but there is nothing preventing an individual from applying 100N or 200N of force, nor are there visual cues. Even if an individual received training on applying the proper amount of force, other factors such as mood, absentmindedness, fatigue, or preference could affect their grip force day-to-day. If proper training was not received, then preference, previous experience, comfort, and even fear of a tool will influence their applied grip force. Visually alerting an individual as to when more force than necessary is being applied has the potential to negate these factors.

Additional benefits may arise from using a grip training system, such as conscientiousness. A worker actively made aware of their applied grip force may also be more aware of the activity they are performing as well as their behaviour; that is to say, they may be more present during the activity. Wallace and Vodanovich demonstrated that cognitive failure can account for workplace safety behavior and accidents, specifically when conscientiousness is low. Cognitive failure can be described as making an error or mistake that "a person should normally be capable of completing" [90]. They found a significant positive correlation between cognitive failure and accidents (0.35, $p < 0.05$) and a significant negative correlation between conscientiousness and accidents (-0.17, $p < 0.05$) in a cohort of 219 production workers [90].

4.4 Secondary Hypothesis

The secondary hypothesis was also proven correct – using a grip training device significantly reduced combined mean muscle activation and grip force compared to a typical condition in which no device is used. Mean (±SD) combined muscle activation for all fastener locations was 9.1%MVE (4.5) with the grip trainer device, and 11.9%MVE (5.8) for the typical scenario, yielding a 23.5% reduction in combined muscle activation. Where the grasp assist device significantly reduced muscle activity specifically in the FDS and FCU, the grip trainer significantly reduced *all* measured muscle activity ($p < 0.001$). The FDS, FCU, EDC, and FCR saw reductions in muscle activities compared to the typical scenario of 33.3%, 32.8%,

13.5%, and 23.2%, respectively. This significant difference between devices highlights the participants ability to control/reduce bulk muscle forces when cognisant of the task requirements. Mean (±SD) grip force for all fastener locations was 73.3N (29.0) with the grasp assist device, and 114.8N (29.6) for the typical scenario – a 36.1% reduction. Mean (±SD) revised strain index values were also found to be significantly less for the grip trainer trial compared to the typical trial, 4.4 (2.8) and 5.2 (3.3) respectively. Both scenarios are "safe" (RSI < 10.0); however, the grip trainer reduced the mean RSI by 17% and its range by 22% compared to without it, illustrated in Figure 55.

4.5 Applicability and Usefulness

A relevant finding from this study is that although both devices significantly reduced muscle activity compared to the typical trial, they were not significantly different from each other ($p = 0.358$). The grasp assist device of the design and input pressure presented in this study reduced combined muscle activity no more than the participant did by consciously using less force. Individual muscles did respond differently to the two devices, with a greater muscle activity reduction in the FDS and FCU using the grasp assist device (37.2% and 42.5% less than typical) than the grip trainer (33.3% and 32.8% less than typical). Given the affect of FDS and FCU on grip force, it follows that mean grip force values were significantly lower for the grasp assist scenario than for the grip trainer ($p < 0.001$). The EDC and FCR muscles responded more favorably towards the grip trainer device with a significant reduction in muscle activity of 13.5% and 23.2% respectively, where no significance was found between the grasp assist and the typical trial. In fact, Figure 53 illustrates that the RSI range of EDC muscle activity for the typical ($RSI = 13$) and grasp assist ($RSI = 13.5$) trials significantly exceeded the hazardous threshold value of 10.0, while the grip trainer trial was at the threshold.

There are many conceivable applications for both devices, but this research focused solely on an industrial environment. The grasp assist device appeared more suited for reducing grip force and could be applied to situations where higher grip force is required such as high torque drills, high force switches, or carrying heavy objects. The grip trainer appeared more suited for applications where lower force is required, but

excessive force can readily be applied, such as lower torque drills, screw drivers, or even handles on carts. Given that pistol grip power tools comprise approximately 40% of all hand held tools in a typical factory and that work-related upper extremity disorders can account for 13% or more of lost work injuries [86], there is a large and definitive population to which these devices may be applied.

Perhaps the most relevant finding of this research was that individuals used significantly more muscle force than required to complete an activity. Given that an activity does not appear visually different depending on force applied, nor is its success determined by applying more than the minimum force, excessive force most often goes unnoticed. This knowledge can be used to better train workers to use the minimum force required for an activity. Furthermore, workers can be educated on the cause and effect between CTD risk factors (posture, repetition, force) and injury. This may improve awareness and conscientiousness in the workplace, resulting in fewer injuries.

4.6 Limitations and Recommendations

The results of this study indicated that a grasp assist device yielded significantly lower grip force than the grip trainer condition, yet the muscle activity between these conditions was not significantly different. This study measured the FDS, FCU, EDC, and FCR muscle activity and while the contribution of these muscles to grip force is well documented [10][11][12][91], additional muscles have been shown to contribute to grip force including the extensor carpi radialis and extensor carpi ulnaris [10][11][91]. It is recommended that future studies investigate the effects on additional superficial muscles including those listed above; however, other non-intuitive muscles may also be affected. For example, Ferrigno et al. showed an approximately 100% increase in trapezius muscle activity when using both a stiff and a commercially available orthosis during a keyboard and mouse activity [40].

The grasp assist device was designed for the right hand, and only fasteners of a right-handed orientation were used in this research. The direction of torque generated by the tool was therefore *into* the participants

right hand, where for left-handed individuals it would be *out of* their left hand. Muscle activation would likely be different under such a configuration and warrants future study.

The design of the study was a limitation of the results. All participants performed the typical trial first, followed by the grip trainer, then the grasp assist trial; therefore, a learning effect is a possible confound to this study. Muscle activation and grip forces may have been lower in the second and third trial as the participants learned to perform the task. As well, the number of participants limited the statistical significance of the results and many more would have been required for a randomized trial study. A larger cohort was not feasible for this study as HCM limited the number participants based on production and availability (participants left their position on the factory line to participate). Both limitations could be addressed in a future study by randomizing the trials and increasing the number of participants.

The Tekscan 9830 pressure sensor was another limitation of the study. Upon recalibrating the sensor after the study, it was determined that four Sensels were not responding. Although a small percentage of the total number of Sensels (5.6%), they were located on/around the DC tool trigger where force was obviously exerted. It is recommended that future studies investigate an improved method for measuring grip force, with a calibration method that can be performed prior to each participant. One such method by Nicholas et al. used a rubber bladder inside an acrylic cylinder to apply a uniform pressure to the sensor [32], but would need to be inverted and adapted to the non-cylindrical tool handle used in this study.

Wrist flexion and extension angles were not measured during this study but can more than double the incidence rate of CTS, especially when combined with high grip force [27]. It has been shown that a neutral position could reduce job-associated upper extremity disorders [92]. When considering the revised strain index, a flexion angle of 45° increases the posture multiplier (PM) to 1.6, and a flexion of 90° increases PM to 2.5. An extension angle of 45° increases PM to 1.1, and 90° to 2.0. Therefore, it is recommended that future studies measure wrist angle to more accurately determine the holistic effects of a grasp assist device.

The failure threshold of the actuators used in the grasp assist device limited its performance. While able to achieve internal pressures greater than 345kPa (~50psi) in the controlled environment of a laboratory, a small number of actuators ruptured at 172kPa (~25psi) for the small/medium size, and 138kPa (~20psi) for the large/x-large size which limited the performance (bending ratio and force output). This limitation was a result of the 3D printing manufacturing process. Anisotropy and stress concentrations introduced by the process reduce the strength of the printed part [93] and are highly subject to the settings, specifically print speed and layer thickness [94][95]. Injection molding is one process that could be used to manufacture the actuators in the future to improve strength and allow for greater input pressure. The process involves melting the material and injecting it into a mold, where it is then cooled and ejected. Using this method would remove both the stress concentrations and anisotropy introduced by 3D printing and is recommended for future developments.

Regarding the Ninjaflex® material characterization of the finite element model, only uni-axial tensile test data was used which is not preferable when applying the Ogden strain energy function [61]. Future work could either improve the material model and optimize the 3D print settings or optimize the material characteristics and find a material or blend of materials to match. The latter would support the injection molding process discussed above.

A stronger, better performing grasp assist device could further reduce required muscle activation for a task; however, such a high performing device may cause adverse repercussions to the dorsal aspect of the hand that should be considered, including reduced blood flow and discomfort. The grasp assist trigger mechanism should also be investigated, as a stronger assistive device may require increased muscle activity to release the DC tool trigger.

5 Conclusion

The purpose of this study was to design a pneumatic grasp assist device and quantify its effects on muscle activation and grip force during a DC tool activity within an industry cohort. A grip training device with real-time grip force visual feedback was also developed and tested for effects on muscle activation and grip force. The following conclusions can be drawn from this research:

- There was a large variation in grip force applied to a DC tool during a common fastening activity ranging from 76N to 142N. Wearing a grasp assist device can reduce the grip force variation (30N to 92N), as can utilizing a visual feedback device (38N to 91N). A slight positive correlation between power tool experience and grip force existed for all three of these conditions (0.21, 0.27, 0.48 respectively) indicating that experience does not translate to lower grip force application.
- A pneumatic grasp assist device was shown to significantly reduce mean grip force compared to without such a device (61.2±25.5N, 114.8±29.6N respectively), as well as significantly reduce combined mean muscle activation (9.7%MVE, 11.9%MVE respectively).
- A grip training system with real-time grip force visual feedback significantly reduced mean grip force compared to without such a system (73.3±29.0N, 114.8±29.6N respectively), as well as significantly reduced combined mean muscle activation (9.1%MVE, 11.9%MVE respectively).
- Mean muscle activation when using a pneumatic grasp assist device was not significantly different than when using a grip training system; however, mean grip force *was* significantly lower.
- With regards to the revised strain index, the activity used in this research was determined to be safe when considering the mean muscle activation ($RSI < 10.0$), although when considering the maximum mean percent muscle activation, the activity entered the hazardous region ($RSI > 10.0$).

References

[1] M. C. T. F. M. De Krom, P. G. Knipschild, A. D. M. Kester, C. T. Thijs, P. F. Boekkooi, and F. Spaans, "Carpal tunnel syndrome: Prevalence in the general population," *J. Clin. Epidemiol.*, vol. 45, no. 4, pp. 373–376, 1992.

[2] T. J. Armstrong, L. J. Fine, S. A. Goldstein, Y. R. Lifshitz, and B. A. Silverstein, "Ergonomics considerations in hand and wrist tendinitis," *J. Hand Surg. Am.*, vol. 12, no. 5, pp. 830–837, 1987.

[3] B. A. Silverstein, L. J. Fine, and T. J. Armstrong, "Hand wrist cumulative trauma disorders in industry.," *Br. J. Ind. Med.*, vol. 43, no. 11, pp. 779–784, 1986.

[4] R. Bakker, M. Kalra, S. S. Tomescu, R. Bahensky, and N. Chandrashekar, "The Effects of Pistol Grip Power Tools on Median Nerve Pressure and Tendon Strains," Unpublished, Waterloo, ON, 2017.

[5] Statistics Canada, "Employment by industry, annual." p. Table 14-10-0202-01, 2016.

[6] Bureau of Labor Statistics, "Employment by major industry sector," *United States Department of Labor*, 2017. [Online]. Available: https://www.bls.gov/emp/tables/employment-by-major-industry-sector.htm. [Accessed: 20-Jul-2019].

[7] "Muscles of the human forearm (anterior view, superficial layer)," *Encyclopædia Britannica*, 2008. [Online]. Available: https://www.britannica.com/science/median-nerve/media/1/372169/111229. [Accessed: 20-Jul-2019].

[8] "The structures of the wrist associated with carpal tunnel syndrome," *Encyclopædia Britannica*, 2007. [Online]. Available: https://www.britannica.com/science/carpal-tunnel/media/1/96673/121609. [Accessed: 20-Jul-2019].

[9] "Muscles of the forearm (posterior view).," *Encyclopædia Britannica*, 2008. [Online]. Available: https://www.britannica.com/science/arm/media/1/35010/121138. [Accessed: 20-Jul-2019].

[10] F. Bano, Z. Mallick, and A. A. Khan, “The effect of grip force, stroke rotation and frequency on discomfort for a torqueing tasks,” *Work*, vol. 53, no. 4, pp. 691–708, 2016.

[11] M. J. M. Hoozemans and J. H. Van Dieën, “Prediction of handgrip forces using surface EMG of forearm muscles,” *J. Electromyogr. Kinesiol.*, vol. 15, no. 4, pp. 358–366, 2005.

[12] Y. Kadowaki, T. Noritsugu, M. Takaiwa, D. Sasaki, and M. Kato, “Development of soft power-assist glove and control based on human intent,” *J. Robot. Mechatronics*, vol. 23, no. 2, pp. 281–291, 2011.

[13] T. J. Armstrong, R. G. Radwin, D. J. Hansen, and K. W. Kennedy, “Repetitive trauma disorders,” *Job Eval. Des.*, vol. 27, no. 1, pp. 325–336, 1986.

[14] A. Moore, R. Wells, and D. Ranney, “Quantifyit1tesng exposure in occupational manual tasks with cumulative trauma disorder potential,” *Ergonomics*, vol. 34, no. 12, pp. 1433–1453, 1991.

[15] S. A. Goldstein, T. J. Armstrong, D. B. Chaffin, and L. S. Matthews, “Analysis of cumulative strain in tendons and tendon sheaths,” *J. Biomech.*, vol. 20, no. 1, pp. 1–6, 1987.

[16] C. D. Jennings, K. Faust, S. J. Fischer, and F. J. Leversedge, “Carpal Tunnel Syndrome,” *American Academy of Orthopaedic Surgeons*, 2016. [Online]. Available: https://orthoinfo.aaos.org/en/diseases--conditions/carpal-tunnel-syndrome/. [Accessed: 21-Jul-2019].

[17] A. Yassi, J. Sprout, and R. Tate, “Upper limb repetitive strain injuries in Manitoba,” *Am. J. Ind. Med.*, vol. 30, no. 4, pp. 461–472, 1996.

[18] B. Silverstein, E. Welp, N. Nelson, and J. Kalat, “Claims incidence of work-related disorders of the upper extremities: Washington State, 1987 through 1995,” *Am. J. Public Health*, vol. 88, no. 12, pp. 1827–1833, 1998.

[19] B. A. Silverstein, L. J. Fine, and T. J. Armstrong, “Occupational factors and carpal tunnel

syndrome," *Am. J. Ind. Med.*, vol. 11, no. 3, pp. 343–358, 1987.

[20] K. Kurppa, E. Viikari-Juntura, E. Kuomas, M. Huuskonen, and P. Kivi, "Incidence of tenosynovitis or peritendinitis and epicondylitis in a meat-processing factory," *Scand. J. Work. Environ. Heal.*, vol. 17, no. 1, pp. 32–37, 1991.

[21] R. A. Werner, A. Franzblau, N. Gell, S. S. Ulin, and T. J. Armstrong, "A longitudinal study of industrial and clerical workers: Predictors of upper extremity tendonitis," *J. Occup. Rehabil.*, vol. 15, no. 1, pp. 37–46, 2005.

[22] A. Fields, S. Uppal, S. LaRochelle-Côté, and Statistics Canada, "Insights on Canadian Society: The impact of aging on labour market participation rates," *Can. Labour Force Surv.*, no. 75, p. 10, 2017.

[23] U.S. Bureau of Labor Statistics, "Labor Force Statistics from the Current Population Survey," 2019. [Online]. Available: https://data.bls.gov/PDQWeb/ln. [Accessed: 21-Jul-2019].

[24] J. Park, "Obesity on the job," *Perspect. Labour Income*, vol. 10, no. 2, pp. 14–22, 2009.

[25] B. P. Bernard, "Musculoskeletal Disorders and Workplace Factors," *Public Health*, no. July 1997, pp. 1-1-7–11, 1997.

[26] T. J. Armstrong, L. J. Fine, R. G. Radwin, and B. S. Silverstein, "Ergonomics and the effects of vibration in hand-intensive work," *Scand. J. Work. Environ. Heal.*, vol. 13, no. 4, pp. 286–289, 1987.

[27] K. T. Palmer, E. C. Harris, and D. Coggon, "Carpal tunnel syndrome and its relation to occupation: A systematic literature review," *Occup. Med. (Chic. Ill).*, vol. 57, no. 1, pp. 57–66, 2007.

[28] T. J. Armstrong and D. B. Chaffin, "Some biomechanical aspects of the carpal tunnel," *J. Biomech.*, vol. 12, no. 7, pp. 567–570, 1979.

[29] R. W. McGorry *et al.*, “Effect of grip type, wrist motion, and resistance level on pressures within the carpal tunnel of normal wrists,” *J. Orthop. Res.*, vol. 32, no. 4, pp. 524–530, 2014.

[30] R. Roy, D. Sikdar, M. Mahadevappa, and C. S. Kumar, “EEG based motor imagery study of time domain features for classification of power and precision hand grasps,” *Int. IEEE/EMBS Conf. Neural Eng. NER*, no. May, pp. 440–443, 2017.

[31] N. J. Seo and T. J. Armstrong, “Investigation of Grip Force, Normal Force, Contact Area, Hand Size, and Handle Size for Cylindrical Handles,” *Hum. Factors J. Hum. Factors Ergon. Soc.*, vol. 50, no. 5, pp. 734–744, 2008.

[32] J. W. Nicholas, R. J. Corvese, C. Woolley, and T. J. Armstrong, “Quantification of hand grasp force using a pressure mapping system,” *Work*, vol. 41, no. SUPPL.1, pp. 605–612, 2012.

[33] P. Marcotte, Y. Aldien, P. É. Boileau, S. Rakheja, and J. Boutin, “Effect of handle size and hand-handle contact force on the biodynamic response of the hand-arm system under zh-axis vibration,” *J. Sound Vib.*, vol. 283, no. 3–5, pp. 1071–1091, 2005.

[34] A. Garg, J. S. Moore, and J. M. Kapellusch, “The Revised Strain Index: an improved upper extremity exposure assessment model,” *Ergonomics*, vol. 60, no. 7, pp. 912–922, 2017.

[35] V. L. Kruger, G. H. Kraft, J. C. Deitz, A. Ameis, and L. Polissar, “Carpal tunnel syndrome: objective measures and splint use.,” *Arch. Phys. Med. Rehabil.*, vol. 72, no. 7, pp. 517–20, 1991.

[36] D. Rempel, R. Manojlovic, D. G. Levinsohn, T. Bloom, and L. Gordon, “The effect of wearing a flexible wrist splint on carpal tunnel pressure during repetitive hand activity,” *J. Hand Surg. Am.*, vol. 19, no. 1, pp. 106–110, 1994.

[37] R. H. Gelberman, P. T. Hergenroeder, A. R. Hargens, G. N. Lundborg, and W. H. Akeson, “The carpal tunnel syndrome. A study of carpal canal pressures.,” *J. Bone Joint Surg. Am.*, vol. 63, no. 3, pp. 380–3, Mar. 1981.

[38] L. Johansson, G. Björing, and G. M. Hägg, “The effect of wrist orthoses on forearm muscle activity,” *Appl. Ergon.*, vol. 35, no. 2, pp. 129–136, 2004.

[39] S. Bulthaup and D. J. C. Iii, “An Electromyography study of wrist extension orthoses and upper-extremity function,” *Am. J. Occup. Ther.*, vol. 53, no. 5, pp. 434–440, 1999.

[40] I. S. V. Ferrigno, A. Cliquet, L. A. Magna, and A. Zoppi Filho, “Electromyography of the Upper Limbs During Computer Work: A Comparison of 2 Wrist Orthoses in Healthy Adults,” *Arch. Phys. Med. Rehabil.*, vol. 90, no. 7, pp. 1152–1158, 2009.

[41] R. A. Bos *et al.*, “A structured overview of trends and technologies used in dynamic hand orthoses,” *J. Neuroeng. Rehabil.*, vol. 13, no. 1, p. 62, 2016.

[42] I. H. Ertas, E. Hocaoglu, and V. Patoglu, “AssistOn-Finger: An under-actuated finger exoskeleton for robot-assisted tendon therapy,” *Robotica*, vol. 32, no. 8, pp. 1363–1382, 2014.

[43] C. G. Rose, F. Sergi, Y. Yun, K. Madden, A. D. Deshpande, and M. K. O’Malley, “Characterization of a hand-wrist exoskeleton, READAPT, via kinematic analysis of redundant pointing tasks,” *IEEE Int. Conf. Rehabil. Robot.*, vol. 2015-Septe, pp. 205–210, 2015.

[44] M. A. Diftler *et al.*, “RoboGlove – A Robonaut Derived Multipurpose Assistive Device,” *Int. Conf. Robot. Autom.*, pp. 78–84, 2014.

[45] M. Nilsson, J. Ingvast, J. Wikander, and H. Von Holst, “The Soft Extra Muscle system for improving the grasping capability in neurological rehabilitation,” *2012 IEEE-EMBS Conf. Biomed. Eng. Sci. IECBES 2012*, no. December, pp. 412–417, 2012.

[46] B. B. Kang, H. In, and K. Cho, “Force transmission in joint-less tendon driven wearable robotic hand,” *Control. Autom. Syst. (ICCAS), 2012 12th Int. Conf.*, pp. 1853–1858, 2012.

[47] “ExoHand,” *FESTO*, 2012. [Online]. Available: https://www.festo.com/group/en/%0Acms/10233.htm. [Accessed: 18-Jul-2019].

[48] J. L. Pons, “Rehabilitation Exoskeletal Robotics,” *IEEE Eng. Med. Biol. Mag.*, vol. 29, no. 3, pp. 57–63, May 2010.

[49] B. Gorissen, D. Reynaerts, S. Konishi, K. Yoshida, J. W. Kim, and M. De Volder, “Elastic Inflatable Actuators for Soft Robotic Applications,” *Advanced Materials*, vol. 29, no. 43. 2017.

[50] J. I. Baer, “Material handling apparatus and the like,” 3,343,864, 1967.

[51] P. Polygerinos, Z. Wang, K. C. Galloway, R. J. Wood, and C. J. Walsh, “Soft robotic glove for combined assistance and at-home rehabilitation,” *Rob. Auton. Syst.*, vol. 73, pp. 135–143, 2015.

[52] H. K. Yap, H. Y. Ng, and C.-H. Yeow, “High-Force Soft Printable Pneumatics for Soft Robotic Applications,” *Soft Robot.*, vol. 3, no. 3, pp. 144–158, 2016.

[53] P. Polygerinos *et al.*, “Modeling of Soft Fiber-Reinforced Bending Actuators,” *IEEE Trans. Robot.*, 2015.

[54] H. K. Yap, J. H. Lim, F. Nasrallah, and C.-H. Yeow, “Design and preliminary feasibility study of a soft robotic glove for hand function assistance in stroke survivors,” *Front. Neurosci.*, vol. 11, no. OCT, pp. 1–14, 2017.

[55] C. W. Nicolay and A. L. Walker, “Grip strength and endurance: Influences of anthropometric variation, hand dominance, and gender,” *Int. J. Ind. Ergon.*, vol. 35, no. 7, pp. 605–618, 2005.

[56] F. Gerr *et al.*, “A prospective study of computer users: I. Study design and incidence of musculoskeletal symptoms and disorders,” *Am. J. Ind. Med.*, vol. 41, no. 4, pp. 221–235, 2002.

[57] B. Mosadegh *et al.*, “Pneumatic networks for soft robotics that actuate rapidly,” *Adv. Funct. Mater.*, vol. 24, no. 15, pp. 2163–2170, 2014.

[58] H. K. Yap, J. H. Lim, F. Nasrallah, J. C. H. Goh, and R. C. H. Yeow, “A soft exoskeleton for hand assistive and rehabilitation application using pneumatic actuators with variable stiffness,” *Proc. -*

IEEE Int. Conf. Robot. Autom., vol. 2015-June, no. June, pp. 4967–4972, 2015.

[59] Dassault Systèmes, “ABAQUS.” Dassault Systèmes, Johnston, RI, 2017.

[60] P. Moseley, J. M. Florez, H. A. Sonar, G. Agarwal, W. Curtin, and J. Paik, “Modeling, Design, and Development of Soft Pneumatic Actuators with Finite Element Method,” *Adv. Eng. Mater.*, vol. 18, no. 6, pp. 978–988, 2016.

[61] M. Shahzad, A. Kamran, M. Z. Siddiqui, and M. Farhan, “Mechanical Characterization and FE Modelling of a Hyperelastic Material,” *Mater. Res.*, vol. 18, no. 5, pp. 918–924, 2015.

[62] D. Systèmes, “Abaqus 6.14 Documentation.” Dassault Systèmes, Providence, RI, 2014.

[63] “Ninjaflex,” *Ninjatek*, 2019. [Online]. Available: https://ninjatek.com/ninjaflex/. [Accessed: 18-Jul-2019].

[64] D. Systèmes, “Introduction to Abaqus.” [Unpublished], Johnston, RI, 2016.

[65] “Mark-10 Force Gauges,” *Mark-10*, 2019. [Online]. Available: http://www.mark-10.com/force_gauge.html. [Accessed: 22-Jul-2019].

[66] J. Prusa, “Prusa i3 MK3,” 2019. [Online]. Available: https://shop.prusa3d.com/en/3d-printers/180-original-prusa-i3-mk3-kit.html. [Accessed: 18-Jul-2019].

[67] Ultimaker, “Cura.” Ultimaker B.V., Cambridge, MA, 2019.

[68] “Atlas Copco,” *Atlas Copco*, 2019. [Online]. Available: https://www.atlascopco.com/en-ca. [Accessed: 18-Jul-2019].

[69] “Tekscan,” *Tekscan, Inc.*, 2019. [Online]. Available: https://www.tekscan.com/. [Accessed: 18-Jul-2019].

[70] E. F. Delagi, A. O. Perotto, J. Iazzetti, and D. Morrison, *Anatomical Guide for the Electromyographer*, Fifth. Springfield, IL: Charles C Thomas Publisher, Ltd., 2011.

[71] "OT Bioelettronica," *OT Bioelettronica s.r.l.*, 2014. [Online]. Available: https://www.otbioelettronica.it. [Accessed: 18-Jul-2019].

[72] "Arduino," *Arduino S.r.l*, 2019. [Online]. Available: https://www.arduino.cc/. [Accessed: 18-Jul-2019].

[73] J. Winkel, S. E. Mathiassen, and G. M. Hägg, "Normalization of upper trapezius EMG amplitude in ergonomic studies," *J. Electromyogr. Kinesiol.*, vol. 5, no. 4, pp. 195–196, 1995.

[74] S. N. McNair, P. J., Depledge, J., Brettkelly, M., & Stanley, "Verbal encouragement: Effects on maximum effort voluntary muscle action," *Br. J. Sports Med.*, vol. 30, no. December 1995, pp. 243–245, 1996.

[75] "MATLAB." The MathWorks, Inc., Natick, MA, 2019.

[76] C. J. De Luca, L. Donald Gilmore, M. Kuznetsov, and S. H. Roy, "Filtering the surface EMG signal: Movement artifact and baseline noise contamination," *J. Biomech.*, vol. 43, no. 8, pp. 1573–1579, 2010.

[77] D. A. Winter, *Biomechanics and Motor Control of Human Movement, Fourth Edition David A. Winter (cloth) 1. Human mechanics. 2. Motor ability. 3. Kinesiology. I. Title. QP303.W59*. 2009.

[78] T. Corser, "Temporal discrepancies in the electromyographic study of rapid movement," *Ergonomics*, vol. 17, no. 3, pp. 389–400, 1974.

[79] P. R. Cavanagh and P. V. Komi, "Electromechanical delay in human skeletal muscle under concentric and eccentric contractions," *Eur. J. Appl. Physiol. Occup. Physiol.*, vol. 42, no. 3, pp. 159–163, 1979.

[80] De Luca. Carlo J, "The Use of Surface Electromyography in Biomechanics," *J. Appl. Biomech.*, vol. 13, no. 2, pp. 135–163, 1997.

[81] A. Burden and R. Bartlett, "Normalisation of EMG amplitude: An evaluation and comparison of old and new methods," *Med. Eng. Phys.*, vol. 21, no. 4, pp. 247–257, 1999.

[82] "SPSS Statistics." IBM, Armonk, NY, 2019.

[83] C. W. Jansen, S. L. Olson, and S. M. Hasson, "The effect of use of a wrist orthosis during functional activities on surface electromyography of the wrist extensors in normal subjects.," *J. Hand Ther.*, vol. 10, no. 4, pp. 283–9, 1997.

[84] S. S. Shapiro and M. B. Wilk, "An Analysis of Variance Test for Normality (Complete Samples)," *Source Biometrika Biometrika Trust*, vol. 52, no. 34, pp. 591–611, 1965.

[85] R. G. Radwin, E. VanBergeijk, and T. J. Armstrong, "Muscle response to pneumatic hand tool torque reaction forces," *Ergonomics*, vol. 32, no. 6, pp. 655–673, 1989.

[86] J. R. Potvin, M. J. Agnew, and C. Ver Woert, "An ergonomic comparison of pneumatic and electrical pistol grip hand tools," *Int. J. Ind. Ergon.*, vol. 34, no. 6, pp. 467–478, 2004.

[87] S. L. Johnson, "Evaluation of Powered Screwdriver Design Characteristics," vol. 30, no. 1, pp. 61–69, 1988.

[88] H. Zhao, Y. Li, A. Elsamadisi, and R. Shepherd, "Scalable manufacturing of high force wearable soft actuators," *Extrem. Mech. Lett.*, vol. 3, pp. 89–104, 2015.

[89] J. Rossi, E. Berton, L. Grélot, C. Barla, and L. Vigouroux, "Characterisation of forces exerted by the entire hand during the power grip: effect of the handle diameter," *Ergonomics*, vol. 55, no. 6, pp. 682–692, 2012.

[90] J. C. Wallace and S. J. Vodanovich, "Workplace Safety Performance : Conscientiousness , Cognitive Failure , and Their Interaction," vol. 8, no. 4, pp. 316–327, 2003.

[91] R. Barański and A. Kozupa, "Hand grip-EMG muscle response," *Acta Phys. Pol. A*, vol. 125, no. 4

A, pp. 7–10, 2014.

[92] M. Fagarasanu, S. Kumar, and Y. Narayan, “Measurement of angular wrist neutral zone and forearm muscle activity,” *Clin. Biomech.*, vol. 19, no. 7, pp. 671–677, 2004.

[93] J. R. C. Dizon, A. H. Espera, Q. Chen, and R. C. Advincula, “Mechanical characterization of 3D-printed polymers,” *Addit. Manuf.*, vol. 20, pp. 44–67, 2018.

[94] K. G. J. Christiyan, U. Chandrasekhar, and K. Venkateswarlu, “A study on the influence of process parameters on the Mechanical Properties of 3D printed ABS composite,” *IOP Conf. Ser. Mater. Sci. Eng.*, vol. 114, no. 1, 2016.

[95] T. Letcher, B. Rankouhi, and S. Javadpour, “Experimental Study of Mechanical Properties of Additively Manufactured ABS Plastic as a Function of Layer Parameters,” no. December, p. V02AT02A018, 2016.